TARTU ÜLIKOOLI
TOIMETISED
ACTA ET COMMENTATIONES UNIVERSITATIS TARTUENSIS

972

EESTI ALUSPÕHJA GEOKEEMIA JA MINERALOOGIA KÜSIMUSI

Töid geoloogia alalt
XIV

TARTU 1994

TARTU ÜLIKOOLI TOIMETISED
ACTA ET COMMENTATIONES UNIVERSITATIS TARTUENSIS
ALUSTATUD 1893. a. VIHIK 972

EESTI ALUSPÕHJA GEOKEEMIA JA MINERALOOGIA KÜSIMUSI

Töid geoloogia alalt
XIV

Tartu
1994

Toimetuskolleegium: Aadu Loog (vastutav toimetaja)
Juho Kirs, Leho Ainsaar

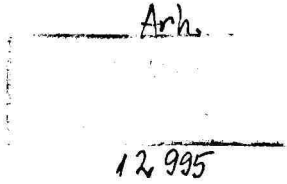

© Tartu Ülikool 1994

Tartu Ülikooli Kirjastuse trükikoda
Tiigi 78, EE 2400 Tartu
Tellimus nr. 282.

AGE AND GEOCHEMICAL CHARACTER OF PLAGIOMICROCLINE GRANITE VEINS IN THE ABJA GABBRO-DIORITIC MASSIF

Juho Kirs, Valter Petersell

The Svecofennian complexes of the burried crystalline basement of Estonia often contain mostly vein-like plagiomicrocline granite bodies of different thickness and shape. By texture the granites are varigrained, more rarely pegmatoid or medium-grained. Their mineralogical composition varies from microcline granite to plagioclase-microcline ones being also charnockitic in the areas of granulitic stage of regional metamorphism. Chemically the granites belong to subalkaline series (Irvine, Baragar, 1971). The rocks are most often correlated with the late — and postkinematic plagiomicrocline granites of the Fennoscandian Shield, which have the ages between 1.85–1.75 Ga. (Nurmi and Haapala, 1986, Andersson, 1991). Similar varigrained K-rich vein-like bodies of plagio-microcline granite intersect also the gabbro-diorites of the Abja massif in Southern Estonia (Fig. 1). The stock under the Paleozoic sedimentary cover 480 m thick was tracked geophysically and opened by the drill core 92 (Puura et al. 1983).

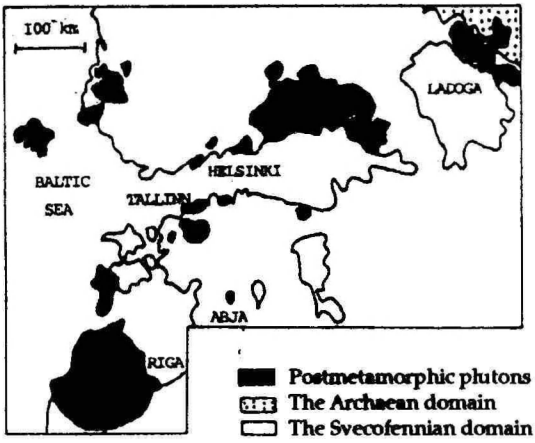

Fig. 1. Map, showing the location of Abja gabbro-dioritic stock in Estonian crystalline basement.

Table 1. Chemical composition of the rocks from drill core 92 (Abja)

Sample	925948	926150	926254	926306	926336	925875	925890	926203	926300
	1	2	3	4	5	6	7	8	9
SiO_2	45.34	50.00	49.44	50.80	51.74	67.12	68.80	73.26	71.92
TiO_2	2.04	2.14	2.14	2.06	1.88	0.42	0.48	0.11	0.18
Al_2O_3	13.04	13.02	13.74	13.02	13.02	13.52	13.63	12.96	13.50
$Fe_2O_3^+$	16.32	13.93	14.64	13.58	13.22	4.79	1.93	1.42	2.26
MnO	0.20	0.14	0.17	0.19	0.16	0.04	0.03	0.02	0.03
MgO	4.74	3.92	4.31	3.79	4.01	0.93	1.26	0.13	0.43
CaO	8.14	7.12	6.88	6.82	6.15	1.51	1.75	1.21	1.69
Na_2O	2.88	3.25	3.16	3.32	3.16	2.50	2.50	2.68	3.41
K_2O	2.58	3.20	3.12	3.18	3.09	7.25	6.65	7.33	6.05
P_2O_5	3.58	1.98	2.04	1.88	1.80	0.18	0.15	0.02	0.08
Total	98.86	98.70	99.64	98.64	98.23	98.26	97.18	99.14	99.55

Sample	925948	926150	926254	926306	926336	925875	925890	926203	926300
	1	2	3	4	5	6	7	8	9
F	0.457	0.331	0.508	0.507	0.589	0.123	–	0.017	0.058
CO_2	0.62	0.62	0.67	0.54	0.62	0.40	–	0.44	0.23
LOI	1.39	0.93	1.26	1.18	1.45	0.98	0.60	0.76	0.66
Pb	55	60	39	57	57	62	–	70	98
Rb	61	62	80	87	86	197	–	185	150
Sr	1423	1586	850	959	1290	608	–	923	1150
Nb	24	19	23	22	27	70	–	16	16
Zr	224	279	356	356	353	330	–	93	184
Ti	12230	12829	12829	12350	11271	2518	2878	659	1079
Y	65	56	66	64	67	119	–	39	36
Th	14	16	16	26	21	111	–	42	67
U	9	6	10	11	10	10	–	6	15

Notes:

$^{+}$Total iron as Fe_2O_3

Samples 1–5 as gabbro-diorites, 6–9 as plagiomicrocline granites.

Major elements: wet chem. an., trace elements: XRF method. Chem. Lab. Geol. Surv. Estonia

Table 2. U-Pb analytical results of zircons from the gabbo-diorites and granites from the drill core 92 (Abja)

N	Fraction (mkm)	Concentration (ppm)		Measured			Atomic ratios		Age (Ma)
		U	Pb	$^{206}Pb/^{204}Pb$	$^{207}Pb/^{206}Pb$	$^{208}Pb/^{206}Pb$	$^{206}Pb/^{238}U$	$^{207}Pb/^{206}Pb$	$^{207}Pb/^{206}Pb$
Sample 926064, interval 606.4–610.0 m. Gabbro-diorite, weakly gnessic									
1.	80-200	267.7	74.07	4015	0.1029	0.2081	0.2433	3.351	1624
2.	200-250	250.6	69.82	6140	0.1019	0.2244	0.2431	3.360	1628
Sample 926110, interval 611.0–617.0 m. Gabbro-diorite, weakly gneissic									
3.	80-200	237.9	70.39	3855	0.1032	0.2693	0.2484	3.439	1632
4.	200-250	194.5	63.85	1175	0.1114	0.3291	0.2620	3.622	1629
5.	80-200+	216.3	83.22	241.7	0.1569	0.4296	0.2620	3.622	1629
Sample 92575, intervals 587.5–589.5, 620.3–620.7, 630.0–630.3, 603.4–604.0 m. Plagiomicroline granite, varigrained									
6.	Slightly coloured	2057	579	4954	0.10193	0.11430	0.26863	3.6770	1610.5
7.	Mediumcolured	2590	636	1535	0.10671	0.11401	0.23160	3.1251	1583.8
8.	Dark-coloured, opaque	3589	686	743.5	0.11280	0.11754	0.17665	2.2974	1514.6
9.	Residues of 7 and 8	248.9	163	620.2	0.11963	0.14659	0.59157	7.9607	1578.7

+ – abrasive treatment

Fraction 9 – residues of the fractions 7 and 8, were processed during 30 minutes in fluoric acid at 210°C

Abja gabbro-diorites

The gabbro-diorites from the Abja drill core form the greenish-grey mediumgrained rock with massif or weakly gneissic texture. Containing SiO_2 about 45–52 wt% the rock nevertheless has the mineralogical composition of quartz-diorite (Puura et al, 1983, Table 32). Of specific character is also the enrichment with the accessory apatite and titanomagnetite. Geochemically the rock belongs to alkaline series with K_2O content of 2.6–3.2 wt%. It is enriched with the P, F, Ti and incompatible trace elements such as Ba, Sn, Zr, Th, REE (Table 1) (Petersell, Kirs 1992).

The isotope age of the gabbro-diorite was determined by the U-Pb method of zircon in the laboratory of Vassiliostrov Association "Ostrov" by IGGD in St. Petersburg under the supervision of Dr. O. A. Levchenkov. Decomposition of zircon and extraction of Pb and U were performed by Krogh's method (Krogh, 1973). Pollution with laboratory Pb and U did not exceed 0.2 and 0.1 ng. The content of Pb and U isotopes was measured by means of the mass spectrometer Finnigan MAT, model 261. Fractionation coefficient of this device is 0.001 to 1 per unit of atom mass. Error by measuring the isotopic ratios 206Pb/238U and 207Pb/235U was up to 1.0%. Establishing of isotopic relations, finding of their analytical points in the concordia plot and calculation of isochronous ages were performed according to Ludwig (Ludwig, 1980).

By calculating the age the following constant values were used: $\lambda_{238} = 0.155125 \times 10^{-9}$ years^{-1}, $\lambda_{235} = 0.984850 \times 10^{-9}$ years^{-1}, 238U/235U=137.88. In meaning of correctional lead the isotopic composition calculated by the model of Stacey and Kramers (Stacey, Kramers, 1975) was used.

Zircons fractionated were translucent with the pale pink (brownish) colour and idiomorphic prismatic habit. Some crystals were weakly zoned. Most grains had dimensions about 0.05–0.3 mm with the elongation less 1.5. Rarely tiny inclusions were detected.

The age of Pb, obtained by single determinations from zircon, as well as the concordant age, were very similar, respectively 1.624–1.632 Ga and 1.635 ± 7 Ga (Table 2, Fig. 2).

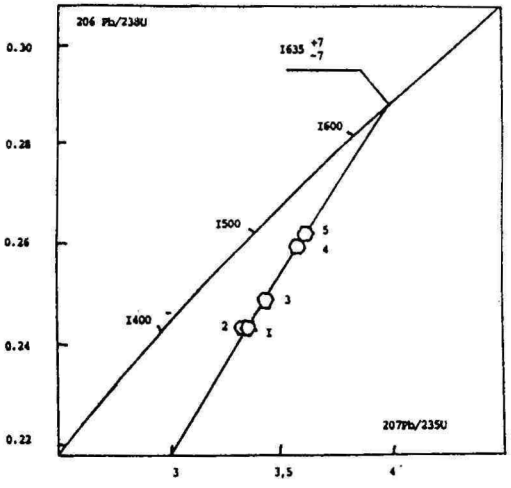

Fig. 2. Concordia plot of U-Pb zircon data on Abja gabbro-diorite. 1–5 – fractions from Table 2.

Veins of plagiomicrocline granite

Gabbroids in the Abja drill core are intersected by five veins of varigrained plagiomicrocline granite, forming an angle of about 40–50° with the vertical line. The thickness of these veins seems to range within 0.2–3.4 m. The rock is fine- to mediumgrained, in places containing coarser K-feldspar crystals which give to it a slightly porphyritic appearance. The mineralogical composition of granite is predominantly as follows: microcline (40–60%), plagioclase (20–30%), quartz (20–25%), biotite (5%). Accessory minerals are represented by apatite, zircon, monazite, orthite and magnetite.

For the isotope age dating rock samples were taken from the drill core 92 at dephts of 577.5, 620.3 and 630.0 ± 0.5 m and were combined into one sample. At the same dephts samples were taken for the determination of major and trace elements in the rock.

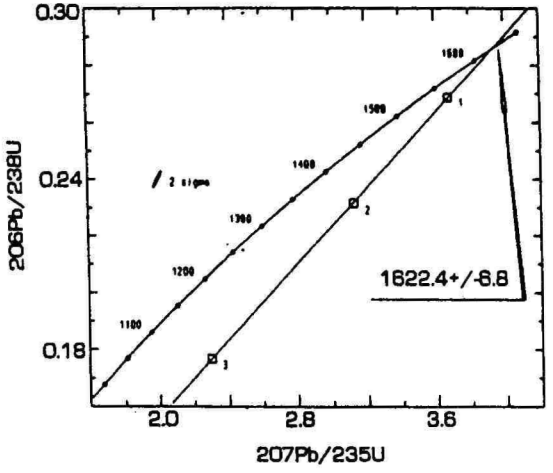

Fig. 3. Concordia plot of U-Pb zircon data on Abja vein granite.
1–3 – fractions from Table 2 (see text).

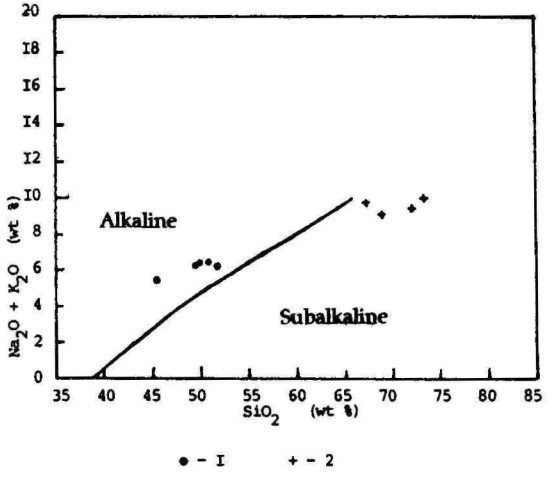

Fig. 4. Compositions of Abja gabbro-diorites (1) and plagiomicrocline granites (2) plotted in Na_2O+K_2O vs. SiO_2 diagram (Irvine and Baragar, 1971).

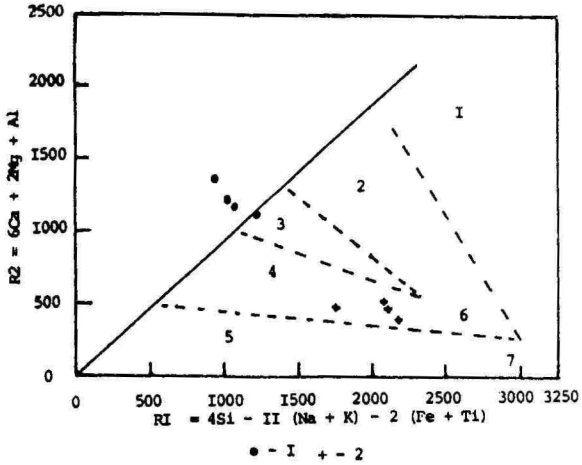

Fig. 5. Compositions of Abja gabbro-diorites (1) and plagiomicrocline granites (2) plotted in de la Roche multicationic RI vs. R2 diagram (Batchelor and Bowden, 1985)
1 – Mantle Fractionates, 2 – Pre-plate Collision, 3 – Post-collision Uplift, 4 –Late-orgenic, 5 – Anorogenic, 6 – Syn-collision, 7 – Post-orogenic

The sample for the isotope age was crushed to 0.25 mm. Zircon, separated from it using the ordinary mineralogical methods, constituted pieces of crystals of one generation broken mechanically.

The isotope age dating was performed also in the above-mentioned laboratory in St. Petersburg under the supervision of Dr. O. A. Levchenkov. The colour of zircons analyzed changed from colourless translucent to dark-brown opaque (Table 2). For the analysis three portions were weighed having different colours: slightly coloured translucent, medium-coloured semi-opaque and dark-coloured opaque. The residues of the two last fractions were processed during 30 minutes in fluoric acid on the temperature of 210°C to investigate of more crystallized mineral parts having less destroyed isotope systems (Krogh, Davis, 1975).

All three zircon fractions of different translucency, separated for the analysis, had a very high U-content exceeding 2000 ppm (Table 2). Radioactive decomposition of U and Th caused considerable metamictisation of crystals finding its expression in lowering of double refraction coefficient. This was the reason for partial loss of radiogenic Pb. There can be observed direct relation between the U-content in zircon and Pb loss.

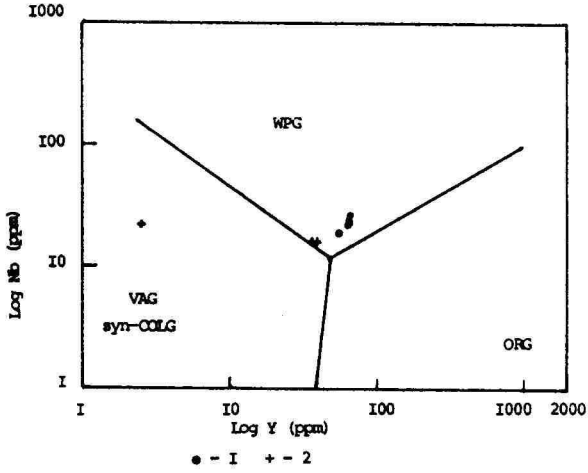

Fig. 6. Compositions of Abja gabbbro-diorites (1) and plagiomicrocline granites (2) plotted in Nb vs. Y diagram (Pearce et al; 1984).
WPG – within plate granites, VAG – volcanic arc granites, syn-COLG – syncollision granites, ORG – ocean ridge granites.

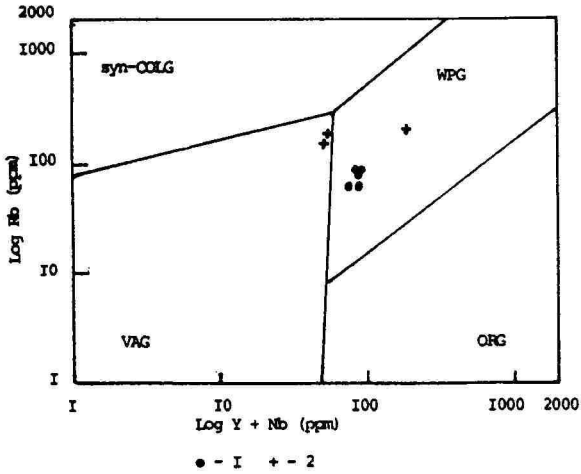

Fig. 7. Compositions of Abja gabbro-diorites (1) and plagiomicrocline granites (2) plotted in Rb vs. (Y+Nb) diagram (Pearce et al; 1984). The fields as in Fig. 7.

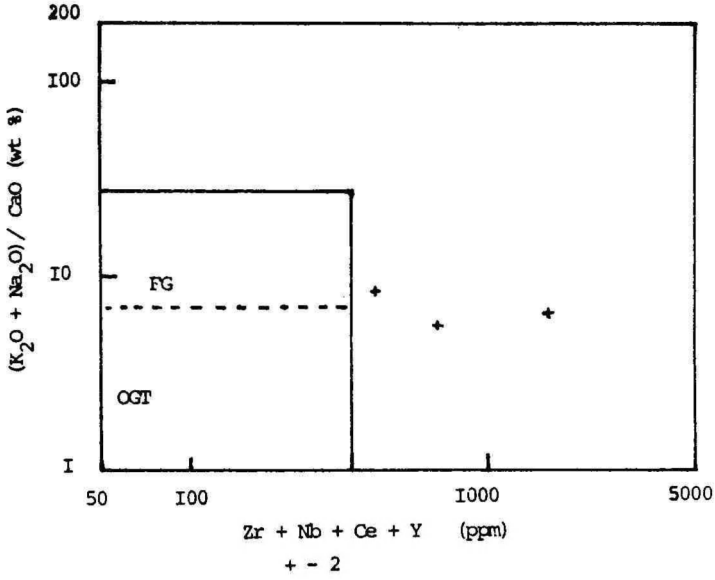

Fig. 8. Compositions of Abja plagiomicrocline granites (2) plotted in $(K_2O + Na_2O)/CaO$ vs. (Zr + Nb + Ce + Y) diagram (Whalen et al; 1987).
FG – fractionated I-type granites, OGT – unfractionated M-, S-, I-type granites.

By the data of analysis of three zircon fractions an isochron was constructed dating the age of zircon occuring in granites as 1622 ± 6 million years (Fig. 3). The fourth fraction was left out of consideration. During its processing with fluoric acid subtraction of U in relation to Pb took place whereas the 207 Pb and 206 Pb ratio remained the same. The Pb-Pb age in different zircon fractions ranges within 1514.6–1610.5 million years, being lower at higher U content in the samples (Table 2).

The contents of major and trace elements in granites were established at the chemical laboratory of the Geological Survey of Estonia, using the classical chemical and XRF methods, respectively, under the supervision of the chemist M. Kalkun (Table 1). The granites under consideration are highly alcalic, particulary rich in K (Table 1). On the SiO_2-alkalies diagram (Irvine, Baragar, 1971) their composition fall into the transition zone from subalkaline to alkaline field (Fig. 4). On the de la Roche R1-R2 multicationic diagram (Fig. 5) (Batchelor and Bowden, 1985) the compositions of vein granites lie on the trend of late

orogenic granitoid series, lieing closely to the field of syn-collisional granites (i.e. towards the minimum melting composition formation of it in many cases coincides with the plate collision event in time). It is worth to note that, the compositions of Estonian subplatform (or rapakivi formation) K-granites (Petersell, Kirs 1992, Table 1), postorogenic age of which has been firmly documented (1.62–1.63 Ga, Kirs et al, 1991), lie exactly on this latter field of this diagram.

Characteristic to Abja vein granites is also high content of U, Th, Sr and Pb. The specific location of the composition points of the plagiomicrocline granites on various tectono-magmatic discrimination diagrams, such as Nb-Y, (Fig. 6), Rb-(Nb+Y) (Fig. 7) (Pearce et al. 1984) and $(K_2O + Na_2O)/CaO - -(Zr + Nb + Y + Ce^*)$ (Fig. 8) (Whalen et al. 1987) allows to connect them with the granitoids of a tensional tectonic regime. Their geochemical parameters are quite close to granitoids of the rapakivi formation of the Estonian crystalline basement, first of all to rocks of the Naissaare stock. The age of the latter is also about 1.626±13 Ga (Kirs et al., 1991). However, the geochemical data refer to a more less fractionated character (lower Rb/Sr ratios, greater difference from a granitic minima) as to a more restricted (and various) extent of source rock melting (little higher, but uneven content of incompatible elements) for Abja vein granites in comparison with the Estonian subplatform K-granites forming an independent stocks.

Conclusions

The data above show the existence of such type plagiomicrocline vein granites in Estonian crystalline basement which have clearly younger age, than Svecofennian, together with the geochemical characteristics proper to anorogenic type magmatic rocks. However to distinct them from the widespread Svecofennian so-called lateorogenic plagiomicrocline granites it demands more detailed geochemical investigations. Considering this, the greatest attention should be paid on alkali-rich ($Na_2O + K_2O = 7 - 10$ wt%) veined bodies of plagiomicrocline

* unpublished data V. Petersell

granite known from the boreholes of Are (171), Häädemeeste (172), Viljandi (91) and also from Seliste (173) borehole. In the last case, the isotopic age of granites determined by the K-Ar method from biotite is 1.545 Ga and 1.540 Ga (Puura, 1974). The pegmatoid varieties of plagiomicrocline granite, having a low isotopic age determined by the K-Ar method from biotite, have been recorded also from the drill cores in North-Eastern Estonia (Jõhvi II – 1.440 Ga, Kabala – 1.683 Ga, etc.) and also from Northern Estonia (Hirvli 8 – 1.345 Ga, F109 – 1.654 Ga) (Puura, 1974).

References

Andersson U. B. 1991. Granitoid episodes and mafic-felsic magma interaction in the Svecofennian of the Fennoscandian Shield, with main emphasis on the 1.8 Ga plutonics. Precambrian Research, vol. 51, p. 127–149.

Batchelor R. A., Bowden P. 1985. Petrogenetic interpretation of granitoid rock series using multicationic parameters. Chemical Geology, vol. 48. p. 43–55.

Irvine T. N., Baragar W. R. A. 1971. A guide to the chemical classification of the common volcanic rocks. Canad. J. Earth Sci., vol. 8., p. 523–548.

Kirs J., Huhma H., Haapala I. 1991. Petrological-chemical features and age of Estonian anorogenic potassium granites. In: I. Haapala and O.T. Rämö (Editors), Symposium on rapakivi granites and related rocks. Abstr. vol., p. 28–29.

Krogh T. E. 1973. A low-contanimation method for hydrothermal decomposition of zircon and extraction of U and Pb for isotopic age determination. Geochim. Cosmochim. Acta 37, p. 485–494.

Krogh T. E., Davis G. L. 1975. Alteration in zircons and differential dissolution of altered and metamict zircon. Carnegie Year Book 1974–1975, p. 619–625.

Ludwig K. R., 1980. Calculation of uncertainties of U-Pb isotope data. Earth Planet. Sci. Lett. vol. 46, p. 212–220.

Nurmi P. A., Haapala I. 1986. The Proterozoic granitoids of Finland: Granite types, metallogeny and relation to crustal evolution. Bull. Geol. Soc. Finl. 58, Part 1. p. 203–233.

Pearce J. A., Harris N. B. W., Tindle A. G., 1984. Trace element discrimination diagrams for the tectonic interpretation of granitic rocks. J. Petrol., vol. 25, p. 956–983.

Petersell V., Kirs J. 1992. Geochemical character of Estonian subplatform granitoids and gabbroids. Geol. Pap. XIII, Acta Comm. Univ. Tartuensis 956, p. 27–43.

Puura V., 1974 – Пуура В. К-Ar изотопый возраст пород кристаллического фундамента Северной Прибалтики. Изв. АН ЭССР Химия, Геология. Т. 23, с. 40–49.

Puura V. et al. – Пуура В. и др., 1983. Кристаллический фундамент Эстонии. М. Наука, 208 с.

Stacey J. S., Kramers J. D. 1975. Approximation of terrestrial lead isotope evolution by two-stage model. Earth and Planet. Sci. Lett. vol. 26, p. 207–221.

Whalen J. B., Currie K. L., Chappel B. W. 1987. A-type granites: geochemical characteristics, discrimination and petrogenesis. Contrib. Min. and Petrol., vol. 95. p. 407–419.

ABJA GABRO-DIORIITSE MASSIIVI PLAGIOMIKROKLIINGRANIIDI SOONTE VANUS JA GEOKEEMILINE ISELOOM

Juho Kirs, Valter Petersell

Resümee

Eesti aluskorra svekofenni kivimikompleksides on sageli soonelised mikrokliin- või plagiomikrokliingraniidi kehad. Neid rööbistatakse Fennoskandia kilbi hilis- osalt ka post-kinemaatiliste graniitidega, mille vanus kõigub vahemikus 1,85–1,75 miljardit aastat. Sellised eriteralise plagiomikrokliingraniidi sooned levivad ka Abja puursüdamikus 92 kohati gneisilist tekstuuri ilmutavas gabro-dioriidis (mineraloogiliselt kvartsdioriidis).

Gabbro-dioriidist eraldatud tsirkooni vanuseks saadi U-Pb isokroonmeetodil 1635 ± 7 ma (tabel 2, jn. 2). Geokeemiliselt on gabrokivimites kõrgenenud K, P, F, Ti, Zr, TR jt. nn. mittekaasnevate elementide sisaldus, mis on väga iseloomulik postorogeenseile magmakivimeile.

Abja soonelise plagiomikrokliingraniidi tsirkoonid annavad isokroon-vanuseks 1622 ± 6 ma. (jn. 3). Multikatioonsel RI-R2 diagrammil (jn. 5) langevad graniidiproovide koostispunktid graniitse ülessulamise miinimumi koostise lähedale. Rabakivigraniitidega võrreldes viitavad Abja soongraniidi geokeemilised andmed aga nii lähtekivimi ülessulamise kui ka tekkinud magma väiksemale fraktsioneerituse astmele.

Toodud andmed näitavad, et Eesti aluskorra kivimeis on Svekofenni orogeneesist selgelt nooremad, valdavalt plagiomikrokliingraniitse koostisega sooned. Sellele viitavad ka V. Puura esitatud soonelist tüüpi graniitide biotiidist K-Ar meetodil saadud isotoopvanused (Puura, 1974).

ON THE GEOLOGICAL STRUCTURE OF THE CRYSTALLINE BASEMENT OF THE SOUTHERN SLOPE OF THE BALTIC SHIELD

Valter Petersell, Oleg Levchenkov

Introduction

The southern slope of the Baltic Shield (SSBS) belongs to the transitional area between the shield in the north and Poland–Lithuania depression and Latvia saddle in the south. It comprises the territory of Estonia and the western part of the Leningrad and the northwestern part of the Pskov regions, also North Latvia (Fig. 1). Its territory on the continent exceeds 66 thousand square km. The western border lies under the Baltic Sea. The northern border proceeds by the contact of the Baltic Shield and Russian Plate along the southern part of the Gulf of Finland. Here the crystalline basement has subsided for 20–40 m. The southern boundary of the slope has not been defined exactly. At present it proceeds by the zone of sublatitudinal subsurface tectonic faults along the slopes of the Lokno–Valmiera basement dome (Tect. map.., 1980). By data of seismic studies this fault ranges into the upper mantle and the displacement of the Mohorovicic discontinuity can reach 6 km and more. SSBS is covered by Vendian, Paleozoic and Quaternary sedimentary rocks with a total thickness from a few meters in the Gulf of Finland up to 400–600 m and more in South Estonia. The relief of the crystalline basement is weakly rugged, in the greatest part of the territory dipping southward for 2–4 m/km (Fig. 2). Near the Lokno–Valmiera basement dome the southward inclination of the basement relief decreases gradually and is replaced by the zone of Lokno–Valmiera domes, with the relative height reaching 37 m.

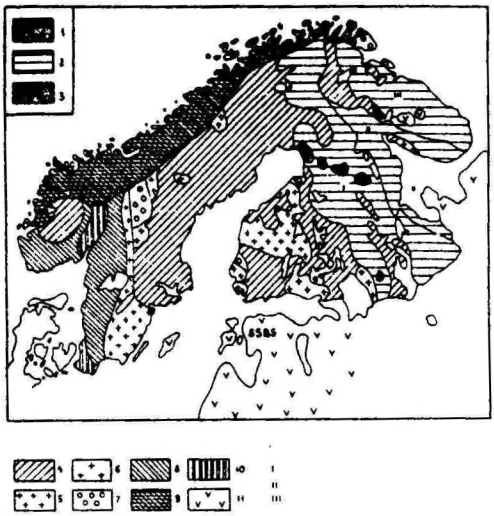

Fig. 1. Geochronological chart of the Precambrian Baltic Shield, compiled by results of U-Pb age dating of zircon in rocks. (By Tugarinov and Bibikova, 1980, with supplements of authors).
1 – main rock mass of Chuna-Moncha-Volchi tundra; 2 – Archean of the Baltic Shield (3.00–2.60 Ga): I – Karelian region, II – White Sea region, III – Kola region; 3 – deep magmatism (2.40 Ga); 4 – Sveco-Karelian formations (2.40 – 1.85 Ga); 5 – Svecofennian magmatism (1.90–1.75 Ga); 6 – rapakivi granites (1.67–1.54 Ga); 7 – Jotnian and Sub-Jotnian formations (1.75–1.67, 1.54–1.27 Ga); 8 – Dalslandian activization zone (1.10–0.90 Ga); 9 – Caledonides; 10 – post Riphean cover of the East European Platform; 11 – Phanerozoic platform Formations.

The units and views on the geological structure of the crystalline basement

Regionalization of the crystalline basement of the SSBS has been carried out by A. Öpik (Öpik, 1935), E. Fotiadi (Fotiadi, 1958), R. Gafarov (Gafarov, 1962), E. Pobul (Pobul, 1960) and by other researchers on the basis of magnetometric and gravimetric data in the years 1936 to 1963. These geological and geophysical source materials allow to subdivide the SSBS into two different structural facies regions — Tallinn–Novgorod and Estonian–Latvian ones which roughly coincide with the subdivision by E. Fotiadi. Considering the geophysical fields, composition, genesis and degree of metamorphism of the rocks, these regions are

subdivided into zones and other structural units. As for their age and structure, views differ considerably and are often contradicting (Dedejev, 1974; Zander et al, 1967, Puura, 1974, Petersell, 1976 etc.).

In the Tallinn–Novgorod region the Tallinn, Alutaguse, Jõhvi and Tapa zones are distinguished. The Estonian–Latvian region is subdivided into the Paldiski–Pskov zone and West and South Estonia with North Latvia (Fig. 2).

In the Tallinn zone in the form of subsurface belts there can be observed mostly metavolcanic quartz-feldspathic, biotite and biotite amphibole gneisses and amphibolites, also metasedimentary biotite and aluminiferous gneisses with interbeds of graphite- and sulphide-bearing varieties ("black" shale). All these belong to the Jägala rock massif (Petersell, 1974).

In the Alutaguse zone there are widely distributed biotite and aluminiferous, more rarely biotite-amphibole gneisses, quartzite and other rocks, interbedded with "black" shale. These different rocks form the Alutaguse rock massif. In the Uljaste Member and its analogues there are distinguished quartzites, interbedded with carbonate rocks, "black" shale, biotite-amphibole gneisses, etc., occurring in the lowermost part of the Alutaguse rock massif (Vaher et al, 1962).

The Jõhvi zone is characterized by mineralogically diverse Mn-rich ferruginous quartzites occurring in biotite and aluminiferous gneisses and acid, intermediate and basic metavolcanites. They all form the Vaivara rock massif (Puura, 1974; Vetrennikov et al, 1986).

In the submeridional Tapa zone the granitized basic rocks border with biotite- amphibole gneisses and amphibolites, also as with the "black" shale interbedded aluminiferous gneisses (Petersell, 1976).

The Estonian–Latvian structural facies region is considerably less studied. The Paldiski–Pskov zone is dominated by metavolcanic quartz-feldspathic, biotite and biotite-amphibole gneisses, more rarely by amphibolites and carbonate rocks. In South Estonia and North Latvia there occur often granulites and charnockites, but also biotite and biotite-amphibole gneisses, more rarely aluminiferous gneisses and other rocks. In Northwestern Latvia Mn-rich ferruginous quartzites were discovered by boring at Staicele locality (Vetrennikov et al, 1986). In West Estonia there prevail biotite and biotite-amphibole gneisses.

Quartz-feldspathic and aluminiferous gneisses and amphibolites occur more rarely. From the Undva core (b.h. 508) on West Saaremaa the subplatform stage (Gothian) quartz-porphyry and plagioclase porhyrites have been recorded (Niin, 1976).

The Estonian crystalline basement supracrustal rocks were metamorphized in the amphibolite facies, those of the South Estonia, Tapa and Jõhvi zones partly also in the granulitic facies of metamorphism, which is represented by the sillimanite-andalusite type (Krist. fund..., 1983) The Pre-Gothian supracrustal rocks are penetrated by metabasites, more rarely by metaultrabasites and granitoids. The whole complex is, in turn, penetrated by late Svecofennian granites causing migmatization and intense, but uneven K-metasomatism. Na- metasomatism has been recorded only in small areas. Intrusive rocks of the subplatform Gothian complex are represented by gabbroids and granitoids of anorthosite- rapakivi formation.

Basing on magnetometric data and on those obtained from single drill cores in North Estonia, in 1935 A. Öpik (Öpik, 1935) suggested the extension of Svecofennian structures and rocks on the territory of Estonia from Central Sweden and South Finland.

L. Vardanjants (Vardanjants, 1960) and S. Tihomirov (Tihomirov, 1966) correlated the above-mentioned rocks with Svecokarelian rocks of the Baltic Shield. A principally similar viewpoint was expressed also by other Soviet scientists (Dedejev, 1974, Zander et al, 1967). However, part of paragneisses in Northeastern Estonia they assigned to the Novgorod Archean massif. V. Petersell (Petersell, 1976) supported the opinion that rocks of the crystalline basement of the SSBS belong to svecofennides-karelides. In 1974–1976 several publications appeared, edited by V. Puura (Puura, 1974; Puura et al, 1976; Koppelmaa et al, 1978) where for the first time rocks of the crystalline basement of South and West Estonia, as also of the Paldiski–Pskov, Tapa and Jõhvi zones were attributed to the Archean. More recently these views have been widely supported and developed by V. Puura, M. Niin, H. Koppelmaa and V. Klein (Geol. map .., 1980; Tect. map.., 1980; Krist. fund.., 1983; etc.). Unfortunately the data, such as the isotopic age, mineralogical, petrochemical and other correlations have not been published by these authors. Archean age was mostly based on high degree of metamorphism and similarity of these rocks with granulites of the Russian Plate and the Kola peninsula.

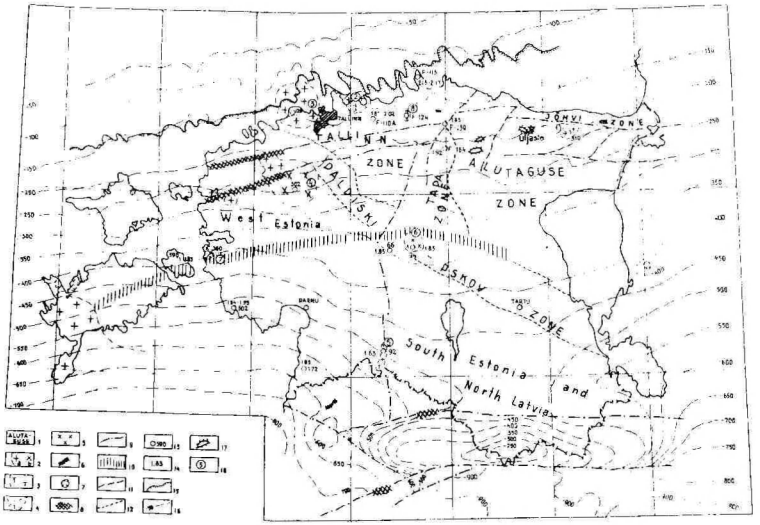

Fig. 2. Scheme of the geological structure of the crystalline basement of the Southern slope of Baltic Shield.
1 – structure zone; 2–4 – anorthosite-rapakivigranite formation, 2 – potassic porphyraceous granite (a) and granodiorite (b), 3 – gabbro-diorite and gabbro-norite, 4 – plagioclase porphyrite and quartz porphyries; 5–6 – Svecofennian complex (5-granodiorite and quartz-diorite, Mn-rich ferruginous quartzites); 7 – ring-shaped structure; 8–9 – faults ranging into the upper mantle surface, 8 – by seismic studies, 9 – by geological features); 10 – zone of fracture and mylonitisation; 11 –proved platform faults; 12 – boundary of zone; 13 – location of samples for U-Pb isotopic age-dating; 14 – isotopic age, Ga; 15 – boundary of Vendian deposits; 16 – contour line of the basement surface; 17 – local rise of the basement; 18 – number of small intrusions (1 – Ereda, 2 – Jägala, 3 – Naissaar, 4 – Märjamaa, 5 – Abja, 6 – Taadikvere, 7 – Virtsu, 8 – Sigula)

As was said before, the "Archean", as well as the Proterozoic, rocks are subjected to intense K-metasomatism and migmatization. This is often accompanied by numerous veins and small "dirty" intrusions of potassic granites with xenoliths of adjacent rocks. In the areas of "Archean" rocks charnockitization as also small charnockite massifs were recorded. All these granites, including charnockite, were not subjected to metamorphism.

By the supporters of the "Archean" age such intense migmatization accounts for the high degree of metamorphism. Ultrametamorphism, in turn, accounts for intense migmatization and charnockitization. Potassium-rich magma and fluids, originated from deeper sources acted as one possible reason for K-metasomatism and migmatization, also charnockitization. These processes, however can be widely observed in the classical Svecofennian area effecting basic and other potassium-deficient rocks (Miner. mest..., 1982, Tugarinov et al, 1980).

Thus, the main problems discussed during the last 30–40 years are the determination of the geological position of the SSBS in the structure of the East-European Platform and the age relations betweeen the regions and structural zones distinguished in the crystalline basement of the SSBS. Only correctly established age relations of rock complexes of the region allow to estimate reliably the perspective of the area as a mineral deposit. This concerns particularly the subsurface territories which are neighbored by well-studied different-aged areas of the shield with different ore perspectives.

Material and methods of the study

The factual material for this paper has been collected during the geological study of the crystalline basement of the SSBS in the years 1965–1990, permanently assisted by one of the author (V. Petersell). Results of spectral, X-ray spectral, atomic-absorption, silicate etc. analyses had been applied together with data on mineralogical, petrographic, petrophysical etc. investigations. Additional samples were taken for determination of the trace elements, REE, gross isotopic composition of Pb in rocks and for U-Pb isotopic age dating of zircon.

Material for establishing gross isotopic composition of Pb in rocks was obtained from duplicates of samples taken for geochemical investigations. The samples were collected by point method from petrographically similar rock intervals of drill cores with the total weight of 150–250 grams and ground up to grain size of 200 mesh.

Samples for U-Pb isotopic age dating were taken from acid metavolcanites, aluminiferous gneisses and intrusive rocks. The samples comprised pieces of drill core without any noticeable marks of migmatization and K-metasomatism, except for the sample from borehole 502. In this borehole aluminiferous gneisses are all migmatized or subjected to K-metasomatism. Therefore also all rock samples bear traces of K-metasomatism. The weight of a sample depended on the zircon content in the rock ranged from 2 kg to 6 kg.

The isotopic analysis of Pb in the rocks was performed by isotopic spectral method in the laboratory of IGFM of the Ukrainian Academy of Sciences by means of a unified interference spectral analyzer (type UISA-2). The relative error of measuring by the concentration of isotopes 208Pb higher than 40%, also 206Pb and 207Pb higher than 20%, does not exceed 1.5 and 2.5%, respectively. The relative error by determination of the isotope 204Pb by the concentration 1.4% does not exceed 5–7% (Zukov, Lesnoi, 1982).

The isotopic age dating of rocks by Pb and U isotopes from zircon was carried out in the laboratory of Vassiliostrov association "Ostrov" by IGGD in St. Petersburg. Decomposition of zircon and extraction of Pb and U were performed by Krogh's method (Krogh, 1973). Pollution with laboratory Pb did not exceed 3 ng. The content of Pb and U isotopes was measured by means of the mass spectrometer Finnigan MAT, model 261. Fractionation coefficient of this device is 0.001 to 1 per unit of at. mass. Error by measuring the isotopic ratios 206Pb/238U and 207Pb/235U was up to 1.5%. Establishing of isotopic relations, finding of their analytical points in the concordia diagram and calculation of isochron ages were performed according to K. Ludwig (Ludwig, 1980). By calculating the age the following constant values were used: $\lambda_{238} = 0.155125 \times 10^{-9}$ years, $\lambda_{235} = 0.984850 \times \times 10^{-9}$ years, 238U/235U = 137.88. In meaning of correctional lead the isotopic composition calculated by the model of J. Stacey and J. Kramers (Stacey, Kramers, 1975) was used.

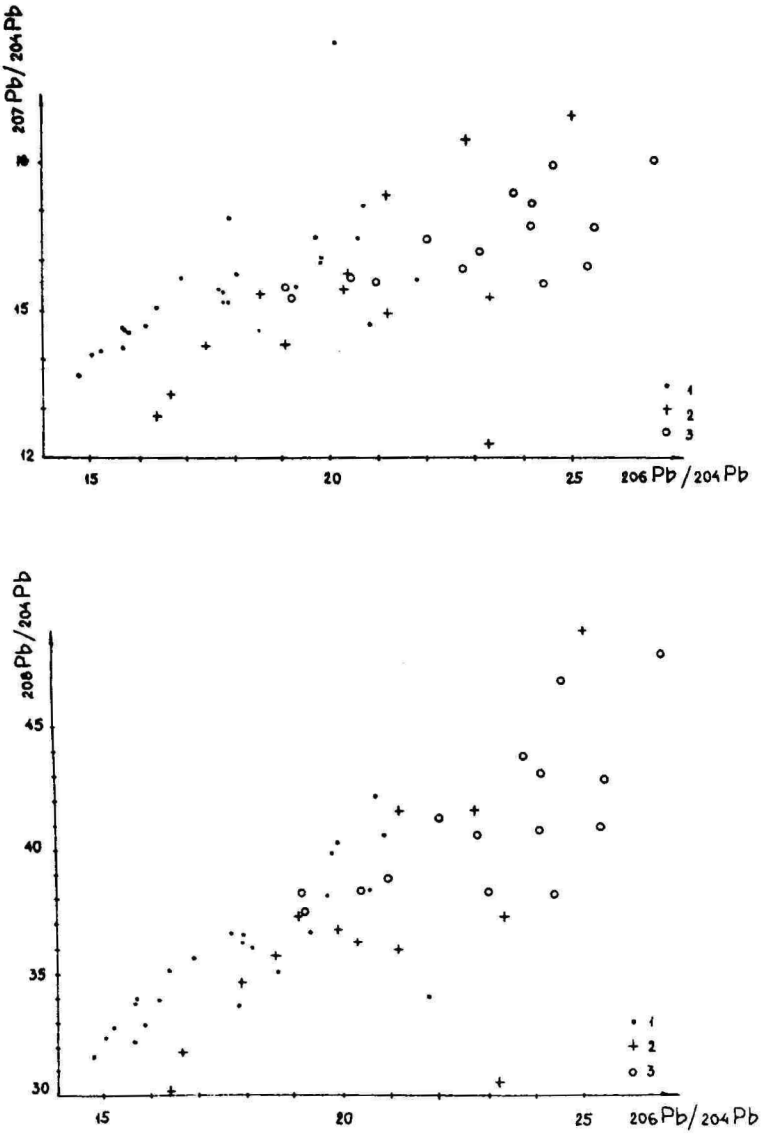

Fig. 3. 207Pb/204Pb – 206Pb/204Pb (a) and 208Pb/204Pb – 206Pb/204Pb (b) diagrams illustrating the Pb isotopic ratios in rocks of the Tallinn and Alutaguse zones;

1 – aluminiferous gneisses; 2 – potassic granites causing migmatization; 3 – metavolcanic quartz-feldspar, biotite and amphibole-biotite gneisses.

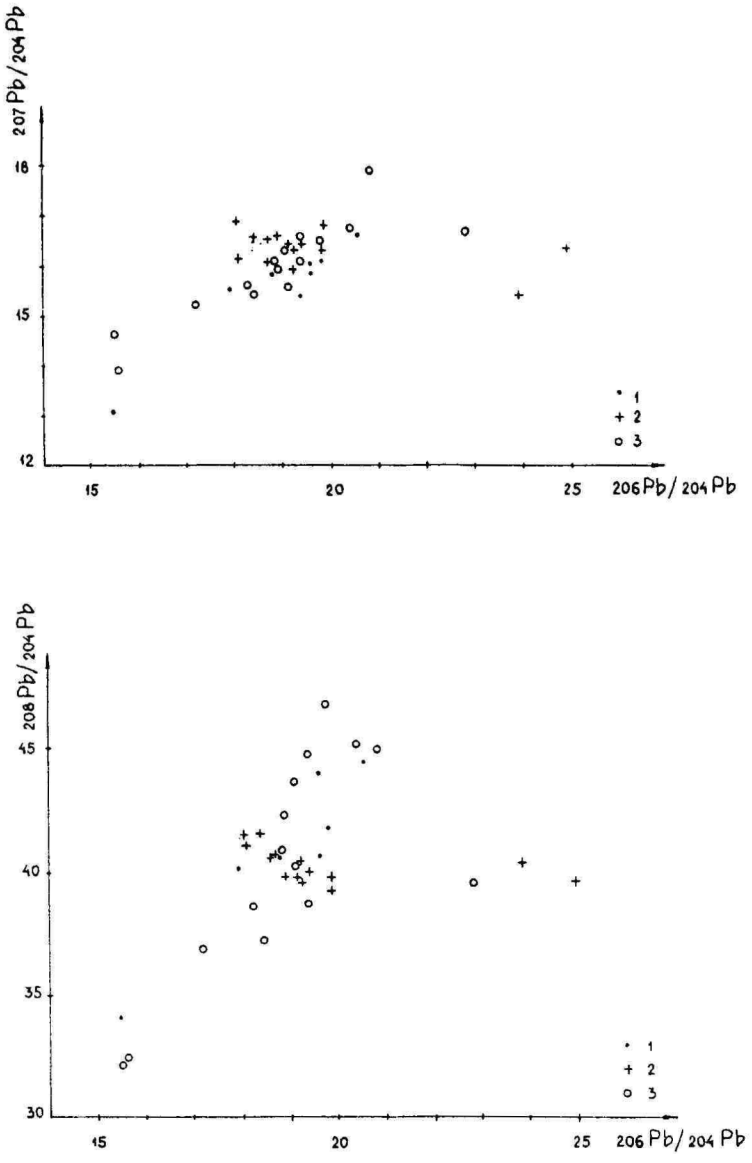

Fig. 4. 207Pb/204Pb – 206Pb/204Pb (a) and 208Pb/204Pb – 206Pb/204Pb (b) diagrams illustrating the Pb isotopic ratios in rocks of West and South Estonia.

1 – aluminiferous gneisses; 2 – potassic granites causing migmatization; 3 – metavolcanic quartz-feldspar and biotite gneisses.

Results

Data on the isotopic composition of Pb from aluminiferous gneisses, metavolcanites and migmatiteforming plagio-microcline granites are plotted in the diagrams 207Pb/204Pb – 206Pb/204Pb (Fig. 3) and 208Pb/204Pb – 206Pb/204Pb (Fig. 4). The fields and trends of points in those diagrams are clearly different.

In the diagram Fig. 3 the fields of Pb isotopic relation points of aluminiferous gneisses from different regions almost coincide, but differ noticeably from those of migmatite-forming granites and metavolcanites. The last-mentioned fields are quite similar and overlapping. Those regularities are followed, although less clearly, in the diagram Fig. 4.

The factual material obtained in this way allows to suggest, that the supposed formation of migmatite plagio-microcline (or orthoclase) granites of the SSBS during metamorphism and ultrametamorphism of aluminiferous and other gneisses seems ungrounded. The most reasonably they correlate with the migmatites and pegmatites of post-folded Svecofennian plagio-microcline granites in the Baltic Shield, intrusion of which took place after the main stage of folding and metamorphism at the interval of 1.850 1.750 Ga at the time of Svecofennian tectono-magmatic activisation (Miner. mest..., 1982, Tugarinov et al, 1980). Certainly this does not exclude the occurrence of ultrametamorphic migmatites.

Petrochemical and geochemical analysis of "Archean" and Proterozoic metavolcanic and intrusive rocks of the SSBS has shown, that by those characteristics they are widely varying — from acid to basic composition — whereas metavolcanites form often differentiated series.

The wide range of variation of petrochemical and geochemical characteristics is also proper to metasedimentary rocks from these regions. Among those in various "Archean" complexes the rocks, similar to rock types, characteristic to the Fennoscandian Svecofennian area (not known from other areas of the Russian Plate) are common. These are: Mn-rich, often sulphide- bearing ferruginous quartzites, recorded from the Jõhvi and Tallinn zones, as also from Northwestern Latvia (Vetrennikov et al, 1986). Such specific rock types include also pre-Gothian P-rich metavolcanites and intrusions in West and South Estonia and beds of calcite-dolomite rocks in metavolcanic sections of the Paldiski–Pskov

zone (Petersell, 1976, Krist. fund., 1983). The latter have typical sedimentary marine isotopic composition of C ($\delta^{13}C$ varies from –0.6 to –1.9‰ pro).

To determine the real stratigraphic position of the observed rocks, of principal importance has the isotopic U-Pb age dating of zircon. Results of those datings are given in Table 1 and in Fig. 5. From this material it can be seen, that in the concordia plot the analytical points of U-Pb age dating by zircon from metavolcanites of amphibolite facies, as well as from granulite facies and from synorogenic granites approximate to a straight line. The isotope ages of rocks are very similar, ranging from 1.833 to 1.827 Ga, by 207Pb/206Pb ratio: from 1.833 to 1.812 Ga. The age of metavolcanites from the Tapa zone, particularly at the granulite facies of metamorphism, is somewhat higher, about 1.918 Ga (Fig. 5), but by 207Pb/206Pb ratio ranges from 1.889 to 1.884 Ga.

At the present time the data that could show the rocks "rejuvenation" during regional metamorphism are still lacking. Results of the studies (Höltta, 1988, Tugarinov, Bibikova, 1980) have not revealed considerable "rejuvenation" of rocks during metamorphism up to amphibolite facies conditions inclusive. Indisputably, the isotope ages show, that the metamorphism of rocks in West and South Estonia has Svecofennian age and there is no reason to attribute these rocks to the Archean.

The analytical points of U-Pb age dating of zircon from aluminiferous gneisses are quite dispersed and they did not approximate to a straight line in the concordia plot (Fig. 5). The age of zircon dated by 207Pb/206Pb ratio ranges from 2.175 to 1.841 Ga (Table 1). The age of aluminiferous gneisses from South Estonia (sample 5026220) is considerably lower than in the Tallinn zone. This may be caused by rejuvenation or partially by the occurrence of younger zircon connected with K-metasomatism of rocks. By zircon the U-Pb age of aluminiferous gneisses is close to that of greywacke from Tampere region (Wetherill et al, 1962) and of quartzite from southeastern Sweden (Aberg, 1978), being also Svecofennian. It is notable that the age of gneisses is older and changeable. The problem whether this was caused partly by an older source of removal or by uneven "rejuvenation" of rocks, remains unsolved.

Thus, the data presented allow most certainly to attribute the supracrustal complexes of West and South Estonia, but also of the Paldiski–Pskov, Tapa and Jõhvi zones to svecofennides and to correlate them with the corresponding rocks of the Baltic Shield.

U-Pb dating of the age of Svecofennian metavolcanites and synorogenic granitoids – gabbroids of the Baltic Shield has shown, that the age of these rocks decreases from the northeast to the southwest, from 2.100–1.950 Ga in Outokumpu–Oravaara region (Huhma, 1986; Wetherill et at, 1962) to 1.940–1.830 in West and South Estonia. Supporting the opinions of G. Gaal and R. Gorbatschev (Gaal, Gorbatschev, 1987) and A. F. Park et al. (Park et al, 1984) we consider that such age trends reflect the direction of the origin of the Svecoennian crust also on the SSBS. The estimated rate of the formation of the Svecofennian crust of the Baltic Shield was about 1 cm per year.

For establishing the geologic structure of the SSBS of great interest are also small intrusions of gabbroids and granitoids (Fig. 2).This group includes gabbro-norites of Sigula (b.h. F-124), gabbro diorites of Abja (b.h. 92), granodiorites of Taadikvere (b.h. 94), Virtsu (b.h. 360) and Märjamaa (b.h. 302), but also potassium granites from Naissaare, Jägala (Neeme) and Ereda stocks. These rocks form a specific association, characterized by the increased content of trace elements (Petersell, Kirs, 1992). Granites of the mentioned massifs, as well as Märjamaa granodiorites, are not subjected to metamorphism. Granites of the Neeme massif are intersected by aplitic, microsyenitic veins. Undoubtedly they belong to rapakivi-granite formation. Gabbro-norites of the Sigula massif are not metamorphised either, but till now assigned to svecofennides (Geol. map.., 1980; Krist. fund., 1983).

Gabbro-diorites of the Abja massif have sporadically weak gneissic texture. Granodiorites of the Taadikvere and Virtsu massifs are as a whole weakly gneissous. Besides, rocks of the first massif are intersected by thin veins of plagiomicrocline granites. They have been considered as Svecofennian or older (Geol. map..., 1980). The age dating by U-Pb method, however, show that granodiorites are of Svecofennian, gabbro diorites of Gothian age (Table 1, Fig. 5). In accordance with the age and geochemical data gabbro-diorite correlates with gabbroids of anorthosite — rapakivi formation of the Baltic Shield and also by geochemical data with gabbro-norite of Sigula massif (b.h. F-124) (Petersell, Kirs, 1992). The occurrence of veins of plagiomicrocline granites in gabbro-diorites of the Abja massif, in turn, gives evidence of post gabbro-diorite intrusion taking place in South Estonia. This may account for the Gothian age of some plagio-microcline granites established by K-Ar method (Krist. fund..., 1983).

Table 1. Pb and U isotopes in the zircons from the rocks of the crystalline basement of the SSBS

No	Fraction mcm	Concentration, ppm		Measured			Atomic ratio		Age, Ma	Zones	Descripton of samples
		U	Pb	206 Pb / 204 Pb	207 Pb / 206 Pb	208 Pb / 206 Pb	206 Pb / 238 Pb	207 Pb / 235U	207 Pb / 206 Pb		
1	2	3	4	5	6	7	8	9	10	11	12
	Borehole 590 (Muhu), sample 5904420, interval 442–452 m										
1	120–250	304.4	94.70	3820	0.1145	0.1280	0.2889	4.431	1820	West Estonia	Finegrained amphibolebiotite gneiss (metavolcanite). Amphibolite facies of metamorphism
2	140–250	316.4	102	3180	0.1154	0.1253	0.3038	4.677	1826		
3	200–250	279.3	101.1	1175	0.1224	0.1668	0.3227	4.973	1828		
4	80–200	295.0	93.34	10340	0.1124	0.1276	0.2956	4.544	1824		
5	150–200	316.7	97.89	3385	0.1152	0.1482	0.2824	4.362	1832		
							Concordant age		1827 ± 7		
	Borehole 066 (Vaki), sample 0664680, interval 468–489 m										
6	100–200 (4)	1051	319	21250	0.11233	0.06157	0.3006	4.639	1830	South Estonia	Finegrained quartz-feldspar gneiss (metavolcanite). Amphibolite facies of metamorphism
7	100–200 (5)	744	217	17225	0.11139	0.06515	0.2883	4.431	1824		
	sample 0664800, interval 480–489 m										
8	100–200 (5)	982	297	44780	0.11204	0.05772	0.3002	4.629	1829		
9	60–80 (z)	518	149	9780	0.11323	0.06740	0.2828	4.370	1833		
							Concordant age		1828 ± 8		
	Borehole 172 (Häädemeeste), sample 1726990, interval 699–702 m										
10	70–150 (3)	658	208	10490	0.11225	0.20056	0.27934	4.2795	1817	South Estonia	Finegrained quartz-feldspathic gneiss (metavolcanite). Granulite facies of metamorphism
11	70–100 (z)	1553	462	6679	0.11206	0.15039	0.27366	4.1566	1802		
12	70–100 (6)	2802	266	3769	0.10215	0.24816	0.08157	1.1092	1598		
13	50– 70	483	354	6273	0.11361	0.22212	0.25369	3.9028	1825		
14	50– 70	412	143	7889	0.11342	0.20737	0.30452	4.6954	1829		
							Concordant age		1832 ± 22		

1	2	3	4	5	6	7	8	9	10	11	12
	Borehole F-164, sample 1643580, interval 358–396 m										
15	80–200 (1)	404	118	4255	0.11553	0.07585	0.2846	4.422	1844	Tapa zone	Finegrained quartz-feldspathic and amphibole-biotite gneiss, in places with rare pyroxenes (metavolcanite). Granulite facies of metamorphism
16	80–100 (z)	479	133	1575	0.12078	0.0945	0.2648	4.116	1844		
17	80–200 (2)	415	121	8330	0.11468	0.06525	0.2886	4.515	1856		
18	50–80 (3)	571	176	1380	0.12373	0.09687	0.3011	4.798	1889		
							Concordant age		1918 ± 10		
	Borehole F-139, sample 1394050, interval 405–408 m										
19		728	211	7310	0.11437	0.11454	0.2744	4.272	1847	Tallinna zone	Rich of quartz aluminiferous gneiss (metasedimentary rock). Amphibolite facies of metamorphism
	Borehole F-113, sample 1134090, interval 409–413 m										
20	80–100	752	700	4983	0.39572	0.82576	0.3338	6.086	2128		
21	60–100 (4)	652	233	1590	0.14039	0.11945	0.3292	5.999	2127		
22	60–100 (5)	460	169	2200	0.14121	0.11921	0.3402	6.370	2175		
	Borehole F-110A, sample 110A3400, interval 340–344 m										
23	80–100 (5)	706	209	7730	0.12581	0.08002	0.2857	4.894	1847		
24	60–100 (4)	510	152	3950	0.12174	0.06283	0.2960	4.866	2018		
25	60–100 (4)	964	284	5890	0.11966	0.03078	0.2993	4.867	1944		
	Borehole 502 (Varbla), sample 5026220, interval 622–628 m										
26	50–100	631	187	2705	0.11789	0.07976	0.2884	4.510	1855	South Estonia	Aluminiferous gneiss (metasedimentary rock), in places weakly subjected to migmatization. Granulite facies of metamorphism
27	50–100	529	161	6980	0.11506	0.06496	0.3035	4.736	1856		
				sample 5026030, interval 603–615 m							
28	50–100 (3,4)	351	103	3570	0.11827	0.03786	0.3115	5.080	1930		
29	50–100 (5)	550	166	4650	0.11446	0.04035	0.3082	4.781	1841		
30	50–100 (5)	582	178	1115	0.12335	0.10514	0.3019	4.4761	1870		
	Borehole 92 (Abja), sample 926064, interval 606–610 m										
31	80–200	267.7	74.07	4015	0.1029	0.2081	0.2433	3.351	1624	South Estonia	Mediumgrained gabbro-diorite, weakly gneissic
32	200–250	250.6	69.82	6140	0.1019	0.2244	0.2431	3.360	1628		
				sample 92611, interval 611–617 m							
33	80–200	237.9	70.39	3855	0.1032	0.2693	0.2484	3.439	1632		
34	200–250	194.5	63.85	1175	0.1114	0.3291	0.2594	3.589	1630		

Table 1 (continued)

1	2	3	4	5	6	7	8	9	10	11	12
35	80–200	216.3	83.22	241.7	0.1569	0.4296	0.2620	3.622	1629		
							Concordant age		1635 ± 7		
	Borehole 94 (Taadikvere), sample 944040, interval 404–424 m										
36	200–250	426	119	9780	0.11256	0.14987	0.2586	3.975	1824	South Estonia	Potassic porphyraceous granodiorite, weakly gneissic
37	80–200	364	109	5725	0.11331	0.14937	0.2775	4.262	1822		
38	80–200	438	127	2030	0.11750	0.16408	0.2610	3.999	1818		
			sample 944540, interval 454–464 m								
39	200–250	372	114	7530	0.11273	0.14227	0.2852	4.381	1823		
40	80–200	390	106	3090	0.11477	0.14920	0.2509	3.831	1812		

Remarks:

Characterization of zircons: 1 – long-prismatic, 2 – short-prismatic, 3 – prismatic corroded, 4 – prismatic, 5 – rounded, 6 – opaque, Z – yellowish, AO – abrasive treatment

Borehole 590 (Muhu), sample 5904420

Zircons subtransparent, prismatic and rounded. Size of grains 0.05–0.2 mm, rarely more, elongation 1.5–2.1. Zoning of crys tals is not observed.

Borehole 066 Vaki), samples 0664680 and 0664800

Zircons subtransparent,often yellowish prismatic and rounded, frequently fractured, but not transformed. Size of grains 0.05–0.2 mm, elongation 1.5. Zoning of crystals is not observed.

Borehole 172 (Häädemeeste), sample 1726990

Zircons from transparent to opaque, yellowish, greenish, prismatic, often rounded (corroded). Size of grains 0.05–0.1 mm, rarely more, elongation 1.5. Zoning of crystals is not observed.

Borehole F-164, sample 1643580

Zircons subtransparent, prismatic, often corroded and rounded. The grains with turbid zoning of crystals are represented, also with nodules of apatite, quartz and ore minerals. Size of grains 0.05–0.25 mm, elongation 2–3.

Borehole F-139, sample 1394050

Zircons subtransparent, prismatic, rounded and corroded. Size of grains 0.1mm. Elongation 2–2.5

Borehole F-113, sample 1134090

Zircons from subtransparent to opaque, prismatic, rounded and corroded, rolled and fine. Size of grains 0.05–0.1 mm. The grains are often fractured, rarely weakly zoning, elongation 2.

Borehole F-110A, sample 110A3400

Zircons subtransparent, often yellowish, prismatic, corroded and rounded. Size of grains 0.05–0.1 mm. In the biggest grains turbid zoning is observed, often also nodules. Elongation 2–2.5.

Borehole 502 (Varbla), samples 5026220 and 5026030

Zircons from subtransparent to opaque, prismatic and rounded, corroded with marks of roundness. Size of grains 0.05–0.07mm, rarely up to 0.1 mm, fractured, elongation 1.5. Some grains have the turbid dark nucleus.

Borehole 92, samples 926060 and 926110

Zircons transparent, light rose-coloured (brownish), pris matics, idiomorphic. Rare grains are weakly zoned. Size of grains 0.05–0.3 mm, elongation 1.5. Rare fine nodules in zircons are observed

Borehole 94 (Taadikvere), samples 944040 and 944540

Zircons greyish transparent and subtransparent, prismatic, often with uneven indented crystal edges and fractured, but not transformed. Size of grains mostly 0.1–0.3 mm, elongation 1.5–3. In the centre of crystals the nodules of ore minerals are observed.

Fig. 5. Concordia diagrams of U-Pb isotopic zircon data of rocks from the Estonia crystalline basement

a–d – metavolcanite: West Estonia, b.h. 590 (a); South Estonia, b.h. (066 (b), b.h. 172 (c); Tapa zone, b.h. F-164 (d); e–f – aluminifwerous gneisses: Tallinn zone, b.h-s F-110A, F-113, F-139 (e); South Estonia, b.h. 502 (f); g–h – intrusive rocks: gabbro and diorite Abja, b.h. 92 (g), granodiorite Taadikvere, b.h. 94 (h); 1–40 – numbers of dating in table 1

a

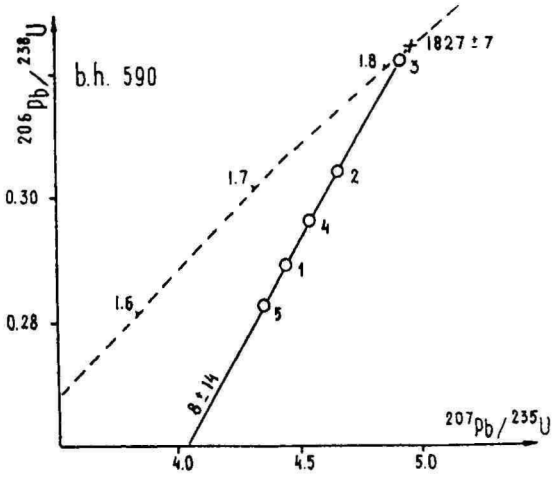

b

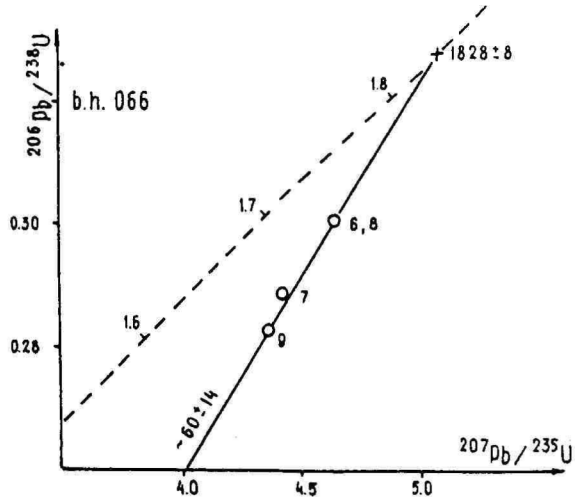

c

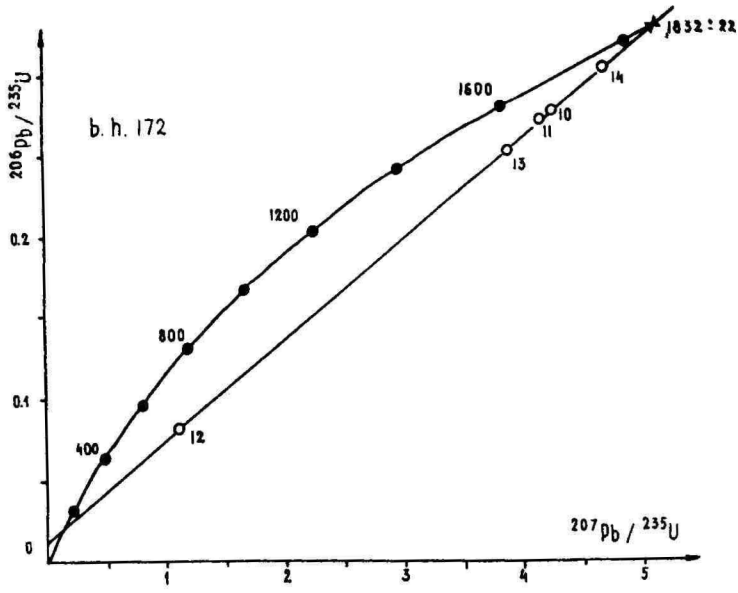
b. h. 172
$^{206}Pb/^{235}U$
$^{207}Pb/^{235}U$
1832 ± 22
1600
1200
800
400
0.2
0.1
0
1
2
3
4
5
10
11
12
13
14

d

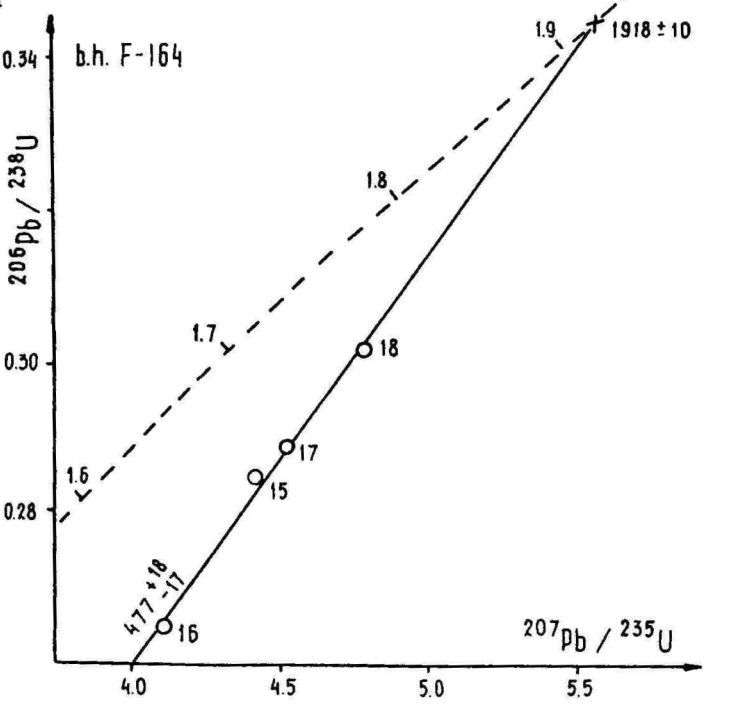
b.h. F-164
$^{206}Pb/^{238}U$
$^{207}Pb/^{235}U$
1918 ± 10
1.9
1.8
1.7
1.6
0.34
0.30
0.28
4.0
4.5
5.0
5.5
15
16
17
18
477 +18 -17

9

e

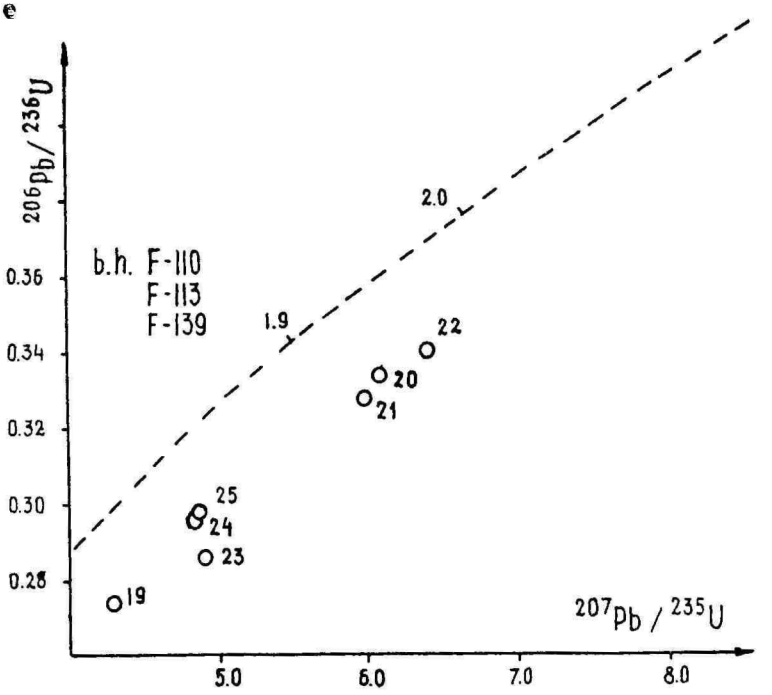
$^{206}Pb/^{236}U$
b.h. F-110
F-113
F-139
2.0
1.9
22
20
21
25
24
23
19
0.36
0.34
0.32
0.30
0.28
$^{207}Pb/^{235}U$
5.0
6.0
7.0
8.0

f

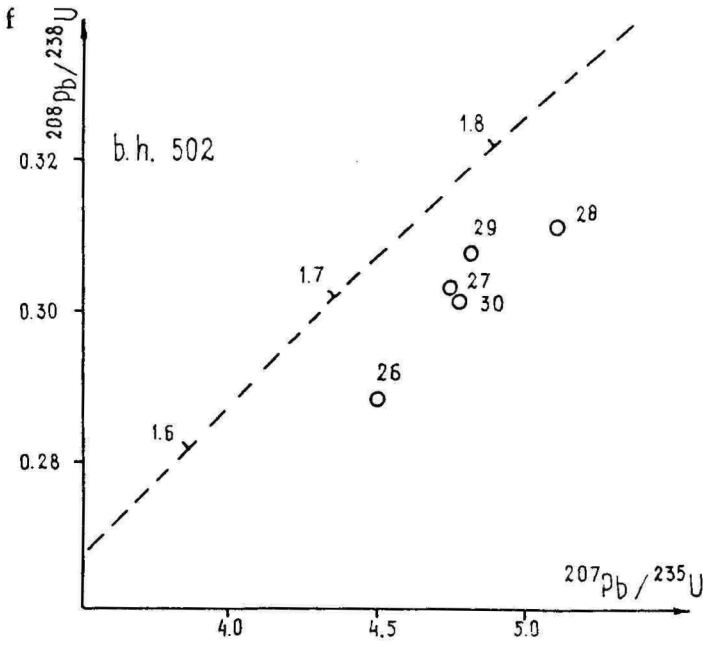
$^{208}Pb/^{238}U$
b.h. 502
1.8
1.7
1.6
29
28
27
30
26
0.32
0.30
0.28
$^{207}Pb/^{235}U$
4.0
4.5
5.0

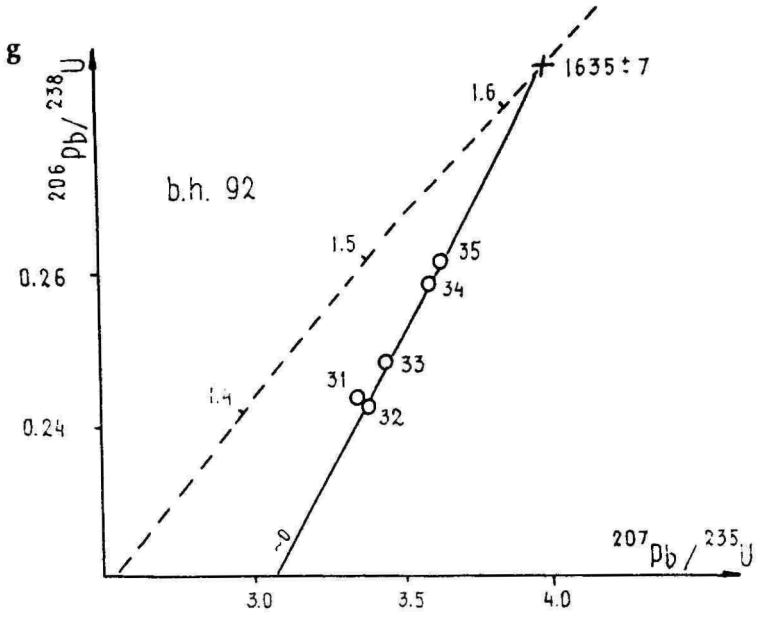
g
b.h. 92
$^{206}Pb/^{238}U$
0.26
0.24
1.6
1635 ± 7
1.5
35
34
33
31
32
1.4
~0
$^{207}Pb/^{235}U$
3.0
3.5
4.0

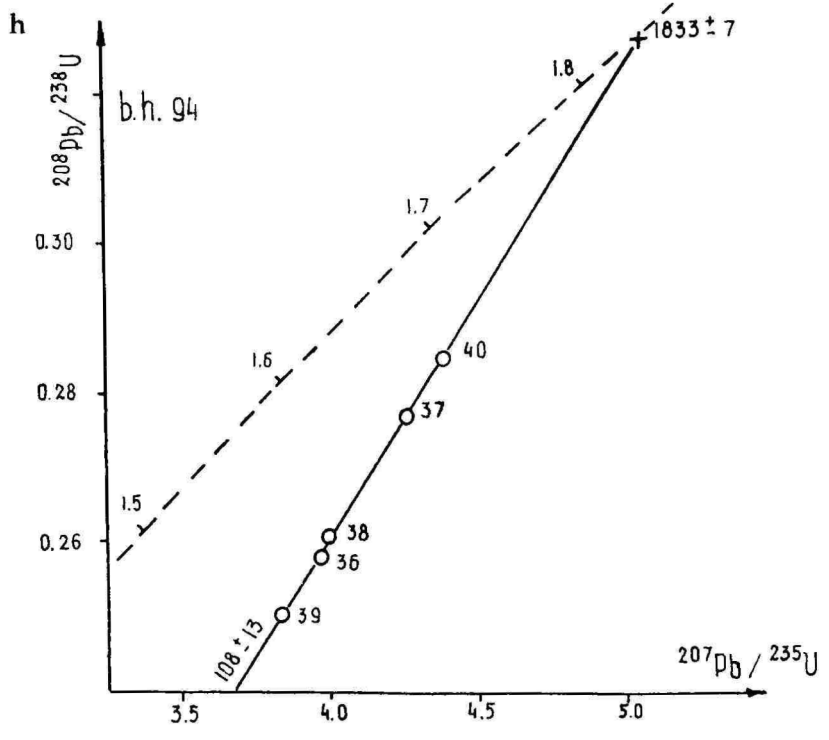
h
b.h. 94
$^{208}Pb/^{238}U$
0.30
0.28
0.26
1.8
1833 ± 7
1.7
1.6
40
37
1.5
38
36
39
108 ± 13
$^{207}Pb/^{235}U$
3.5
4.0
4.5
5.0

Acknowledgements

The authors thank the geologists- researchers of the crystalline basement of Estonia, Dr-s V. Klein and J. Kivisilla, geologists H. Koppelmaa, M. Niin, K. Suuroja, E. Kala, and also the lecturer of the Tartu University J. Kirs for kindly providing unpublished data on geology and useful discussions about the structure of the crystalline basement of Estonia.

We greatly acknowledge the help of Dr. F. I. Zukov from the Ukr. Acad. Sci., who initiated and guided isotopic Pb datings. The authors are also indebted to Prof. A. Loog from Tartu University, thanks to whom the publication of this paper was possible.

References

Aberg G., 1978. Precambrian geochronology of southeastern Sweden. Geol. fören. förhandl. 100, p. 1–37.

Dedejev, 1974 – Дедеев В. А., 1974. Раннедокембрийские складчатые структуры и массивы фундамента Русской плиты. Вкн: Структура фундамента платформенных областей СССР. Л: Наука.

Gaal G., Gorbatschev R., 1987. An outline of the Baltic Shield. In: Precambrian Geology and Evolution of the Central Baltic Shield, Gaal, G. and Gorbatscev, R. (eds.). Precambrian Res. 35, 15–52.

Gafarov, 1962 – Гафаров Р. А., 1962. Строение складчатого фундамента Восточно-Европейской платформы по геофизическим данным. Изв. АН СССР. Сер. геол. 8 с. 56–67.

Geological map of the Crystalline basement of the Soviet Baltic Republics. Scale 1 : 500000. 1980. Leningrad. NEDRA.

Fotiadi, 1958 – Фотиади Э.Э., 1958. Геологическое строение Русской платформы по данным региональных геофизических исследований опорного бурения. М.: Госгеолтех издат. 244 с.

Huhma H. 1986. Sm-Nd, U-Pb and Pb-Pb isotopic evidence for the origin of the Early Proterozoic Svecokarelian crust in Finland. Geol. Surv. of Finland. Bull. 337. 52 p.

Hölttä P. 1988. Metamorphic zones and the evolution of granulite grade metamorphism in the early Proterozoic Pihlavesi area, central Finland. Geol. Surv. of Finland. Bull. 344. 50 p.

Koppelmaa et al., 1978 – Коппелмаа Х, Клейн В. М., Пуура В. А., 1978. Метаморфические комплексы кристаллического фундамента Эстонии. – В кн: Метаморфические комплексы фундамента Русской плиты. Л. Наука с. 43–76.

Krogh T. E. 1973. A low-contamination method for hydrothermal decomposition of zircon and extraction of U and Pb for isotopic age determinations. Geochim. Cosmochim. Acta 37. N.3. p. 485–494.

Krist. fund. ..., 1983 – Кристаллический фундамент Эстонии. 1983. М.: Недра. 208 с.

Ludwig K. R. 1980. Calculation of uncertainties of U-Pb isotope data. Earth Planet. Sci. Lett. 46. p. 212–220.

Luha A. 1946. Eesti NSV maavarad. R.K. Teaduslik-tehniline kirjandus. Tallinn. 178 lk.

Miner. mest ..., 1982 – Минеральные месторождения Европа. Северо-Западная Европы. 7, М. Мир. 583 с.

Niin, 1976 – **Ниин М. И.** 1976. К стратиграфии хогландской серии среднего протерозоя Северной Прибалтики. В кн: Материалы по стратиграфии Прибалтики. Вильнюс: ЛитНИГРИ. с. 15–17.

Park A. F., **Bowes** D. R., **Halden** N. M., **Koistinen** T. J. 1984. Tectonic evolution at an Early Proterozoic continental margin: The Sveco-karelides of eastern Finland. J. Geodynamics 1. p. 359–386.

Petersell, 1974 – **Петерселль В. Х.,** 1974. О сульфидной минерализации в кристаллических породах ягалаской толщи Изв. АН ЭССР. Геология. 2, с. 142–148.

Petersell, 1976 – **Петерселль В. Х.,** 1976. Основные черты геологии и рудоносности кристаллического фундамента южного склона Балтийского щита. Автореф. дисс. – канд. геол-мин. наук АН ЭССР. Таллинн ИГ АН ЭССР, 28 с.

Petersell, V., **Kirs,** J., 1992. Geochemical Character of Estonian Subplatform Granitoids and Gabbroids. Tartu Ülikooli Toimetised. 956. Töid geoloogia alalt XIII, p. 27–43.

Pobul, 1962 – **Побул Э. А.,** 1962. О строении кристаллического фундамента Эстонии по данным геофизики Тр. Ин-та геологии АН ЭССР, т. 10. Геология палеозоя. Таллинн, с. 309–318.

Puura, 1974 – **Пуура В. А.,** Структура Южного склона Балтийского щита. Автореф. дисс. канд. геол-мин. наук. Таллинн, ИГ АН ЭССР, 28 с.

Puura et at., 1976 – **Пуура В. А., Куусмаду Т. И., Биркис А. П.,** 1976. Главные черты геологического строения докембрийского фундамента Прибалтики. В кн: Геология, петрология и металлогения кристаллических образований Восточно-Европейской платформы. Т.III.М. Недра. с. 27–40.

Stacey J. S., **Kramers** J. D., 1975. Approximation of terrestrial lead isotope evolution by a two-stage model. Earth Planet. Sci. Lett. 26. p. 207–221.

Tectonic map of the Soviet Baltic Republics. Scale 1 : 500000. 1980. Leningrad. NEDRA.

Tihomirov, 1966 – **Тихомиров С. Н., 1966.** Геологическое строение докембрийского фундамента в пределах Ленинградской области и Прибалтики. Автореф. дисс. ... канд. геол.-мин. наук Л: ВСЕГЕИ, 24 с.

Tugarinov, Bibikova, 1980 – **Тугаринов А. И., Бибикова Е. В., 1980.** Геохронология Балтийского щита по данным цирконометрии. М: Наука, 132 с.

Vaher et al., 1962 – **Вахер Р. М., Пуура В. А., Эрисалу Э. К., 1962.** Тектоническое строение Северо-Восточной Эстонии. – Тр. Ин-та геологии АН ЭССР, т. 10, с. 319–335.

Vardanjants, 1960 – **Варданянц Л. А. 1960.** Геологическая карта докембрийского кристаллического фундамента Русской платформы м-ба 1 : 500000. Объяснительная записка. М: Госгеолтехиздат. 48 с.

Vetrennikov et al., 1966 – **Ветренников В. В., Петерселль В. Х., Пыллузере А. А., 1986.** Марганценосная железорудная формация докембрия и происхождение горных пород кристаллического фундамента Белоруссии и Прибалтики. Минск. с. 86–97.

Öpik A. 1935. Eine mögliche geologische Deutung der magnetischen Anomalien Estlands. – In: C.r. Comiss. Geodes. Baltiq. reunie a Tallinn et Tartu 20–30 about 1935. p.287–288.

Zander et al., 1967 – **Зандер В. Н., Томащунас Ю. И., Берковский А. Н., 1967.** Геологическое строение фундамента Русской плиты. Л: Недра, 122 с.

Zukov, Lesnoi, 1982 – **Жуков Ф. И., Лесной Д. А., 1982.** Изотопы серы и углерода в стратиформных месторождениях складчатых областей. Киев. „Наукова Думка". 160 с.

Wetherill G. W., Kouvo O., Tilton G. R., Gast P. W. 1962. Age measurements on rocks from the Finnish Precambrian. – J. Geol. 70. N 1. p. 74–88.

BALTI KILBI LÕUNANÕLVA KRISTALSE ALUSKORRA GEOLOOGILISEST EHITUSEST

Valter Petersell, Oleg Levchenkov

Resümee

Balti kilbi lõunanõlva piiridesse arvatakse Eesti territoorium, Leningradi oblasti lääne- ja Pihkva oblasti loodeosa ning Põhja-Läti. Nõlva kristalses aluskorras levivad valdavalt metavulkaniidid ja metasedimendid. Intrusiivsete kivimite levik on tunduvalt tagasihoidlikum.

Gneisilised kivimid on enamasti metamorfiseeritud regionaalse metamorfismi amfiboliitse ja granuliitse faatsieste tingimustes, ning

on sageli mõjustatud K-metasomatoosist, migmatiseeritud ja ganuliitse faatsiese levilas ka tšarnokiidistunud.

Viimastel aastakümnetel on osa Eesti ja Läti geolooge käsitlenud migmatisatsiooni ja tšarnokiidistumist kivimite osalise sulamise tulemusena *in situ* tingimustes mitte ainult kivimite kõrge metamorfismiastme tõendina, vaid ka nende arhailise vanuse peamise kriteeriumina. Nii korreleeritakse Balti kilbi lõunanõlval suurtel aladel varem svekofenniidide struktuurivööndisse loetud varaproterozolisi kivimeid Koola poolsaare ja Vene lava arhailise vanusega kivimitega.

Metasedimentide, metavulkaniitide ja migmatiite moodustavate K-rikaste graniitide Pb isotoopkoosluse eripära ja sarnasus (jn. 3 ja 4) lubavad migmatiite moodustavaid K-rikkaid graniite rööbistada Balti kilbil paljanduvatele svekofenniididele omaste kurrutusjärgsete K-rikaste, samuti migmatiitemoodustavate graniitidega.

Tsirkoonide järgi määratud metavulkaniitide ja granitoidide U-Pb isotoopvanused nii amfiboliitse kui granuliitse metamorfismi vööndite arhaikumi kivimitest näitavad, et tegemist on tüüpiliste varaproterozoiliste svekofenniidide kurrutusvööndi kivimitega. Nende samaaegsust svekofenniididega rõhutavad ka ainult viimastele Ida-Euroopa platvormil iseloomulike Mn-rikaste rauakvartsiitide jt. kivimitüüpide esinemine ning metasedimentide teistest veidi kõrgem isotoopvanus sõltumata metamorfismi faatsiesest (jn. 5, tabel 1).

U-Pb isotoopvanuse määrangud kinnitavad ka Balti kilbi lõunanõlva P-rikaste subleeliseliste gabroidide anortosiit-rabakiviformatsiooni kivimitega üheaegset teket.

Seega jätkuvad Balti kilbi lõunanõlval vähemalt valdavas enamuses kilbil paljanduvate svekofenniidide analoogid. Esitatud kivimite U-Pb isotoopvanuse määrangud tunnistavad svekofenniidideaegse kontinentaalse koore kasvu lõuna- ja edelasuunas.

KVARTS RAKVERE ÜMBRUSE FOSFORIIDIKIHINDIS

Tiia Kurvits

Sissejuhatus

Alamordoviitsiumi Pakerordi lademe liivakivi (oobolusliivakivi) paljandub Põhja-Eesti klindil arvukates kohtades ja tema aineline koostis on seetõttu hästi uuritud (Loog, 1968; Heinsalu, Viiding, 1978; Mens jt., 1989; Heinsalu jt., 1991). 1980. aastatel lisandus võimalus uurida neid kihte ka klindist lõunapool. Rakvere fosforiidiuuringute käigus rajatud puuraukude rohkus andis võimaluse valida hea väljatulekuga puursüdamikud, mis on nõrgalt tsementeerunud liivakivide uurimisel oluline.

Pakerordi lademe Kallavere kihistu mineraalset koostist analüüsiti kolmes Kabala piirkonnast võetud puursüdamikus (P-2003, P-2087, P-2162), vt. jn. 1. Ilmnes, et tavalisest suurema paksusega ja jämedama lõimisega kivimiga, mis kuulub Kallavere kihistu Rannu kihistikku (Heinsalu jt., 1993), kaasneb tüüpilisest erinev mineraalne koostis. Kõige selgemini väljendavad seda kvartsiterade tüpomorfsed tunnused, mis ongi järgneva käsitluse teemaks.

Uurimistulemused

Kallavere kihistu liivakividele omaselt moodustab uuritud läbilõigetes >90% allotigeensetest mineraalidest kvarts. Eripäraks on see, et kvartsiterad jagunevad selgelt kahte rühma:

1) ümardamata õhukesekilluline ehk plaatjas, sageli kumera karpja pinnaga, suletisteta või suletistevaene, normaalse kustumisega kvarts (tahvel I, 1–6); 2) hästi või keskmiselt ümardatud, enamasti suletisterohke, normaalse ja lainelise kustumisega kvarts (tahvel I, 8).

Kvartsi ümardamata terade sisaldus jämedates fraktsioonides on <5% tõustes hüppeliselt fraktsioonis 0,25–0,1 mm ja suurenedes fraktsioonis 0,1–0,05 mm veelgi. Andmed viimases fraktsioonis esineva killulise kvartsi jaotumise kohta (uuritud immer-

sioonimeetodiga ja kasutades 200–600 x suurendust) on toodud joonisel 2. Nähtub, et kirjeldatud kvarts levib kogu Rannu kihistikus ja tema sisaldus ulatub 50%-ni kogu kvartsi hulgast. Vähemalt kolmandik killulisest kvartsist on suletisteta. Killuline kvarts on koondunud ülemisse jämedateralisemasse ossa, kuid selget korrelatsiooni lõimise ja ümardamata terade leviku vahel pole. Lamavates Tsitre kihistu ja Maardu kihistiku setendites teda ei leidu. Klindipaljandites eelnimetatud kahe rühma eristamine raskeneb, sest kvartsiterade ümardatus ühtlustub. Käsitletud alale lähimad paljandid, mida uuriti, olid Saka idas ja Vihula läänes. Sakas võib ümardamata kvartsi leida Rannu kihistikus kuni 5%, Vihulas Suurjõe kihistikus kuni 20%. Läänepoolsemates paljandites pole esimesse rühma kuuluvat kvartsi võimalik eristada. Seega on ta lokaalse levikuga. Stratigraafiline levik Kabala väljal on piiratud konodontide tsoonidega *Cordylodus proavus* –*C. lindströmi* (Heinsalu, Raudsep, 1993).

Teise rühma kuuluvad kvartsiterad on klindil Kallavere liivakividele iseloomulikud ja nende ümardatus ehk kulutatus sõltub settimiskeskkonna hüdrodünaamilistest omadustest ning ümbersettimise määrast. On loomulik, et nõrga hüdrodünaamilise toime puhul kuhjub peeneteralistesse vähesorteeritud setetesse keskmiselt ja halvasti ümardatud kvarts. Peene- ja keskmiseteralisi hästi sorteeritud liivu, mis on kujunenud liikuvaveelises keskkonnas, iseloomustab hästi ümardatud kvarts (Loog, 1968; Mens jt., 1989). Brahhiopoodkonglomeraadis, mis sisaldab jämedaimat terrigeenset materjali, on kvartsiterad rohkem ümardunud kui mujal (Loog, 1968).

Kvarts alamordoviitsiumi, kambriumi ja vendi setendites ning kristalses aluskorras

Kvartsi tüpomorfseid tunnuseid Kallavere liivakivides ning lamavas settekivimite kompleksis on käsitlenud mitu uurijat. Rakverest läände jäävates paljandites alamkambriumi Tiskre kihistu ja kambriumi-ordoviitsiumi piirikihtide setendite fraktsioonis 0,1–0,25 mm ümardamata teri ei ole ja suletisteta kvarts praktiliselt puudub (Heinsalu, Viiding, 1978). Ümardamata kvartsiteri märgitakse Toolse fosforiidikihi fraktsioonis <0,1 mm (Raudsep, 1975). Leningradi oblasti ümbruse paljandite põhjal on analoogi-

lisi uuringuid fraktsioonis 0,25–0,5 mm tehtud kambriumi lademe Lükati, Sablinka, Laadoga kihistutes ning alamordoviitsiumi Tosno, Türisalu ja Leetse kihistutes (Kuljamin, Hazanovitch, 1971). Uurijad on arvanud ühte rühma suletisteta ning poolläbipaistva väikeste punktsuletistega kvartsi, pidades nendevahelist piiri üleminekuliseks. See rühm on kõige valdavam ning tema levik on muutusteta nii vertikaalis kui horisontaalis. Läbipaistva kvartsi hulk ümardatuse suunas suureneb, mis on tingitud tema suuremast vastupidavusest võrreldes suletisterikka ja lõhelise kvartsiga.

Liikudes läbilõikes allapoole on Eesti piires saadud kvartsi uurimisel järgmisi tulemusi: alamkambriumi Lontova kihistus on fraktsioonis 0,1–0,05 mm suletisteta normaalse kustumisega kvartsi 7%, millest on ümardamata <1%, ümardamata teri kokku on 8% (Viiding, Konsa, 1976); vendis ei ulatu suletisteta ümardamata kvartsi hulk alumistes kihtides üle 6%, mis ülespoole veelgi kahaneb, ümardamata terade sisaldus kokku on 10–80%, suurenedes kristalse aluskorra suunas (Viiding, Konsa, 1976).

Kristalse aluskorra kivimites märgitakse suletisteta normaalse kustumisega kvartsi biotiitgneissides ja Al-gneissides (13–18%), granitoidides (9%), teistes vähem (Konsa, 1989).

Kabalale lähedase Uljaste piirkonna kristalseid ning nendel lasuvaid vendi settekivimeid käsitlevas uurimuses (Konsa, 1993) märgitakse, et kristalsetes kivimites ja murenemiskoorikus varieerub suletisteta kvartsi sisaldus suures ulatuses. Settekivimite kompleksis omandab kvarts ümardatud piirjooned, v.a. kerke võlvi läheduses, mis viitab lokaalse murendmaterjali allikale.

Kvartsi päritolu

Esiteks. Eelnevast nähtub, et Eestis uuritud kivimiga samavanuselistes ja vanemates settekivimites ei kirjeldata killulist suletisteta kvartsi hulgal, mis võimaldaks tema pärinemist lamami kulutusel ümbersettinud materjalist, seda enam, et ümbersettimisel kvarts kulutub ning nurgelised terad säilivad vaid eluviaalsetes-deluviaalsetes setetes (Konsa, 1989). Sankt-Peterburgi ümbruses on uuritud kahjuks ainult võrdlust raskendavat liiga jämedat fraktsiooni, kuid ka selles ei ole eraldi nimetatud ümardamata suletisteta kvartsi esinemist (Kuljamin, Hazanovitch, 1971).

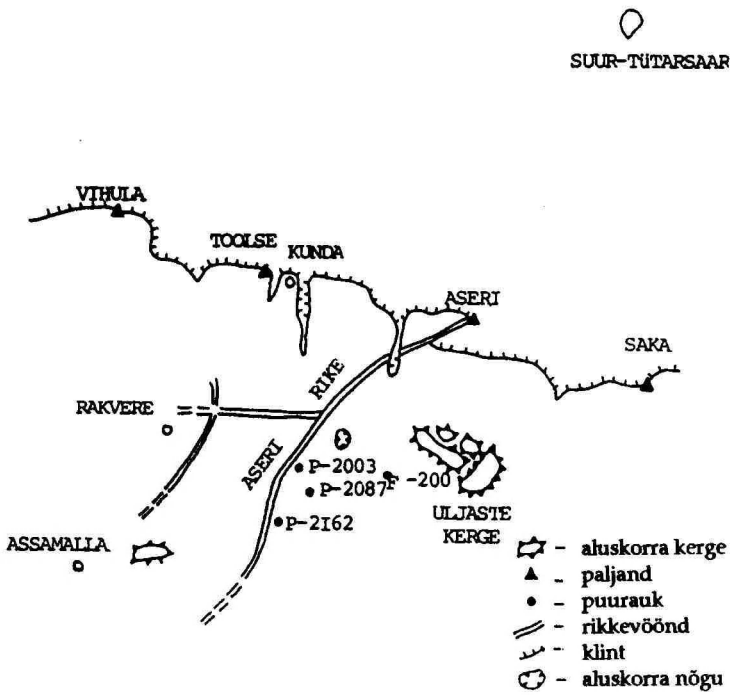

Jn. 1. Paljandite, puuraukude ja aluskorra tektooniliste struktuuride skeem Rakvere ümbruses.

Fig. 1. Scetch-map of the outcrops, boreholes and tectonic structures locations in Rakvere area.

Teiseks. Võib oletada ümardatud jämedate lõheliste kvartsiterade purunemist aktiivse lainetuse piirkonnas. Selliseid teri kahtlemata on, kuid kirjeldatud killulisel kvartsil fraktsioonis 0,25–0,1 mm lõhed puuduvad, mis ei anna võimalust nende edasiseks peenenemiseks. Selle vastu on ka asjaolu, et suletisteta ja suletistevaene kvarts on struktuurilt vastupidavam ning eelkõige puruneb suletisterohke või mõnel teisel moel struktuurselt rikutud kvarts (Kuljamin, Hazanovitch, 1971; Simanovitch, 1976).

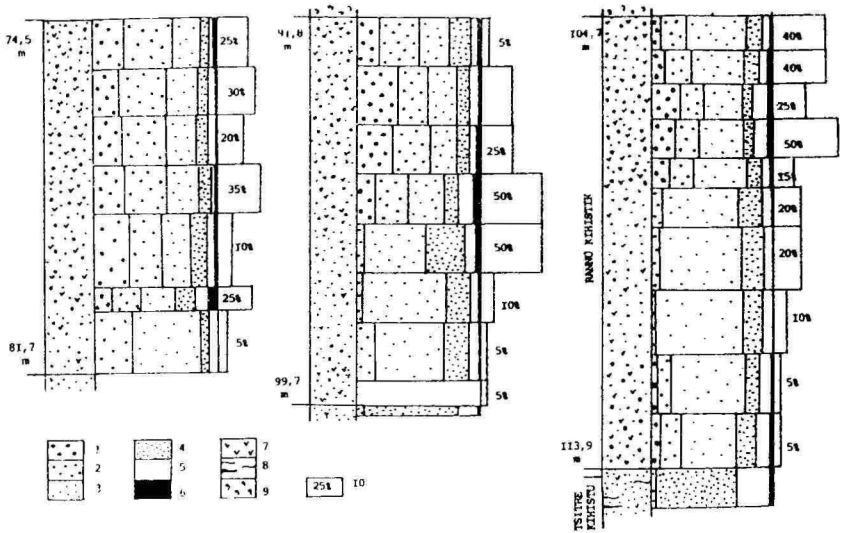

Jn. 2. Lõimis ning killulise kvartsi jaotumine (fr. 0.1–0.05 mm) Kallavere kihistus Kabala piirkonnas.
Legend: 1 – fr. >1.0 mm, 2 – fr. 1.00–0.5 mm, 3 – fr. 0.5–0.25 mm, 4 – fr. 0.25–0.1 mm, 5 – fr. 0.1–0.01 mm, 6 – fr. < 0.01 mm, 7 – brahiopoodide detriit, 8 –savikihid, 9 – glaukoniitliivakivi, 10 – killulise kvartsi sisaldus kogu kvartsi hulgas fraktsioonis 0.1–0.05 mm.

Fig. 2. Grain-size distribution of analysed sandstone and content (in %, relative to all quartz grains) of angular quartz (fraction 0.1–0.05 mm) in Kallavere Formation, Kabala district.
Legend: 1 – fr. > 1.0 mm, 2 – fr. 1.00–0.5 mm, 2 – fr. 0.5–0.25 mm, 4 – fr. 0.25–0.1 mm, 5 – 0.1–0.01 mm, 6 – < 0.01 mm, 7 – sceletal debris of brachiopods, 8 – clay beds, 9 – glauconite sandstone, 10 – content of angular quartz in fr. 0.1–0.05 mm.

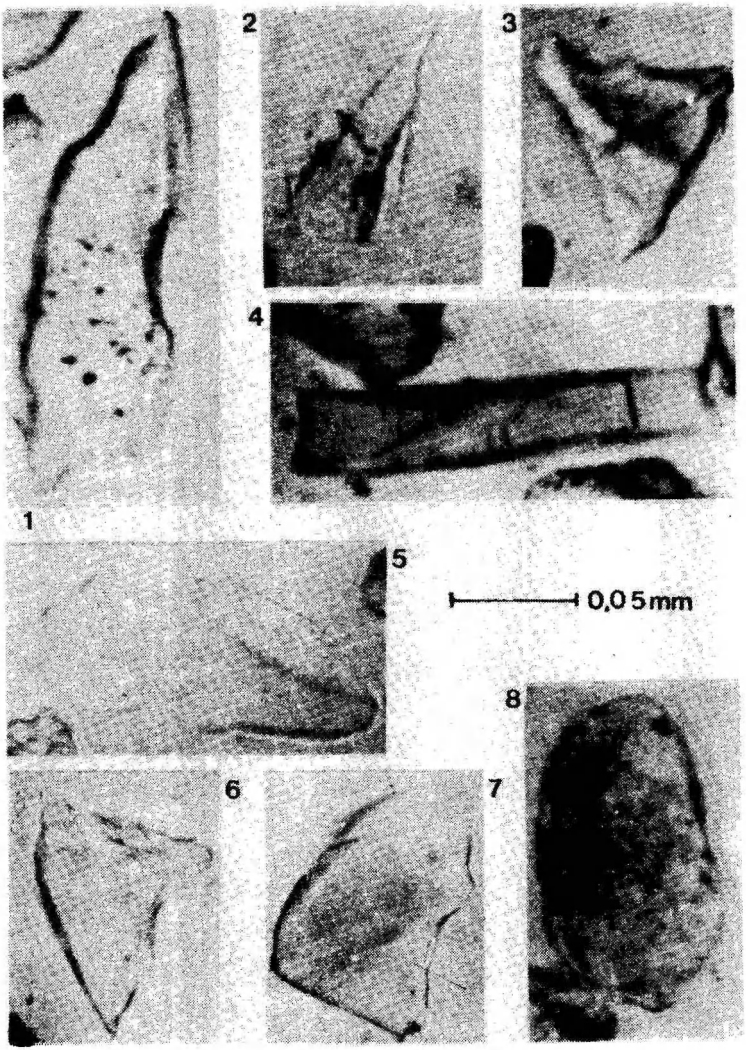

Tahvel 1. 1–3 – väheste suletistega ümardamata kvarts Rannu kihistikus; 4–6 – suletisteta ümardamata kvarts samas; 7 – kvarts Keskordoviitsiumi K-bentoniidist; 8 – ümardatud suletistega kvarts Rannu kihistikus.

Plate 1. 1–3 – angular quartz with a few inclusions in the Rannu Mb.; 4–6 – angular quartz without inclusions in the Rannu Mb.; 7 – quartz from K-bentonite (Middle Ordovican); 8 – rounded quartz with inclusions in the Rannu Mb.

Kolmandaks. Suletisteta õhukesekilluline ja sageli kumerate piirjoontega või kiilulaadne normaalse kustumisega tähelepanualune kvarts on tüüpiline K-bentoniitidele (Hagemann, Spjeldnaes, 1955; Bystöm,1956; Jürgenson, 1958; võrdle fotosid 4–6 ja 7). Vulkanogeense kvartsi identifitseerimiseks liivakivides on vajalik ja piisav, kui kvartsil puuduvad suletised, optiliselt määratavad struktuursed defektid ning sellega kaasnevad iseloomulik kuju ja/või klaasi suletised (Simanovitch, 1976, Blatt jt., 1980). Uuritud kvartsil on kõik loetletud tunnused olemas, määratud pole vaid klaasi suletisi. Seega ei saa välistada suletisteta killulise kvartsi vulkanogeenset päritolu, pidades silmas ka seda, et nende sisaldus tõuseb peenemates fraktsioonides. Vulkaanilise tegevuse peegeldumine Eestis alamordoviitsiumi Tremadoci setendites ei näi täiesti võimatuna, kuna samavanuselise vulkanismi ilmingud on Poolas Püha Risti mägedes (Chlebovski, 1978). Effusiivsete kivimite tükke on leitud alamordoviitsiumi liivakivis ka Leningradi oblastis (Gorbunova, 1979) ja odalaadseid ning sirbikujulisi kvartsiteri samavanuselistes argilliitides Eestis (Zhukov jt., 1987).

Neljandaks. Tuleb otsida kristalse aluskorra tektoonilisi struktuure, mis võisid olla värske murendmaterjali allikaks. Lähimateks on Uljaste ja Assamalla kerkestruktuurid, mis asuvad uuritud puuraukudest ligikaudu 10–15 km kaugusel ning Aseri rike (jn. 1). Senised uuringud on näidanud, et nad mattusid juba vara-kambriumis ja on kaetud vähemalt 85 m paksuse kambriumi ladestu settekompleksiga (Vaher jt., 1964; Puura jt., 1987). R. Raudsepa suulistel andmetel on käsitletaval alal väikseim kambriumi kihtide paksus 20 m. Lähim teadaolev kristalsete kivimite paljand kambriumi-ordoviitsiumi vahetusel oli tõenäoliselt Suur-Tütarsaar (jn. 1), mille kaugus (70 km) tingib settematerjali kulutuse transpordil.

Kristalsest aluskorrast pärinemise kasuks räägib suletisteta ja suletistevaese killulise kvartsi koosesinemine ning tüpomrfsete tunnuste sarnanemine puursüdamikust F-200 (jn. 1) kirjeldatud kvartsi omaga Al-gneissides (Konsa, 1989). Käesolevas töös käsitletud puursüdamikud asuvad platvormi tektooniliselt aktiivses osas (Raudsep, Kivisilla, 1992), kus plokilised liikumised on jätkunud ka pärast varaordoviitsiumit (Vaher jt., 1964), seetõttu pole võimatu, et mõni kristalsete kivimite plokk käsitletud ajal paljandus.

Vulkaanilist päritolu toetab kvartsiterade suur sarnasus keskordoviitsiumi K-bentoniitide kvartsiga.

Kokkuvõte

Rakvere piirkonnas alamordoviitsiumi fosforiidikihindis (Pakerordi lade, Kallavere kihistu, Rannu kihistik) sisaldub neile setenditele mitteomane killuline suletisteta või suletistevaene, sageli kumerate pindadega või kiilulaadne normaalselt kustuv kvarts, mille päritolu on problemaatiline. Killulise kvartsi levik on nii pindalaliselt kui ajaliselt piiratud. Uuringutest järeldub, et nimetatud tüpomorfsete tunnustega kvarts ei saa pärineda lamavast settekivimite kompleksist, ebatõenäoline on ka just suletisteta ja suletistevaesete terade purunemine lainetuse vööndis. Järelejäänud võimalused on: pärinemine tundmatust varaordoviitsiumis avatud olnud kristalse aluskorra kerkest või vulkaaniline teke.

Tänuavaldused

Autor on tänulik Rein Raudsepale oobolusliivakivi proovide eest ja Leho Ainsaarele K-bentoniitide materjali kasutamise võimaluse ja kasulike nõuannete eest.

Kirjandus

Blatt H., Middleton G., Murray R., 1980. Origin of sedimentary rocks. Second ed.. Prentice – Hall, Inc., Englewood Cliffs, New Jersy, 782 p.

Bystrōm M., 1956. Mineralogy of the Ordivician bentonite beds at Kinnekulle, Sweden. Sveriges Geologiska Undersökning, ser. C, N. 540, 62 p.

Chlebovski R., 1978. Petrografic study of early Palaozoic tuffogenic rocks from the Holy Cross Mts. Archivum Mineralogiczne, t. 34, z. 1, p. 69–134.

Gorbunova, 1979 – **Горбунова Л.И.**, 1979. Состав легкой и тяжелой фракций пород. В кн: Фосфатоносные отложения ордовика Прибалтики. Наука, М., с. 46–47.

Hagemann F., Spjeldnaes N., 1955. The middle Ordovician of the Oslo region, Norway. 6. Notes on bentonites (K-bentonites) from the Oslo-Asker district. Norsk Geologisk Tidskrift, b. 35, p. 29–52.

Heinsalu jt., 1991 – **Хейнсалу Х., Курвитс Т., Оя Т.,** 1991 Литолого-минералогическая характеристика стратотипического разреза раннуской пачки ($Є_3$-O_1klR) в Сака-II, Северо-Восточная Эстония. Изв. АН Эстонии. Геол., 40, 1, с. 1–7.

Heinsalu H., Raudsep R., 1993. Lithostratigraphic subdivision of the phosphate-bearing ($Є_3$-O_1kl) strata in the Rakvere area of northern Estonia. Bull. of the Geological Survey of Estonia, 3/1, p. 4–12.

Heinsalu, Viiding, 1978 – **Хейнсалу Х., Вийдинг Х.,** 1978. О минеральном составе нижнеордовикских фосфатоносных и подстилающих их отложений в Северной Эстонии. Изв ЭССР. Геол., 25, 2, с. 46–52.

Jürgenson, 1958 – **Юргенсон Э.,** 1958. Ментабентониты Эстонской ССР. Труды Института геологии АН ЭССР, II, с. 73–85.

Konsa, 1989 – **Конса М.,** 1989. Типоморфные особенности кварца в породах кристаллического фундамента и базалных отложений. Изв. АН. ЭССР. Геол., 38, 1, с. 1–9.

Konsa, 1993 – **Конса М.,** 1993. Отражение локальных тектонических структур района Усльясте в минеральном составе базальных отложений осадочного чехла. Изв. АН Эстонии. Геол., 42, 2, с. 41–47.

Kuljamin, Hazanovitch, 1971 – **Кулямин Л.Л., Хазанович К.К.,** 1971. Обломочный кварц из кембро-ордовикской печаной толши Ленинградской области. Литология и полезные ископаемые, 4, с. 88–94.

Loog, 1968 – **Лоог А.,** 1968. О литологии песчано-алевритовой толши лакеортского горизонта на полосе выхода. Ученые записки ТГУ, вып. 221, Труды по геологии 5, с. 49–74.

Mens, K., Viira, V., Paalits, I., Puura, I., 1989. Cambrian — Ordivician boundary beds at Mäekalda, Tallinn, North Estonia. Proc. Acad. Sci. ESSR. Geol., 38, 3, p. 101–111.

Puura jt., 1987 – **Пуура В., Вахер Р., Туулинг И.,** 1987. Тектоника. В кн: Геология и полезные ископаемые Раквереского фосфоритоносного района. Таллинн, с. 90–103.

Raudsep, 1975 – **Раудсеп Р.,** 1975. Вещественный состав фосфатоносных пород месторождения Тоолсе. Изв. АН ЭССР. Геол. Химия, 24, 2, с. 134–144.

Raudsep, Kivisilla, 1992 – **Раудсеп Р., Кивисилла Я.,** 1992. Об условиях накопления фосфоритоносных отложений Раквереского фосфоритоносного района. В кн: Геология ракушечных фосфоритов Прибалтики. Таллинн, с. 86–90.

Simanovitch, 1976 – **Симанович И. М.,** 1976. Определение первичных источников сноса по обломочному кварцу. Литология и полезные ископаемые, 3, с. 50–59.

Zhukov jt., 1987 – **Жуков Ф., Петерселль В., Фомин Ю.,** 1987. Признаки палеозойского вулканизма в Эстонии. Изв. АН ЭССР. Геол., 36, 1, с. 6–13.

Vaher jt., 1964 – Вахер Р., Куусмаду Т., Пуура В., Эрисалу Э., 1964. О геологическом положении сульфидных рудопроявлений в районе Ульясте. В кн: Литология палеозойских отложений Эстонии. Таллинн, с. 33–53.

Vilding, Konsa, 1976 – Вийдинг Х., Конса М., 1976. Учет данных по типоморфным разновидностям минералов терригенных отложений. В кн: Методика и интерпретация результатов минералогических и геохимических исследований. Мокслас, Вильнюс, с. 60–67.

QUARTZ IN PHOSPHORITE-BEARING BEDS OF RAKVERE AREA

Tiia Kurvits

Summary

Angular detrital quartz in Lower Ordovician sandstone of Rannu Member (Kallavere Formation, Pakerord Stage), not typical for this beds, has been described from Rakvere area. This angular quartz is monocrystalline, lacking inclusions or with small content of them, exibits nonundulatory extintion and often has concave or wedges-like outlines. Described above quartz cannot be redeposited from older sedimentary rocks because of its absence there. The provenance of angular quartz from rocks of crystalline basement or its volcanic origin is discussed in the paper.

RAKVERE MAARDLA FOSFORIIDI HAPNIKU, SÜSINIKU JA VÄÄVLI ISOTOOPSEST KOOSTISEST

Valter Petersell, Aadu Loog

Põhja-Eesti alamordovjitsiumi Pakerordi lademe liivakivis ja aleuroliidis on lukuta brahhiopoodide karbipoolmeid või nende tükke (detriiti). Fosfaatsete karbipoolmete või nende tükkide massilise leiu alad on tuntud Balti fosforiidibasseini fosforiidimaardlatena. Tänapäevase uurituse poolest on nende hulgas kahtlemata suurim Rakvere maardla, kuhu on koondunud üle 80% kogu basseini potentsiaalsetest tööstuslikest fosforiidivarudest.

Pakerordi lademe liivakive ja aleuroliite on enamik geolooge vaadelnud tüüpilise normaalsoolsusega madalmere moodustisena.

Viimastel aastatel on kogunenud üha uut faktilist andmestikku, mis eeldab nende F-, P-, U-, Sr- ja Ln-rikaste, oma põhiolemuselt biogeensete fosforiitide kujunemises ka endogeensete protsesside ja materjali osalust. Mõningat lisateavet aitavad tuua käesolevas artiklis vaadeldavad fosfaatsete karbipoolmete CO_2, hapniku, fosforiidi karbonaatse tsemendi süsiniku ja sulfiidse väävli isotoopkoostis.

Hapniku isotoopmäärangud tehti mass-spektromeetri MI-1201B-ga Nõukogude-Poola ühisettevõttes Balto-Tervas 1989. a. rahvusvahelise standardi SMOW suhtes. Määrangute täpsus on +0,3%. Süsiniku ja väävli isotoopkoostise määrangud tegi Ukraina TA IGFM laboratoorium rahvusvahelise standardi PDB ja troiliidi suhtes täpsusega vastavalt +0,4% ja +0,1% (Zukov, Lesnoi, 1982).

Fosfaatsetes karbipoolmetes leiduva isomorfse CO_2 hapniku isotoopkoostis selgitati Rakvere maardla keskse osa dolomitiseerumata läbiõikes. Saadud andmed näitavad (tabel 1, jn. 1), et fosfaatsetes karbipoolmetes on $\delta^{18}O$ sisaldus oluliselt suurem kui ookeanivees ja märgatavalt suurem kui kaasaja mereloomade fosfaatsetes karpides (Teis, Naidin, 1973). Fosforiidilasundi läbilõikes kõiguvad $\delta^{18}O$ arvulised väärtused fosfaatsete karpide kodades +12,6 kuni +16,6‰ piirides ja on küllalt selgelt jälgitavas seoses P_2O_5 sisalduse muutusega lasundis. Fosforiidilasundi lantanoidide spektri ja Ln/P_2O_5 analüüs kinnitas, et pärast fosfaatse mater-

jali settimist pole see märkimisväärses ulatuses ümber paigutunud või ümber jaotunud (Petersell jt., 1986). Just sellega on seletatav $\delta^{18}O$ seaduspärane muutus fosforiidilasundi läbilõikes ja ta seos P_2O_5-ga. Ühemõtteliselt on jälgitav, et koos P_2O_5 sisalduse suurenemisega suureneb $\delta^{18}O$ väärtus fosforiidilasundi alumises osas +12.6-st +14,5‰-ni. Seejärel läbilõikes alt ülesse P_2O_5 sisalduste vähenemisel $\delta^{18}O$ väärtused suurenevad. Võib eeldada, et $\delta^{18}O$ seaduspärased muutused on tingitud paleobasseini vee temperatuuri kõikumisest. Fosforiitide kujunemine algas paleobasseinis kõrgendatud temperatuuril, mis omakorda oli oluliselt kõrgem karbonaatsete setete kujunemise temperatuurist.

Rakvere, Toolse, Kingissepa ja teiste Balti fosforiidibasseini maardlate fosforiit on paljudes kohtades dolomitiseerunud. Hulk geolooge rõhutab dolomitisatsiooni seost tektooniliste rikkevööndidega. On ka levinud arvamus, et fosforiidil lasuva karbonaatse veekompleksi vesi infiltreerub Pakerordi lademe liivakivisse, kus temast välja langev karbonaat tsementeerib fosforiidi (Geoloogia..., 1980). Probleemi olemust selgitati Rakvere fosforiidimaardla kesksest osast tugevasti dolomitiseerunud fosforiidilasundist kogutud proovide analüüsiga (tabel 2, jn. 2). Saadud andmetest selgub, et fosforiidi karbonaatse tsemendi $\delta^{13}C$ on Rakvere maardla keskses osas kogu dolomitiseerunud läbilõike piires on püsiv ja võrreldes kõrgemal lasuvate karbonaatsete kivimite süsiniku isotoopkoostisega nihkunud kergema isotoobi suunas. Ta on lähedane tüüpilise hüdrotermaalse karbonaadi ja Kovdori apatiidimaardla kaltsiidi, samuti Narva fosforiidimaardla kemogeense fosforiidi $\delta^{13}C$-le (tabel 2). Hüdrotermidele omase $\delta^{13}C$ koostisega karbonaat tsementeerib ka fosforiidi all lasuvaid Tiskre kihistu liivakive, samal ajal kui lasuvate karbonaatsete kivimite $\delta^{13}C$ (jn. 2) jääb standardseks mereliseks (Petersell, 1991). Seega on alust arvata, et Balti basseini fosforiitide dolomitisatsiooni põhjused on tunduvalt komplitseeritumad ja mitmekesisemad kui varem arvatud. Fosforiitide dolomiitse tsemendi $\delta^{13}C$-le lähedus hüdrotermaalse karbonaadi $\delta^{13}C$-le vihjab sellele, et dolomitisatsiooni üheks põhjuseks on tõenäoliselt ka süvapäritoluga karbonaatse materjali sissekanne. Sellega on seletatav ka dolomitiseerunud fosforiitide levimine paljudes kohtades tektooniliste rikete vööndites.

Selle seisukoha kasuks räägib samuti dolomitisatsiooniga kaasneva püriitse väävli isotoopkoostis, mis 3 määrangu järgi on stabiilne, kõikudes ainult –2,7‰-st kuni –2,8‰-ni. Kõige suurema tõenäosusega on ta samuti süvapäritolu.

Seega on alust arvata, et nii Balti basseini fosforiitide kujunemise ajal kui ka hiljem, graptoliitargilliidi tekke perioodil (Petersell jt., 1987) oli kõrgema temperatuuriga, süvapäritolu hüdrotermide sarnastel voolustel settebasseinis küllalt oluline osa.

Table 1. Rakvere maardla fosforiidi hapniku isotoopkoostis

Proovi nr.	Proovimise sügavus		Sisaldus fosforiidiproovis			$\delta^{18}O$ brahhiopoodide kaantes		
			P2O5	MgO	Fe2O3	1	2	keskm.
				‰			‰	
6297	91,1	91,6	16,99	0,60	2,09	+16,7	+16,4	+16,6
6298	91,6	92,4	17,10	0,77	1,21	+15,6		+15,6
6299	92,4	93,0	19,50	0,68	1,54	ei määratud		
6300	93,0	93,6	21,20	0,51	1,98	+13,9	+13,2	+13,5
6301	93,6	94,7	22,10	0,38	1,11	+15,7		+15,7
6302	94,7	95,9	8,72	0,76	0,45	+16,6		+16,6
6303	95,9	95,9	12,27	0,54	0,48	+15,9	+16,3	+16,1
6304	96,9	97,5	16,90	0,56	0,60	+15,9	+15,5	+15,7
6305	97,5	97,9	21,07	0,70	0,83	+14,7	+14,4	+14,5
6306	97,9	98,2	5,39	4,06	0,88	+12,5	+12,6	+12,6

Proovide asukohad vt. joonisel 1

Table 2. Rakvere maardla fosforiidi süsiniku ja väävli isotoopkoostis

Proovi nr.	Proovimise sügavus m		Sisaldus fosforiidi proovis			C_{karb}	$\delta^{13}C$ karb ‰	$\delta^{34}S$ pür ‰
			P_2O_5	MgO	Fe_2O_3			
0931	93,0	93,2				10,33	–0,9	
0948	94,7	94,9				13,44	–1,1	
0960	95,9	96,1	2	1,4		0,26	–10,7	
0962	96,1	97,2	25,25	0,91	1,74	3,22	–6,8	
0986	98,3	98,8	14,33	3,06	1,17	3,20	–6,9	
1008	100,2	101,1	7,58	1,04	0,56	1,57	–6,6	
1022	101,8	102,6	2,82	4,44	0,70	2,76	–8,3	
1041	103,6	104,6	7,38	3,87	0,92	2,74	–7,9	
1049	104,8	105,0	1,0	2,4		0,96	–7,5	–2,8
0873	87,2	87,4				1,19	–7,9	–2,7
0877	87,6	87,8				2,84	–8,7	–2,7
Narva H-6							–11,6	
Kovdor 91-K							–11,5	

Proovide asukohad vt. joonisel 2

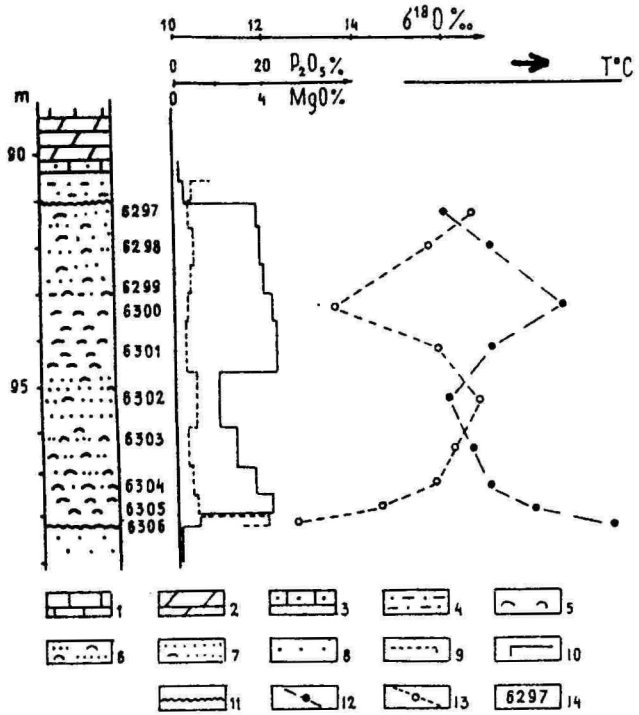

Jn. 1. Rakvere maardla fosforiidi hapniku isotoobid (puurauk 2027):
1 – dolomitiseerunud lubjakivi; 2 – dolomiit; 3 – glaukoniitlubjakivi; 4 – glaukoniitliivakivi; 5–7 – fosforiit: 5 – detriit, 6 – detriitne liivakivi, 7 – detriidikas liivakivi; 8 – liivakivi (Tiskre kihistu; 9 – MgO sisaldus; 10 – P_2O_5 sisaldus; 11 – settelünk; 12 – fosfaatsete karbipoolmete CO_2 hapniku $\delta^{18}O$‰; 13 – paleotemperatuuri muutumine; 14 – proovi number.

Fig. 1. The oxygen isotopic content in the phosphorite from the Rakvere deposit (drill core 2027).
1 – dolomitized limestone; 2 – dolomite; 3 – glauconitic limestone; 4 – glauconitic sandstone; 5–7 – phosphorite: 5 – bioclasts, 6 – bioclastic sandstone, 7 – bioclasts containing sandstone; 8 – sandstone (Tiskre Member); 9 – MgO content; 10 – P_2O_5 Content; 11 – sedimentation gap; 12 – $\delta^{18}O$ values from the phosphoritic shell valves (in ‰); 13 – the variation curve at paleotemperature; 14 – sample number

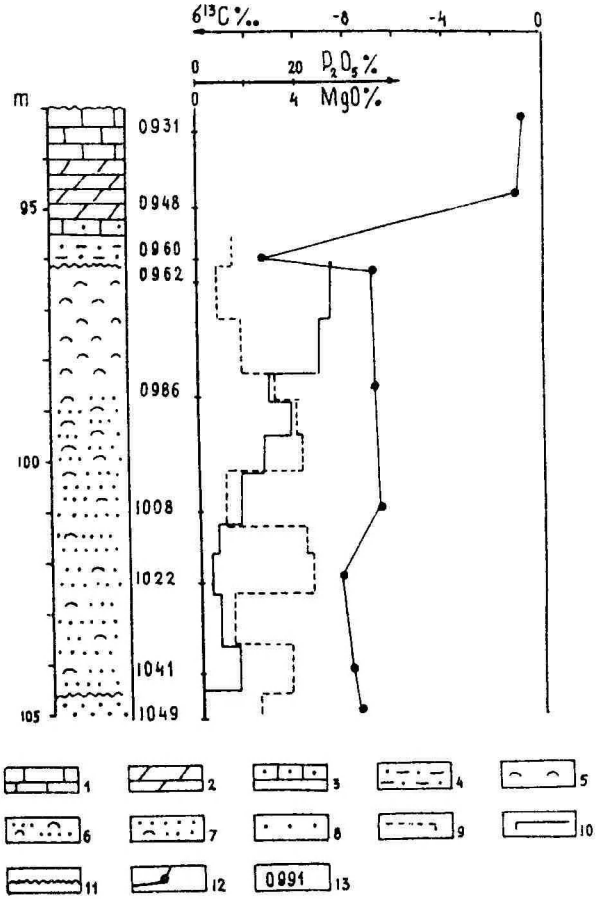

Jn. 2. Süsiniku isotoobid Rakvere maardla fosforiidis (puurauk 2145).
1 – dolomitiseerunud lubjakivi; 2 – dolomiit; 3 – glaukoniitlubjakivi; 4 – glaukoniitliivakivi; 5–7 – fosforiit: 5 – detriit, 6 – detriitne liivakivi, 7 – detriidikas liivakivi; 8 – liivakivi (Tiskre kihistu); 9 – MgO sisaldus; 10 – P_2O_5 sisaldus; 11 – settelünk; 12 – karbonaatse tsemendi süsiniku $\delta^{13}C$ ‰; 13 – proovi number

Fig. 2. The carbon isotopic content in the phosphorite from the Rakvere deposit (drill core 2145).
1 – dolomitized limestone; 2 – dolomite; 3 – glauconitic limestone; 4 – glauconitic sandstone; 5–7 – phosphorite: 5 – bioclasts, 6 – bioclastic sandstone, 7 – bioclasts containing sandstone; 8 – sandstone (Tiskre Member); 9 – MgO content; 10 – P_2O_5 Content; 11 – sedimentation gap; 12 – the $\delta^{13}C$ content in carbonate content (in ‰); 13 – sample number.

Kirjandus

Geoloogia – Геология месторожений фосфоритов. 1980. Методика их прогнозирования и поисков. - М.: Недра. - 243 с.

Petersell jt.; 1987 – **Петероселль В.Х., Жуков Ф.И., Лоог А.Р., Фомин Ю.А.,** 1987. Происхождение тремадокских керогенсодержащих алевролитов и аргиллитов Северной Эстонии. Горюче сланцы, 4/1, с. 8-13.

Petersell jt., 1986 – **Петерселль В.Х., Лоог А.Р., Минеев В.А., Петрина О.И.** 1986. Фтор, стронций и редкие земли в фосфоритах Раквереского фосфоритоносного района. Уч. зап. Тартуского ун-та, вып. 759. Труды по геологии. Т.Х. с. 27-55.

Petersell, 1991. Geochemistry of F, Sr, TR and U in. phosphprites of the East Baltic phosphorite basin. Exploration geochemistry. Proceedings of the Third International Joint Symposium of the IAGC and the AEG. Prague. p. 278–290.

Zukov, Lesnoi, 1982 – **Жуков Ф.И., Лесной Д.А.,** 1982. Изотопы серы и углерода в стратиформных месторождениях складчатых областей. Киев. „Наукова Думка". 160 с.

ON THE PHOSPHORITE OXYGEN, CARBON AND SULPHUR ISOTOPIC COMPOSITION IN RAKVERE DEPOSIT

Valter Petersell, Aadu Loog

Summary

In the Lower Ordovician Pakerort Stage these are complexes of the inarticulate brachiopod shells, which form in places the industrial deposits, the greatest of them is the Rakvere Phosphorite Deposit. The phosphorites here have biogenic nature, containing great concentrations of P, F, U, Sr and La. A lot of data refer to the endogenses processes as a source for many elements.

In this article the data about the isotopic composition of oxygen, carbon and sulphur from the materials of the shell valves, carbonate cement and sulphides accordingly are presented. The valves of $\delta^{18}O$ from the brachiopad shell valves vary between the +12 and 16.6‰. The correlation between the $\delta^{18}O$ and P_2O_5 content is distinet

(Table 1, Fig. 1). The $\delta^{13}C$ values from the carbonate cement in the dolomitineds section of Rakvere phosphorite deposit is quite constant and close to ones for carbonates of typical hydrothermal origin (Table 2, Fig. 2). This gives the basic to the ideas that the dolomitization of phosphorites has been a coplicated process with the influx of deep carbonate material. This view point is corroborated also by the pyritic sulphur isotopic composition which varies between the values of –2.7 to –2.8‰.

The results presented here are of preliminary ones and need more complementary investigation.

THE DISTRIBUTION OF MICROELEMENTS IN TREMADOC GRAPTOLITIC ARGILLITE OF ESTONIA

A. Loog, V. Petersell

Tremadoc graptolitic argillite of Estonia (Dictyonema shale) forms the upper part of the rocks of the Cambrian-Ordovician "black shale" formation distributed in northwestern Europe. In Sweden they are known under the name of Alum shale (Andersen et al., 1985) and are everywhere characterized by increased contents of several microelements, first of all U, Mo and V, but also of S and organic carbon (Safronov, 1971). The content of microelements in Tremadoc graptolitic argillite of Estonia has been treated by several researchers (Loog, 1962; Loog, Petersell, 1981; Pukkonen, 1989; Pukkonen, Rammo, 1992). In these studies the main stress has been laid on the analysis of the mean content of microelements in the sections of outcrops and drill cores with an attempt to find out general regularities in their distribution.

Particularly significant is the study of the occurrence of elements in concrete vertical sections as this permits to get an idea about their distribution in space and time, possible direct and indirect sources of their intrusion and relations with other elements, with rock and its components, etc., i.e. to draw conclusions about the geochemical evolution of the basin.

Basing on the more detailed analysis of the published data, as well as on the materials of archives and those additionally collected by the authors, in the present paper the distribution of the organic matter (OM), mineral CO_2 $(CO_2)m$, uranium (U), molybdenum (Mo), vanadium (V), lead (Pb) and zinc (Zn) is considered on the example of concrete core sections (Fig. 1).

For this purpose three north-southerly profiles (Figs. 2, 3, 4) have been compiled in different parts of the distribution area of graptolitic argillite, i.e. they are directed from the areas of greater thicknesses to the southern margin where argillite thins out. Fig. 5 presents the contents of the corresponding elements on the west-easterly profile.

In all sections the boundary between argillite and overlying beds is lithologic, without a break in sedimentation. The upper boundary of graptolitic argillite is, however, erosional. Sampling of all sections was performed by means of the trenching. Determination of the conventional OM and (CO_2) m were carried out at the former specialized oil shale laboratory of the Kohtla-Järve Geology Department, microelements were established at the laboratory of the Geological Survey of Estonia (U, Mo and Pb by the X-ray fluorescence and V, Zn by the emission spectroscopy methods. High Zn contents were checked on AAS).

As is seen in the figures, the OM, as the concentrator and carrier of generally known microelements, first of all U, Mo and V in the formations of black shales, is of quite even distribution within the strata of graptolitic argillite (Table 1), also in the vertical section, the carbon content of OM exceeding the clark of black shales (Vine, Tourtelot, 1970) 3–4 times.

Only in some core sections the content of OM is notably higher in the lower or middle part of the section boreholes (b.h.-s D-78, D-155, etc.). Also certain increase in the mean content of OM from east to west has been recorded (Fig. 5), whereas in north-south profiles its values are similar ewerywhere. Still, some increase in the mean OM content with the growth of the thickness of the graptolitic argillite strata has been recorded. Contrasting minimums of OM in graptolitic argillite are due to occurrence of silt interbeds in Toolse region and of carbonate-rich interlayers (?) in western Estonia (Figs. 2–4).

Against the background of such relatively even distribution of OM, we can observe extremely uneven distribution of microelements in the vertical section and its alteration, compared to their mean content in concrete sections. Considering the uneven distribution of microelements, contents of separate elements in the vertical section of the strata are changing according to very different regularities.

The U content is differing in separate parts of the distribution area of graptolitic argillite, but exceeds the clark of black shales in all core sections 5 to 14 and more times. The mean U content decreases from west to east up to Maardu, being again high in the east, in Toolse and particularly Sillamäe regions. In the west and middle parts of the area the mean U content of the strata increases also southwards.

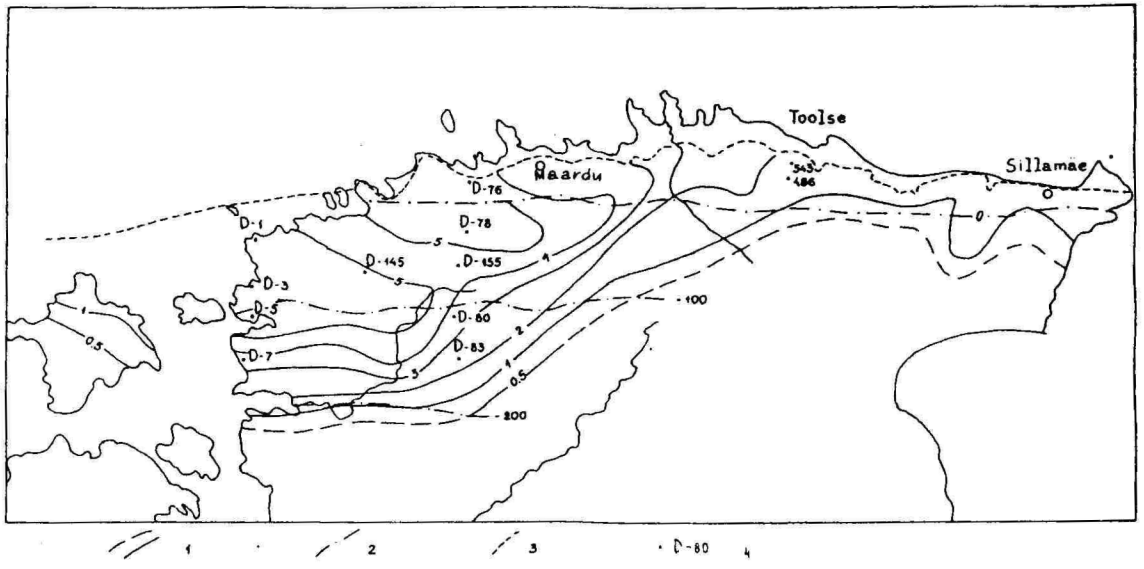

Fig. 1. Occurrence of graptolitic argillie strata in northern Estonia:
1 – isopachyte of the strata, m; 2 – isobath of the upper surface of the strata, m; 3 – erosional northern boundary of the strata; 4 - borehole

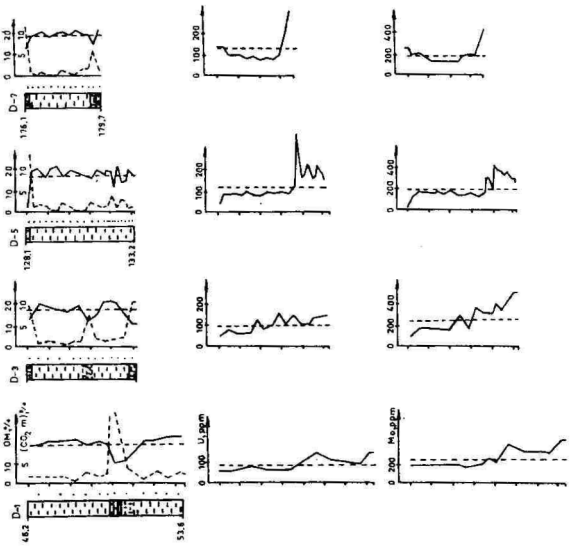
0 10 20
0 5 10
D-7
176.1
179.7
0 100 200
0 200 400
D-5
128.1
132.1
D-3
D-1
46.2
53.4
OH-/2+
(CO3 m)2+
0 100
Li ppm
Mg ppm

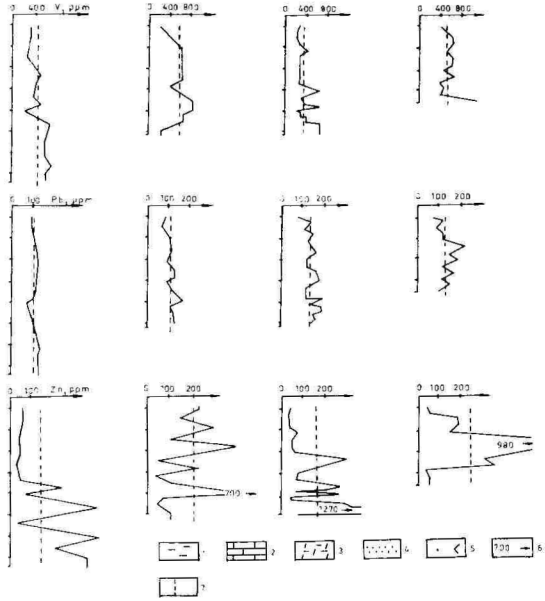

Fig. 2. Distribution of OM, (CO2)m, U, Mo, V, Pb and Zn in the north-south directed western profile of the graptolitic argillite strata:

1 – graptolitic argillite; 2 – carbonate-rock interbed; 3 – carbonate-rich interbed; 4 – silt interbed; 5 – centre of trenching; 6 – high concentration of the element, ppm; 7 – mean concentration.

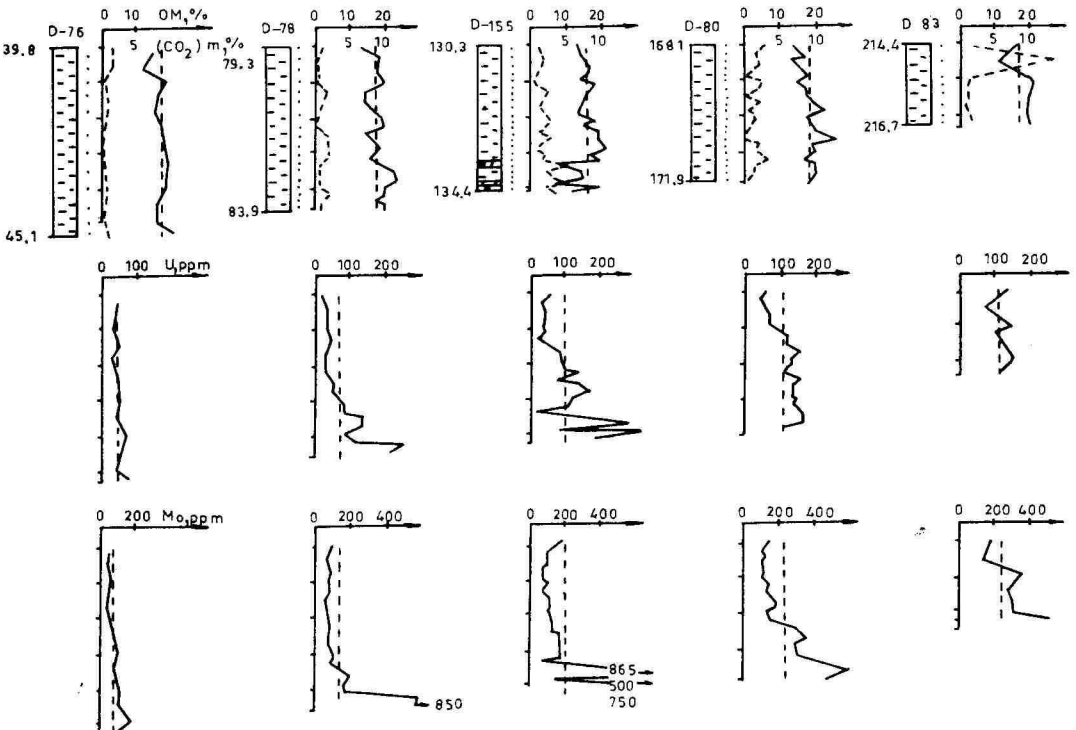
D-76
39.8
45.1
0 10 OM,%
5 (CO2) m,%
D-78
79.3
83.9
0 10 20
5 10
D-155
130.3
134.4
0 10 20
5 10
D-80
168.1
171.9
0 10 20
5 10
D 83
214.4
216.7
0 10 20
5 10
0 100 U,ppm
0 100 200
0 100 200
0 100 200
0 100 200
0 200 Mo,ppm
0 200 400
850
0 200 400
865
500
750
0 200 400
0 200 400

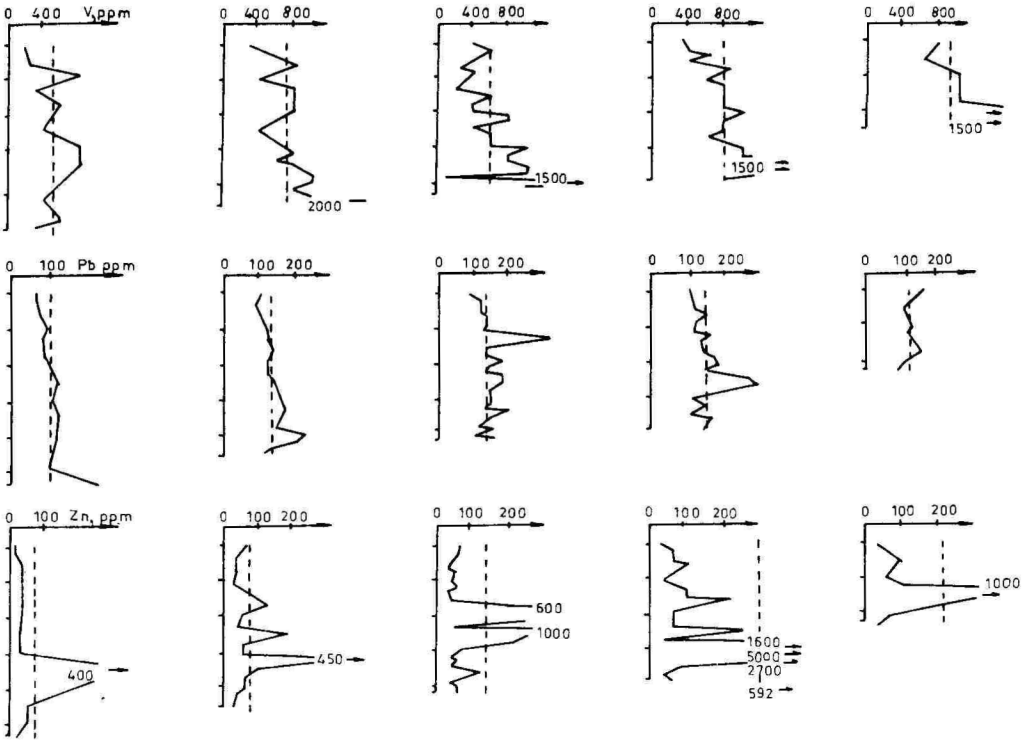

Fig. 3. Distribution of OM, (CO2)m, U, Mo, V, Pb and Zn in the north-south directed middle profile of the graptolitic argillite strata. Symbols as in Fig. 2.

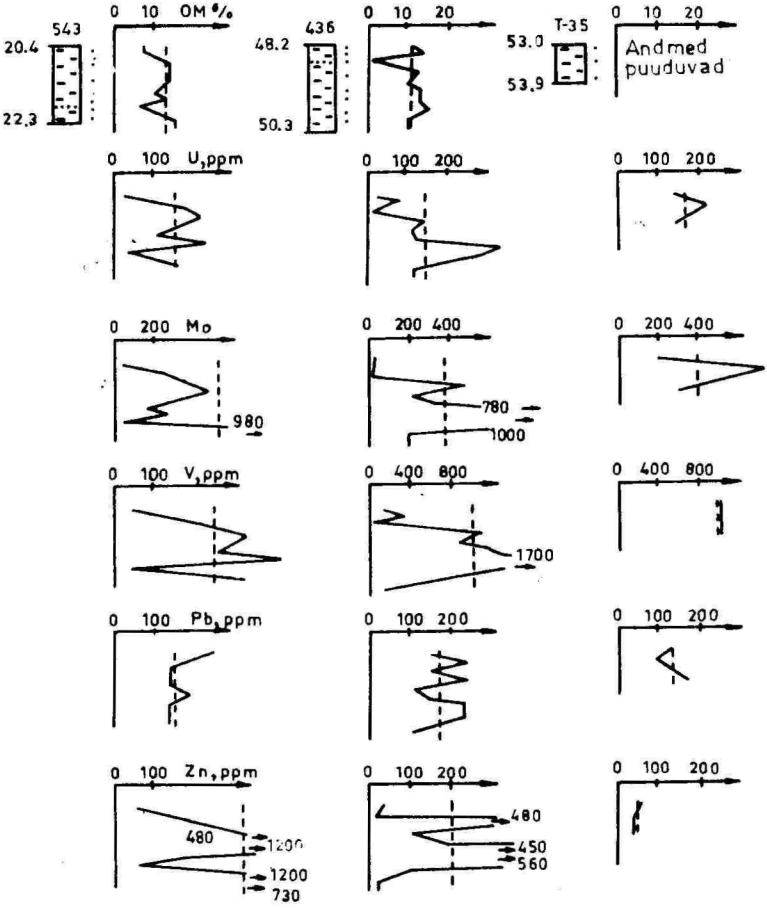

Fig. 4. Distribution of OM, U, Mo, V, Pb and Zn in the north-south directed eastern profile of the graptolitic argillite strata. Symbols as in Fig. 2.

Characteristically in most of the sections the U content increases in the lower part of the strata. In 0.3–0.6 m thick layers of several cores from the belt, lying close to the southern boundary of the distribution area, the U content is up to 200–300 ppm (Figs. 2–5), in the region of Sillamäe exceeding these values.

The content of Mo in graptolitic argillite is high and exceeds the clark of black shales 25 and more times. Its vertical and areal distribution is extremely uneven. In the vertical section the maximum contents have been registered in the basal part of the graptolitic argillite strata where in layers of some tens of a centimetre in thickness the Mo content may rise very high, up to 1000–1500 ppm. Higher Mo contents in the strata are observed in the eastern and western parts of the distribution area of graptolitic argillite. In the middle part of the area, in the region of Maardu the Mo content is low and distribution even.

The distribution pattern of V in the vertical core sections, also its mean content changes in the graptolitic argillite strata from north to south and from west to east are generally analogous to those of U and Mo, although somewhat more even in nature. Its concentration coefficient is also considerably lower than that of the above- discussed elements, exceeding the clark value of black shales only 2 to 6, very rarely more times. In concrete core sections the vertical distribution of V is rather uneven.

Profile II displays clearly the decrease in the V content from base to top, particulary in more southern core sections. At the same time in core sections of profile I such a change is either missing or hardly observable. Distinct increase in the V content is registered from west to east, from profile I towards profile II, followed by its lowering down to the minimum again in the region of Maardu (Fig. 5).

The contents are considerably higher in the eastern part of the distribution area of graptolitic argillite at Toolse and Sillamäe. Maximum V contents of up to 2000 ppm were recorded in the lowermost part of the strata.

The content of Pb in graptolitic argillite is everywhere high and unaltered, almost always exceeding the clark of black shales 5–8 times. Anomalously high concentrations are either lacking or occur very rarely. Neither has there been observed strict regularity in the distribution of Pb in vertical sections. Thus, in the western part of the distribution area the contents are somewhat higher in the lower beds of the section, in the east of the area

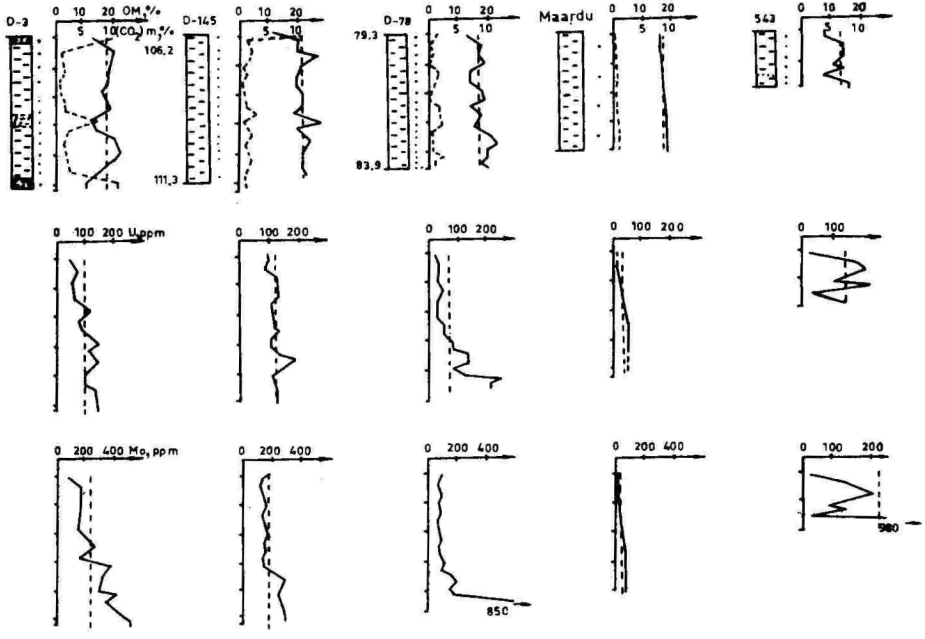
D-2
0 10 20 OM,%
5 10 (CO2) m,%
106,2
111,3
D-145
0 10 20
5 10
D-78
79,3
83,9
0 10 20
5 10
Maardu
0 10 20
5 10
543
0 10 20
5 10
0 100 200 U,ppm
0 100 200
0 100 200
0 100 200
0 100
0 200 400 Mo, ppm
0 200 400
0 200 400
850
0 200 400
0 100 200
980

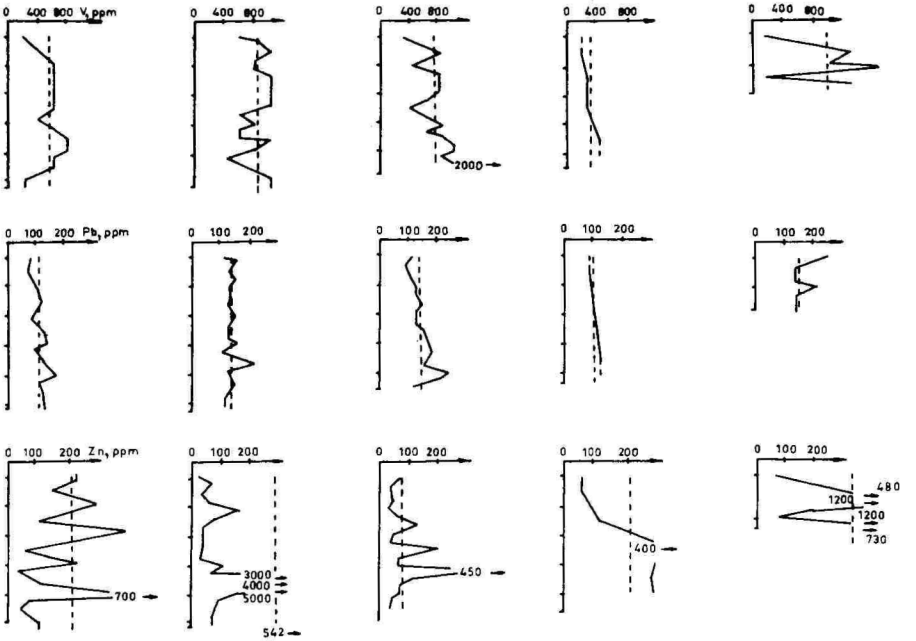

Fig. 5. Distribution of OM, (CO2)m, U, Mo, V, Pb and Zn in the west-eastern profile of the graptolitic argillite strata Symbols as in Fig. 2.

(Toolse), however, in its upper part. At the same time, on several levels some samples have yielded increased Pb contents, which is directly related to the occurrence of ore minerals. In the north-south direction there occur no changes in the mean lead content within the graptolitic argillite strata (Fig. 2), but in the eastern part of the area the Pb content is somewhat higher (Fig. 5) than in its middle and western parts.

Among the elements considered, Zn is the only one, the content of which in graptolitic argillite is often lower than the clark of not only black shales, but also below that of the earth crust, in places, however, being very high. Its mean content in the core sections of the western part of the distribution area increases from north to south. Differently from Mo and Pb, the maximum Zn contents occur in the western part of the distribution area of graptolitic argillite, in the region of the greatest thicknesses (Figs. 1 and 2), in the whole distribution area of graptolitic argillite almost all core sections show the presence of intervals with a high and very high Zn content. In the vertical section they may be observed mainly in the lower part of the strata, more rarely also in the middle part. In the limits of these intervals the Zn content rises to 0.5–1% and they related to the occurence of sphalerite in a few mm to 2–3 cm thick silty interlayers of graptolitic argillite.

Sphalerite and pyrite constitute the main ore minerals in these interlayers, the amount of sphalerite reaching up to 8–10% of the whole rock mass.

In publications very often the distinct correlation between OM and the content of microelements in graptolitic argillite has bees pointed out (Loog, 1962; Petersell et al., 1981; Pukkonen, 1992). Data of paired correlation have also revealed positive relation between OM and U, Mo, V and Pb contents in the core sections of the western part of the area.

The possibility of such a relation between the elements and OM is, however, very different in the core sections studied (Table 1). There appears regularity — the more positive anomalies the element considered form in the graptolitic argillite strata, and the more contrastive they are, the smaller will be be the probability of positive correlation between the elements and OM. By the decreasing probability of positive paired correlation the microelements form an order Pb, V, U and Mo. There is no correlation between Zn and OM in the core sections considered, thus their relations are neutral.

Fig. 6. Relation between OM and U (a), Mo (b), V (c), Pb (d), Zn (e) in differnt sections of graptolitic argellite strata 1–4 – boreholes:
1 – D-3, 2 – D-145, 3 – D-78, 4 – 543; 5 – Maardu quarry; 6 – high concentration of the element, ppm.

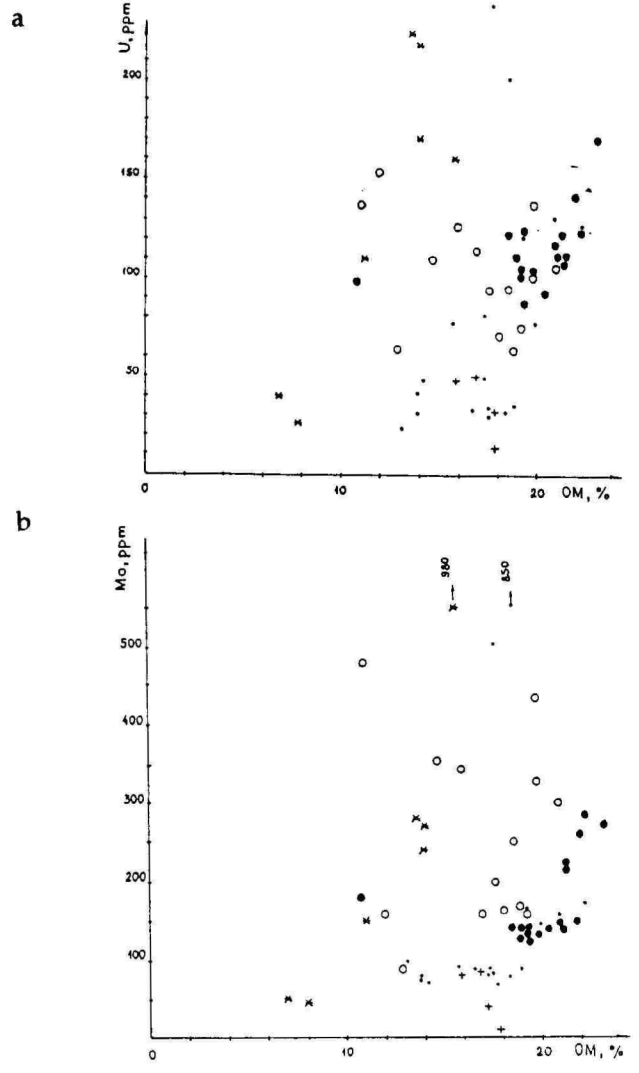

c

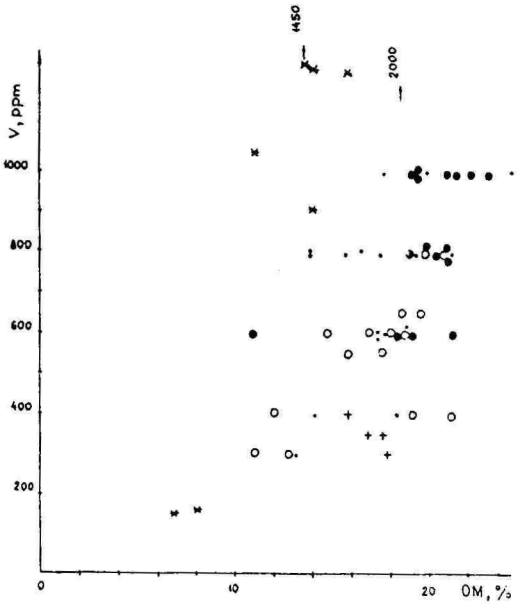
V, ppm
1000
800
600
400
200
0
10
20
OM, %
450
2000

d

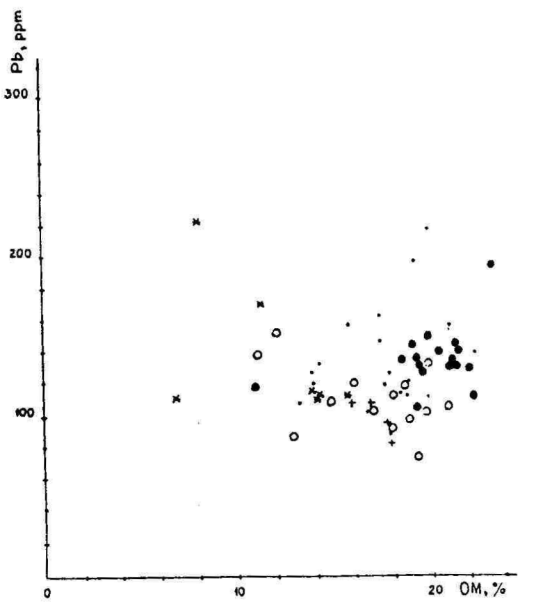
Pb, ppm
300
200
100
0
10
20
OM, %

e

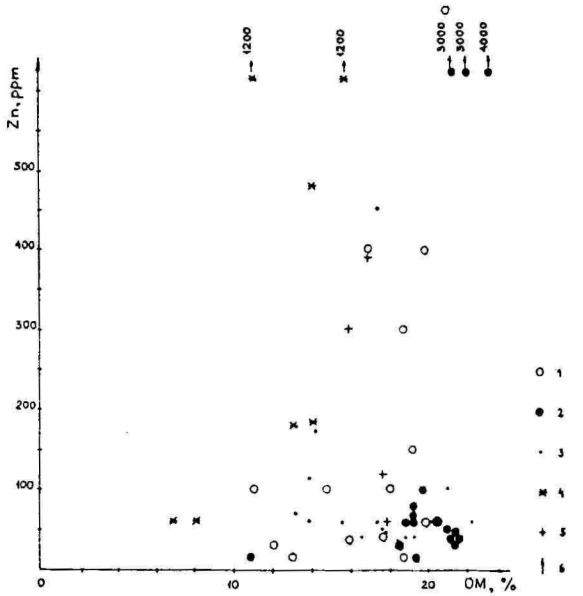

Table 1. Probability of positive correlation between OM and microelements

Borehole nr.	Number of samples	Probability of correlation					
		U	Mo	V	Pb	Zn	(CO_2)m
D-1	12	–	–	–	+++	–	—
D-3	14	+	–	++	+	–	–
D-5	22	–	+	+	++	–	—
D-7	13	–	+	+++	+++	–	–
D-76	12	+++	++	+++	+++	–	–
D-78	19	++	–	++	++	–	–
D-155	24	++	–	++	+	–	–
D-80	20	+++	++	+++	+++	–	–

correlation lacking (–), positive correlation with probabilities of 90–95% (+), 95–99% (++), more 99% (+++); negative correlation (—)

Table 2. Mo, V, Pb and Zn contents in monomineralic pyrite of graptolitic argillite and in graptolitic argillite (ppm)

	Monomineralic pyrite						Graptolitic argillite				
Borehole nr.	Sampling depth, m	Pyrite-bearing rock	V	Mo	Pb	Zn	Sampling depth, m	V	Mo	Pb	Zn
4 (Ellamaa	139.6	S.i.b.	24	130	1600	4200	139.6–140.5	780	110	140	100
	140.2	S.i.b	60	92	320	30					
	141.6	P.c.	300	66	680	24	141.3–142.2	830	220	230	150
	142.0	S.i.b.	100	66	610	2100					
	142.6	S.i.b.	69	210	460	10000	142.2–143.2	1010	200	220	1850
	143.1	P.c.	100	99	460	30					
	143.9	P.c.	24	66	76	35	143.8–144.5	1500	87	120	630
F-237	61.0	P.c.	12	450	27	40	61.0–61.5	420	110	90	80
	62.2	S.i.b.	27	530	30	240	61.5–62.5	410	285	105	90
	62.3	P.c.	35	320	37	60					
	62.6	P.l.	80	110	610	30	62.5–63.0	350	60	120	490
	63.6	S.i.b.	80	230	460	10000	63.5–64.0	490	60	110	320
	66.6	S.i.b.	10	280	30	24	66.3–67.0	690	490	170	30

S.i.b.– up to 3-cm-thick silt interbed
P.c.– pyrite concretion
P.l.– pyrite lens

More detailed observation of the relations between OM and microelements on the reverse diagrams (Fig. 6) shows, that the contents of elements in core sections fall into different parts of the diagrams, stressing in this way the different relations between OM and microelements in separate areas. These data, together with the ones presented in Figs. 2–5, allow to state that positive anomalous contents of different microelements occur frequently on different levels in graptolitic argillite, they are not correlating.

In several publications pyrite is mentioned as the main concentrator and bearer of microelements (Mo, Pb, Zn) in graptolitic argillite (Maldre, 1976, Kallaste, Pukkonen 1992). The significance of pyrite in this respect is considered basing on the data of spectral analysis of monomineralic pyrite collected from core sections 4 (Ellamaa) and F-257 (Table 2). The pyrite analysed has been separated from point samples under binocular microscope, but the analysis of graptolitic argillite has been performed on samples, taken using the trenching, due to which the results cannot be compared unambiguously. Still, they permit to get a general idea about the problem.

Characteristically the content of the elements studied is very heterogeneous in pyrite. Quite clearly there can be observed a low V content in pyrite. It is everywhere lower than that of the host rock, exceeding the clark of the lithosphere only in one case. Therefore pyrite is not the carrier and concentrator of V in graptolitic argillite. The content of Mo, Pb and Zn in pyrite is variable. In some samples their content is higher than in the surrounding graptolitic argillite, in several cases however, being lower. It should be noted that often pyrite is enriched with Mo, as well as with Pb, particularly with Zn, their amounts being larger in pyrite than in the host rock. There occur also samples in which pyrite is enriched with only one or two of the elements considered, or where the content of all three elements – Mo, Pb and Zn is lower than in graptolitic argillite. Therefore pyrite serves often as the concentrator and carrier of Mo, Pb and Zn. Such a characteristic distribution of microelements in pyrite can be explained by the variable content of elements in the sedimentary basin, on one hand, and by different possibilities of the appearance of mineral forms in natural conditions, on the other hand.

Main mineral forms of Mo, Pb nad Zn are sulphides. In pyrite they either replace Fe or occur as an independent sulphide phase depending on the degree of concentration in the sedimentary basin. V occurs predominantly in non-sulphide minerals, the formation or concentration of which in pyrite had no geochemical preconditions in the sedimentary basin.

Reasons of relatively high contents of OM, U, Mo, V, Pb, Zn and other elements in graptolitic argillite are not understood unambiguously. The associations, occurrence and distribution patterns of these elements, the isotopic composition of S, C and Pb (Petersell et al., 1987), chemical and mineralogical composition of graptolitic argillite permit to suggest the concentration of these elements to be related to deep geology.

At that, Caledonian folding and the accompanying magmatic activity caused activation of tectonic deep latitudinal dislocations in the Tremadoc, which resulted in the inflow of subaqueous hydrothermas into the Baltic paleobasin. There appeared in the geological sense short-term specific paleoecological conditions which caused stormy development of organisms and preservation of organic matter. The enviromental settings formed were favourable for mass occurrence of only some species. In the result

of all this metal-rich organic material was accumulated in clay muds. By the burial into sediments and during the following diagenesis they turned into argillite containing OM (mostly 13–19%). Burial of abundant OM in clay facies was possible due to mass occurrence of bacterial mats and algae in the basin water. Therefore sea-water served as one of immediate sources of elements concentrated in the clay facies. This is also evidenced by a stable mineralogical composition of sediments, even distribution of numerous non-hydrothermal elements and their content nearing the clark of the lithosphere. Local anomalously high contents of U, Mo, Zn, Pb, and other elements in graptolitic argillite as well as in pyrite could be explained only by their local concentration changes in sea water. Occurrence of contrasting geochemical anomalies and polymetallic ore formation, often the predominance of mantle sulphur, show directly that the material, carried into the basin water, come not only from the denudation areas and from the ocean with possible deep currents, but included also considerable amounts of endogenic matter.

Proceeding from the above standpoints, in the last years more and more attention has been paid to polymetallic ore formation in graptolitic argillites, also to contrasting anomalies of Au, Pt and other elements. Yet, additional detailed mineralogical, geochemical, etc. investigations are needed in order to prove the existence of the endogenic source of several elements.

References

Andersson, A., Dahlman, B., Gee, D. G., Sna"ll, S., 1985. The Scandinavian alum Shales. Sver. Geol. Unders., The Scandinavian alum Shales. Sver. Geol. Unders., Ca56, 50 p.

Kallaste T., Pukkonen E. 1992. Pyrite varieties in Estonian Tremadocian argillite (Dictyonema Shale). Proc. Estonian Acad. Sci. Geol, 41. No 1. p. 11–22.

Loog, 1962 – **Лоог А.,** 1962. К геохимии нижнего ордовика Эстонии. Тр. Ин-та геол. АН ЭССР, Т. X. с. 273–291.

Loog, Petersell, 1978 – Лоог А., Петерселль В., 1978. Геохимические особенности граптолитовых аргиллитов (диктионемовых сланцев) Эстонии. В кн: Тез. докл. совещ. „Геохимия горючих сланцев". Таллин, с. 109–110.

Maldre, 1976 – **Малдре Я. Я.**, 1976. Молибден в диктионемовых сланцах Северной Эстонии. Литология и Полезные Ископаемые, 5, с. 94–98.

Petersell et al., **Петерселль В., Минеев Д., Лоог А.**, 1981. О минералогии и геохимии оболовых песчаников и диктионемовых сланцев Северной Эстонии. Уч. зап. Тарт. ун-та. Вып. 759: Труды по геологии, м. X. с. 27–55.

Petersell et al., 1987 – **Петерселль В., Жуков Ф., Лоог А., Фомин Ю.**, 1987 – Происхождение термадоксеих керогенсодержащих алевро, литов Северной Эстонии. Горючие сланцы 4/1, с. 3–13.

Pukkonen, 1989 – **Пукконен Э.**, 1989. Макроэлементы и малые элементы в граптолитовом агриллите Эстонии. Горючие сланцы 6/1, с. 11–18.

Pukkonen, E., Rammo, H., 1992. Distribution of Molybdenum and Uranium in the Tremadoc Graptolitic Argillite (Dictyonema Shale) of North-Western Estonia. Bull. of the Geol. Sur. of Estonia, 2/1. p. 3–15.

Safronov, 1971 – **Сафронов Н. И.**, 1971. Основы геохимических методов поисков рудных месторождений. Изд. „Недра", 164 с.

Vine J. D., Tourtelot E. B., 1970. Geochemistry of black shales — A Summary Report. Econ. Geol., 65, p. 253–272.

MIKROELEMENTIDE JAOTUSSEADUSPÄRASUSTEST EESTI TREMADOCI GRAPTOLIITARGILLIIDIS

Aadu Loog, Valter Petersell

Resümee

Vaadeldakse orgaanilise ainese, mineraalse CO_2, uraani, molübdeeni, vanaadiumi, plii ja tsingi jaotust graptoliitargilliidis puuraukude näidete varal (jn.1).

Graptoliitargilliidi levila piirkondades on koostatud 3 põhjalõunasuunalist läbilõiget (jn. 2. 3. 4), s.o. suurema paksusega aladelt levila lõunapiirile, kus argilliit suidub. Joonisel 5 on esitatud elementide sisaldused lääne-idasuunalisel läbilõikel.

Proovimisel on kasutatud vaomeetodit. Orgaaniline aines (OM) ja mineraalne CO_2 on määrangud endises Kohtla-Järve Geoloogiatöökonna põlevkivi spetsialiseeritud laboratooriumis, mikroelemen-

did Eesti Geoloogiakeskuse laboratooriumis; U, Mo ja Pb RF-meetodil, V ja Zn spektraalanalüüsi meetodil.

Orgaanilise ainese suhteliselt ühtlase jaotuse taustal (jn. 2–5) on jälgitav, et mikroelementide jaotumine vertikaalses läbilõikes, võrreldуna läbilõigete keskmiste sisaldustega, on äärmiselt ebaühtlane ja elemenditi erinev. Paariskorrelatsiooni andmetel on positiivne seos orgaanilise ainese ja U, Mo, V ning Pb sisalduste vahel jälgitav levila läänepiirkonna puuraukude läbilõigetes. Selgub seaduspärasus mida rohkem positiivseid anomaaliaid moodustab element ja mida kontrastsemad nad on, seda väiksemaks muutub elemendi positiivse korrelatsiooni tõenäosus orgaanilise ainesega (tabel 1 ja 2).

Graptoliitargilliidis on Mo, Pb ja Zn kontsentraatoriks ja ka kandjaks ka püriit (tabel 2).

Graptoliitargilliitides OM, U, Mo, V, Pb, Zn jt. elementide suhteliselt kõrge sisalduse lähteallikate kohta pole üheseid arusaamu. Vaadeldavate elementide assotsiatsioonid, leviku- ja jaotusseaduspära, väävli, süsiniku ja plii isotoopne koostis ning graptoliitargilliidi mineraalne koostis viivad järeldusele nende elementide kontsentratsioonide tekke seosest süvageoloogiaga.

GEOCHEMICAL ZONATION OF MAARDU MINE TAILINGS DUMP

Erik Puura

Introduction

Opencast mining of phosphorite in Maardu pit near Tallinn has lead to pollution of surrounding hydrosphere due to inaccurate disposal of Dictyonema shale, layer of which was a part of the overburden of phosphorite layer (Naumov, 1991). Total area of disposal site is about 10 sq km, thickness of disposed rocks and sediments 12–18 m, and slope angle of the edges 30–40 degrees. Dictyonema shale contains pyrite (average 4–6%), organic matter (15%) and anomalously high concentrations of a range of heavy metals (V 800 ppm, Mo 130 ppm, U 50 ppm; Pukkonen, 1989; Maremäe, 1988); main rock-forming minerals are quartz, illite and orthoclase (Palvadre et al., 1984).

High porosity and permeability of disposed rocks and sediments favours oxidation of fine-grained shale pyrite, followed by release of sulphur and heavy metals from the shale. Sulphates and heavy metals are distinguished as main pollutants, leached out from the site and entering ground water, lake Maardu and the Baltic Sea (via Kroodi gully). Analyses, however, have shown, that major part of a range of heavy metals (V, Mo, U, Cu etc.), released from the shale, is not entering watercourses according to the release rate, i.e. is adsorbed and/or precipitated within the dump. This occurs mainly because of large amounts of limestone in the dump, what buffers the acidity produced by pyrite oxidation and natural acidity of infiltrating water. Long-term performance of the dump should therefore be of serious concern because of possible depletion of buffering capacity. Due to heterogeneity of dumped material and different physico-chemical processes, regions with different characteristic mineral associations are formed within the site both in vertical and horizontal dimension. Recognition of these regions assists to find areas which may serve as geochemical barriers for different pollutants.

The aim of this study was to distinguish these regions on the light of governing physico-chemical processes together with dis-

cussion from the point of possible accumulation of pollutants according to obtained field-data. Kinetic information about these governing processes should assist to make long-term predictions in future.

Materials and methods

Approximate lithological composition of disposed rocks and sediments in Maardu South Pit dump is assessed to be: Dictyonema shale 37%, limestone 26%, glauconite sandstone 10%, quartz sandstone 18%, quaternary sediments 8%, pyrite and pyrite sandstone 1% (Naumov, 1991). Approximate mineral content calculated according to this composition appears to be: calcite 21%, dolomite 2%, quartz 33%, feldspars 11%, clay minerals 16%, pyrite 3%, glauconite 7%, organic matter 6%.

Great variations in particle sizes of dumped rock and sediment types, and consequently in particle size distributions occur throughout the site. When sandstones and quaternary sediments have quite uniform particle size distribution (dominating fraction 0.05–0.5 mm), that of limestone and Dictyonema shale varies from clay fraction to big lumps. Mine tailings were dumped on the areas of worked-out Maardu North and Maardu South pit for almost 40 years (1955–1992). Presumably, oxidation of shale pyrite in earlier dumped areas has developed further inside the dump. In addition, approximately 10% of the area has suffered under self-ignition, especially near the edges of the dump and in case of unevenness of the surface.

In order to get insight in both fast (years and tens of years) and slow (hundreds and thousands of years) developing processes, as well as to compare areas, where self-ignition has and has not been followed (self-ignition areas are easily detected by gas emissions, risen surface temperature and consequent lack of snow cover in winter), detailed survey area was chosen in Maardu South Pit. Approximate boundary between burnt and unburnt area was fixed by records of Dr. Naumov (Institute of Geology, Estonian Academy of Sciences). Tailings samples from this area were taken by author in summer 1993. Core drilling at two locations (both dumped 10 years ago, but of different distance from the edge — 10 and 200 m) was carried out by EKE EMV and core sampled in the field by author. Samples were also taken from the

levelled-up surface and from the slope of the dump. Altogether, 30 tailings samples were taken, pulverized and scanned on X-Ray diffractometers DRON. Powder diffraction patterns were compared with JCPDS files and catalogues of Tartu University Mineralogy Laboratory. In addition, 3 samples were analyzed by differential thermal analysis using Derivatograph.

Heterogeneity of the dump, as well as heterogeneity of drilling core material made questionable representativeness of core sampling. To overcome this problem, material with grain size <1mm was comparatively analyzed from both drilling cores at different depth intervals, assuming that a large part of this fraction originates from decomposition of the shale. This assumption was controlled by determination of concentrations of other minerals (quartz, illite, orthoclase) which occur in the shale in characteristic ratios. Shale particles and new-formed minerals from different depths were analyzed separately.

Representative sampling of surface layers and the slope of the dump was also complicated due to visible heterogeneity of the material. Dictyonema shale and soil samples were taken from different locations on the surface. Visually fixed new-formed minerals from the cover layer of the shale lumps were analyzed. Samples taken from the slope represented clayey material of different colour (yellow, white, green), formed in the process of weathering of the shale and other rocks.

Except X-Ray powder diffraction analysis, all samples were semi-quantitatively analyzed for wide range of elements (Si, Al, Fe, Mg, Ca, Sc, Ti, V, Cr, Mn, Co, Ni, Cu, Pb, Zn, Mo, Ag, Sn, Li, B, Be, Sr, Ba, P, U, Zr, Nb, La, Ce, Gd, Dy, Ho, Er, Yb, Y, Ga, Ge, As, Tl, W) using plasma emission spectroscopy in the Laboratory of Geological Survey of Estonia. This was done in order to make preliminary assumptions about possible anomalies. From these elements, Fe, V, Co, Ni, Cu, Zn, Mo, P and U were chosen to be further discussed on the basis that

(i) concentration of element may produce environmental hazard, and/or

(ii) concentration of element in particular location in the dump cannot be explained by heterogeneity only (i.e. accumulation is taking place).

All the data were overlooked from theoretical approach discussing governing physico-chemical processes and their possible impacts in both short- and long-term.

Results

Summarized results of drilling core and soil samples analyses are given in Table. These data are used to discuss possible redistributions of pollutants within the site, and their migration into watercourses.

Drilling cores (samples 1–21 in Table).

Minerals. Pyrite (FeS_2), gypsum ($CaSO_4 \cdot 2H_2O$) and anhydrite ($CaSO_4$) were used as indicators of processes. Anhydrite was found in the region of supposed hot spot only (see samples 13, 14, 20, 21 in Table). Semi-quantitative analysis methods enabled to determine percentage of these minerals in each sample. Approximate assessment of pyrite oxidation was done by quantitative comparison of pyritic iron content with total iron in the sample. These results are presented on Figure 1. Other determined minerals were quartz, illite, feldspars, glauconite, apatite, chlorite, and calcite.

Elements. After 10 years of changes, V, Mo and U do not tend to concentrate in higher concentrations than those in original shale. Concentrations of Fe in observed hot spot are higher than in upper layers. Below hot spot, in dolomite- and calcite-rich layers, Co, Ni and Zn are observed to be concentrating (see sample 14 in Table). The same phenomena is followed in sulphate covers of limestone lumps in the hot spot area (see sample 21).

Surface, slope and near-by ditch of the dump.

On the levelled-up surface of the dump, water is leaching elements from the shale into the dump. Jarosite is observed to be formed in a cover layer of shale lumps with considerable amounts of V and Mo carried into the dump (see samples 22 and 23 in Table). On overall scale, however, importance of this phenomena is insignificant. On the slope of the dump, surface runoff and exit of water from inside the dump are also important. This allows formation of new minerals, especially jarosite, gypsum, smectite and amorphous ferric hydroxide. Presence of ferric hydroxide was determined in samples 24–26 by differential thermal analyses. Concentrations of other metals except iron in these sediments are not significantly higher than those in original Dictyonema shale. In the peat of near-by ditch, Zn and P tend to concentrate (see sample 27 in Table).

	1	2	3	4	5	6	7	8	9	10	11	12	13	14	15	16	17
	Location	Type	Depth,m	Fe, %	V, ppm	Co, ppm	Ni, ppm	Cu, ppm	Zn, ppm	Mo, ppm	P, ppm	U, ppm	Main minerals	Py %	Gy %	Anh %	Py/Fe
1	DC 1	fr <1mm	1,1	4,8	600	10	60	100	100	200	1000	40	Q,Or,Ill,Gy	1,6	12,4	0	0,3
2	DC 1	fr <1mm	1,8	4,9	600	6	60	80	120	100	nd	nd	Q,Or,Ill Gy	2,5	7,9	0	0,5
3	DC 1	fr <1mm	2,4	1,4	600	3	25	30	60	80	nd	nd	Q,Or,Ill,Gy	2,2	5	0	1,6
4	DC 1	fr <1mm	3,1	2,8	300	6	40	60	80	60	2000	nd	Q,Or,Ill,Gy	3,2	20	0	1,1
5	DC 1	fr <1mm	6	2,1	200	9	50	80	40	30	6000	nd	Q,Or,Ill,Py	4,4	0	0	2,1
6	DC 1	fr <1mm	8,2	2,6	150	9	40	80	100	30	8000	nd	Q,Or.Ill,Py,Ap	5,7	0	0	2,2
7	DC 1	Dict shale	0,9	2,8	400	6	60	150	150	300	nd	40	Q,Or,Ill	2,9	0	0	1,0
8	DC 1	Dict shale	1,8	2,1	600	8	80	60	600	80	nd	nd	Q,Or,Ill,Py	4,5	0	0	2,1
9	DC 1	Dict shale	2,4	3,5	600	8	80	100	100	150	nd	nd	Q,Or,Ill	3	2,7	0	0,9
10	DC 1	Dict shale	3,1	2,1	400	8	80	100	100	80	nd	nd	Q,Or,Ill	4,3	0	0	2,0
11	DC 2	fr <1mm	2,5	3,5	600	10	70	100	200	35	nd	nd	Q,Or,Ill	3,9	0	0	1,1
12	DC 2	fr <1mm	5,7	5,6	400	10	80	100	300	100	300	nd	Q,Or,Ill	4,5	4,9	0	0,8
13	DC 2	fr <1mm	7,2	10,5	200	15	60	50	150	30	600	nd	Q,Or,Ill,Anh	0	4,1	9,6	0,0
14	DC 2	fr <1mm	9,1	5,5	300	40	200	60	1500	40	2000	nd	Do,Ka,Ill,Gl	0	0	5,8	0,0
15	DC 2	fr <1mm	11	4,2	200	7	60	80	150	40	10000	nd	Q,Ill,Or,Py	7,2	2,1	0	1,7
16	DC 2	fr <1mm	12,7	2,8	200	8	60	80	200	40	4000	40	Q,Ill,Or	3	4,7	0	1,1
17	DC 2	fr <1mm	14	2,9	100	6	25	25	70	7	3000	nd	Q,Ka,Do,Or,Gl	0	0	0	0,0
18	DC 2	Dict shale	2,5	2,8	600	13	100	100	250	60	nd	40	Q,Or,Ill	4,6	0	0	1,6
19	DC 2	Dict shale	5,7	2,6	1000	10	90	130	250	150	nd	60	Q,Or,Ill	4,2	0	0	1,6
20	DC 2	Dict shale	7,2	5,6	500	8	60	100	100	60	nd	40	Q.Or,Ill	2,6	6,1	3,2	0,5
21	DC 2	Gy cover	7,2	10,5	250	40	300	20	2000	8	3000	nd	Gy,Anh,Q,Ill	0	28	14	0,0
22	Surface	Dict shale	0	2,8	800	4	40	30	40	100	nd	nd	Q,Or,Ill,Jar	0	0	0	0,0
23	Surface	Dict sh cover	0	2,7	300	3	20	40	30	60	nd	nd	Q,Or,Ill,Jar	0	0,8	0	0,0
24	Slope	yellow clay	0	5,5	250	7	40	40	200	250	nd	40	Q,Jar,Gy,Sm,Ill	0	20	0	0,0
25	Slope	Gy cover	0	10,4	150	10	40	60	300	40	2000	nd	Gy,Q,Ill,Jar	0	35	0	0,0
26	Slope	brown cover	0	14	100	10	40	70	200	25	6000	nd	Gy,Ill,Q	0	30	0	0,0
27	Ditch	peat	0	1,1	10	10	20	80	1000	10	40000	nd	Ka,Q	0	0	0	0,0
	DETECTION	LIMIT		0,1	3	3	1	1	10	1	300	40		1	0,8	2	

Table 1. Selected data of solid phase analyses. Minerals: Q-quartz, Or-orthoclase, Ill-illite, Py-pyrite, Gy-gypsum, Ap-apatite, Jar-jarosite, Sm-smectite, Ka-calcite, Do-dolomite, Gl-glauconite. DC1-drilling core 1 (in the middle part), DC2-drilling core 2 (near the slope).

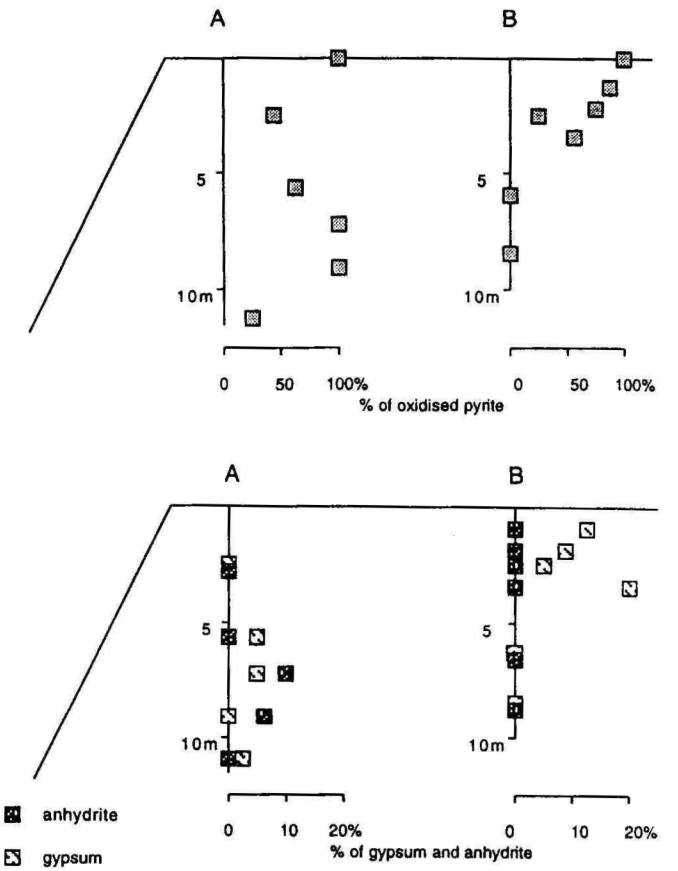

Fig. 1. Schematic diagram of pyrite oxidation and content of calcium sulphates in drilling core materials from near the edge (A) and in the middle (B) of the dump.

Governing physico-chemical processes

Oxidation

The fine-grained character of the shales (1–10μ) determines, that rate limiting factor of pyrite oxidation should be either reaction kinetics, micropore diffusion in shale particles, or macroscopic transport of oxygen by diffusion and convection into the dump. On the surface and upper layers of the dump, kinetics and diffusion of oxygen through shale particle pores are rate limiting, domination of one or another depends from shale particle size. Inside the dump, macroscopic transport of oxygen through porous media of the dump appears to be rate limiting. In middle parts of the site (over several tens of meters from the edge), oxidation of pyrite is controlled by oxygen diffusion, accompanied by moderate temperature rises (20–30°C) inside the dump. Near the edges of the dump, however, convective air currents cause self-ignition of disposed material with temperature rises over 200°C. Schematic diagram of the dump showing governing processes in three different zones is presented on Fig.. 2.

Zone 1: Surface and upper layers of the dump. Reaction rate of pyrite oxidation is limited by reaction kinetics or oxygen diffusion in shale particles. On the surface, characteristic time scale of shale pyrite oxidation ranges from several months to several years. Bacterial activity and climatic conditions are most important.

Zone 2: Deeper layers in the middle of the dump. Reaction rate of pyrite oxidation is limited by oxygen diffusion through porous media. Reaction front is moving towards the depth, but this front is not sharp. Oxygen transport is a two-stage process, diffusion through the pore space of the dump followed by diffusion into reaction sites within the shale particles comprising the dump, second stage however contributes insignificantly to characteristic time scale of oxidizing all shale pyrite in Maardu (several hundreds of years). Temperature is risen due to heat released in pyrite oxidation for about 20–30°C.

Zone 3: Deeper layers near the edges of the dump. Diffusion-caused temperature rise induces convective air currents, which are going to dominate in oxygen transport within this zone, if permeability is high (in order of 10^{-9}–10^{-10} m^2). When temperature is risen up to 60–70°C, organic matter starts actively

participate in oxidation reaction, leading to self-ignition with temperature rises of hundreds of degrees. Characteristic time scale of 'hot spot' formation in Maardu is few years, however it may range from several months to tens of years (Pihlak, 1986). Location and size of each 'hot spot' depends from configuration of the dump edge and heterogeneity of disposed material. In Maardu case self-ignition is often followed along all continuity of the edge. Front between this and other zones is sharp, with transition layers.

Reactions

At low temperatures, overall reaction of pyrite oxidation in Maardu may be expressed as

$$FeS_2 + 15/4\ O_2 + 7/2\ H_2O + 4\ H^+ + 2\ SO_4^{2-} \quad (1).$$

This reaction is catalyzed by bacteria *Thiobacillus ferrooxidans* or *Thiobacillus thiooxidans*. Acidity produced in reaction (1) is neutralized by calcite, the main mineral in limestone from overburden, disposed mixed with the shale; at low temperatures, gypsum is produced:

$$H_2O + CaCO_3 + H_2SO_4 = CaSO_4 \cdot 2H_2O + CO_2\ (g) \quad (2).$$

Reactions (1) and (2) contribute to temperature rises in zones 1 and 2, and to initial temperature rise in zone 3. In hot spots, overall reaction of pyrite oxidation and anhydrite formation may be expressed as

$$FeS_2 + (6+x/2)\ O_2 + 2\ CaCO_3 = 2\ CaSO_4 + 2\ CO_2 + FeO_x \quad (3),$$

where x is 1, 4/3 or 3/2 depending from availability of oxygen, with wuestite (FeO), magnetite (Fe_3O_4) or hematite (Fe_2O_3) formed, respectively. If temperature in hot spot exceeds 800–900°C, calcite decomposes:

$$CaCO_3 = CaO + CO_2 \quad (4).$$

When hot spot is cooled down, CaO and $CaSO_4$ react with water, with portlandite ($Ca(OH)_2$) and gypsum formed:

$$CaO + H_2O = Ca(OH)_2 \quad (5);$$

$$CaSO_4 + 2\ H_2O = CaSO_4 \cdot 2H_2O \quad (6).$$

Reaction (6) may have temporary stage with $CaSO_4 \cdot 0.5H_2O$ formed.

Overall complex of reactions, especially range of those occurring in hot spots at different temperatures, is much more complicated, as shown for example in Veski et al., 1990. Analyze of presence of minerals, formed according to reactions (1)–(6),

however, allows to make simplified assumptions about processes, taking place inside the dump. New-formed calcium and iron minerals are used as indicators to describe these processes.

Leaching

The leaching of a wide range of metals depends on the oxidation of largely insoluble metal sulphides to the much more soluble sulphates. Best practice of alum shale handling has shown, that engineered barriers for the prevention of weathering reduce leaching rates of metals such as Fe, Cu and Ni by several orders of magnitude (Allard et al., 1991). Experiments carried out to determine leaching rates of metals from Dictyonema shale ash show considerable rise in leaching rates of U and V in comparison with unburnt shale (Palvadre, Kleemeier, 1982). Leaching rates are higher also from unburnt shale at risen temperatures (Palvadre et al., 1990). Hence hot spot areas appear to be significantly increasing pollution load from the dump in short term. Reactions (2) and (3) however define buffering capacity inside Maardu dump. The pH of leachate from the site has been recorded to range from 7.4–8.3 (Naumov, 1991). According to approximate calculations, 1 000 000 kg of SO_4^{2-}, 300 000 kg of Ca^{2+}, 150 000 kg of Mg^{2+} and 500 kg $Fe^{2+,3+}$ is leached out from 1 sq km of the pit per year (Naumov, 1991). Assuming that most of sulphur and iron originates from pyrite, mobility (here defined as amount of element in pyrite carried out from the site per unit of time) of S in form of SO_4^{2-} is somewhat 600 times higher than mobility of $Fe^{2+,3+}$. Iron and supposedly a range of other metals released from the shale after pyrite oxidation (including some potentially hazardous ones) remain in large extent trapped inside the dump through precipitation and adsorption. Mass balance according to reactions (1) and (2) interpolated on all waste rock material shows excess of calcite for about 3–6 times (for different sites) in order to neutralize all acidity produced by pyrite oxidation. Limestone, however, is dumped mainly as big lumps, cover layer of which only participates in these reactions. This is a subject of serious concern regarding to dump performance in long term. When rates of pyrite oxidation and acidity generation are relatively easily predictable, assessment of buffering capacity and the rate of its depletion appears to be complicated, and most significant regarding to the dump performance.

Discussion

Based on theoretical approach and analyses of samples from Maardu site, summarized prediction of accumulation and leaching of elements, ions, or complexes is given on Fig. 3.

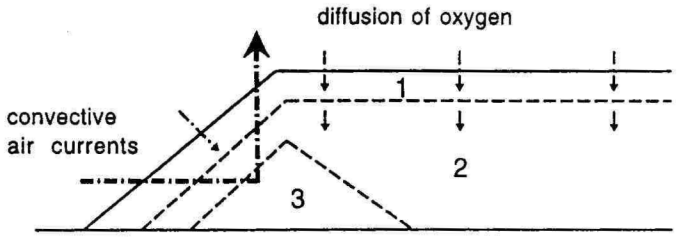

Fig. 2. Schematic diagram of Maardu dump zonation depending on character of oxidation.
Zone 1: surface and upper layers, zone 2: deeper layers in the middle, zone 3: deeper layers near the edges.

In long term, overall performance of Maardu dump is mainly affected by processes inside the dump in the middle areas (see zone 2 on Fig. 2), as contaminants from upper layers will be leached downwards by infiltrating water. Main phenomena to account for in consideration of possible barriers for pollutants in this zone are:

(1) Slowly downwards moving redox front (according to preliminary assumptions, 5 cm/yr as average; see (1) on Fig. 3);

(2) Sharp pH front mainly depending on location and particle size of disposed limestone (Fig. 3, (2));

(3) Increasing towards depth (until redox front, where exothermal reactions occur) temperature of disposed tailings (gradient in order of 3–10°C per m with maximum temperature rise of 30°C);

(4) Slowly decreasing towards depth temperature beneath the redox front, and decreasing temperature of the groundwater when moving to surroundings;

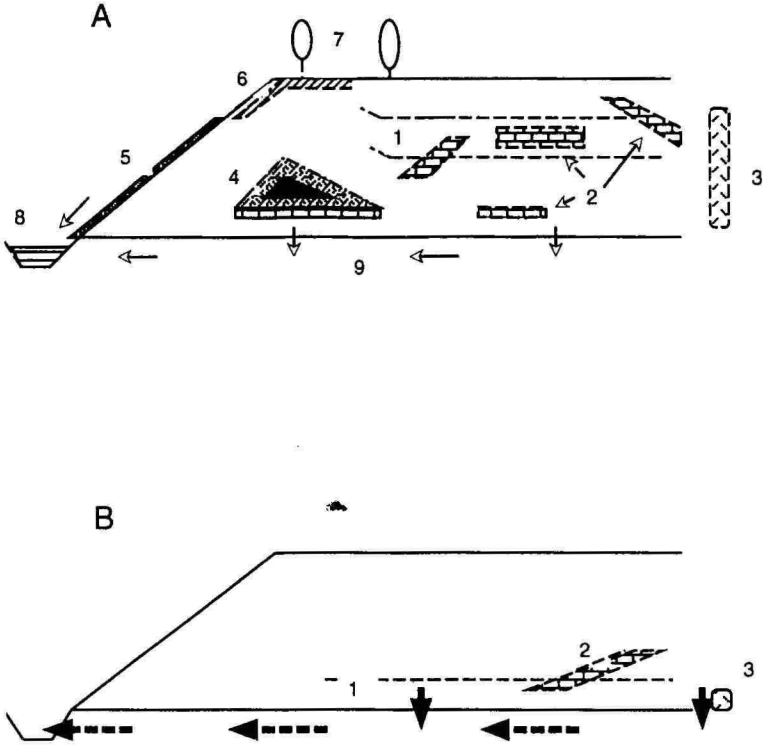

Fig. 3. Short-term (A; during tens of years) and long-term (B; hundreds and thousands of years) accumulation and migration of possible contaminants in Maardu.

1 – redox front inside the dump; 2 – buffering capacity of limestone, 3 – adsorption capacity, 4 – self-ignition hot spot; 5 – redox front on the slope; 6 – precipitation from hot gases; 7 – bioaccumulation in plants; 8 – accumulation in near-by ditch; 9 – migration.

(5) Adsorption capacity of different types of disposed materials, in most cases a function also of pH and redox potential (Fig. 3, (3)).

Other main items to discuss are bacterial activity, heterogeneity of the dump, possible channeling in contaminant transport, and seasonal variations in oxygen supply (for pyrite oxidation) and water supply (for contaminant transport). However, assuming, that accumulation of particular contaminant is favoured by any of listed above mechanisms or their interaction (through precipitation, coprecipitation or adsorption), rates of release of these contaminants into groundwater and surface water bodies should be expected to increase after certain time period, when breakthrough occurs. Hence calculations to predict time scale of leaching out certain contaminant according to presently measured concentrations (Naumov, 1991) could be misleading. Long term behaviour of the dump has to be assessed in complex way with special attention to possible depletion of pH buffering capacity and adsorption capacity inside the dump. Decrease of pH leads inevitably to dissolution and desorption of accumulated elements (see Fig. 3, b). Assessment has to be carried out, how seriously Maardu dump should be considered as 'geochemical time bomb'.

In short term, surface runoff from slopes and leachate originating from cooled-down hot spots (see Fig. 3, (4)) are significantly contributing into pollution load from the site. Places on the slope were waters from the dump are reaching the surface should be surveyed for redox barriers (Fig. 3, (5)). In deeper layers near the edges of the dump, where hot spots occur (zone 3 on Fig. 2 and (4) on Fig. 3), wide range of different reactions takes place. Important is to assess thermal decomposition of Dictyonema shale organic matter in anaerobic conditions, which produces liquid and gaseous organic contaminants. Hot gases emitted during burning are impeding both infiltration and pyrite oxidation in upper layers. Hence concentration of pyrite in upper layers near the edges of the dump may be even higher than that in the middle of the site (see Fig. 1). Precipitation of elements from hot gases is also possible (Fig. 3, (6)). On the surface of the site, plants uptake certain range of elements (Fig. 3, (7)), what is also important to analyze because of possible land use problems. Some ions however (Ca^{2+}, Mg^{2+}, SO_4^{2-}) tend to migrate into surface water bodies and groundwater (Fig. 3, (9)). Tendency of

peat in near-by ditch to adsorb pollutants (Zn, P) needs also to be followed (Fig. 3, (8)).

Geochemical zonation

Majority of studies of metal pollution from waste dumps and mining sites have focussed on division of metals, ions and complexes according to decreasing mobility, determined from leachate samples and overall dump mass balance. Based on these data, time scale of leaching out of particular contaminant may be calculated. In particular cases, these calculations make misleading and even dangerous assumptions about performance of the dump in long term. Much less data is available about actual processes and developing fronts inside the dump. Because of heterogeneity and variety of disposed materials, it is economically unfeasible to carry out representative sampling on the site, as well as to include all data in calculations using geochemical codes. There are some processes however which can be quite easily described and rate of which is possible to calculate, as for example pyrite oxidation reaction controlled by macroscopic oxygen transport mechanisms in Maardu case. Using theoretical approach, geochemical zonation of a dump may be carried out, getting overview of main processes, reactions and developing fronts. Then, more or less representative sampling of the site may be done. On the basis of theoretical information bound with actual empirical representative data from the site, predictions can be given.

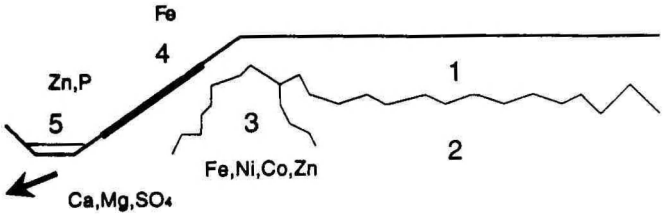

Fig. 4. Geochemical zonation of Maardu dump with elements accumulating in these zones in short-term.
1 – upper layer, 2 – bottom layer; 3 – self-ignition areas; 4 – slopes; 5 – ditches.

Available data and theoretical considerations allow to divide Maardu dumps into following geochemical zones (see Fig. 4):

1. Upper layer of the dump. Aerobic conditions. Shale pyrite oxidized, iron hydroxide and sulphuric acid produced. In case of availability of reactive limestone, gypsum is precipitated and heavy metals coprecipitated and/or adsorbed. Lack of limestone and depletion of its buffering capacity followed by leaching of metals towards depth. Heterogeneity of the dump depends on distribution and particle size of dumped limestone and distribution of Dictyonema shale, complicating the predictions. Zone develops towards depth with decreasing velocity, supposedly reaching bottom layers in 200–300 years. Bacterial activity determines the kinetics of pyrite oxidation. Surface temperature is 10–20°C higher than average atmospheric. Temperature increases towards depth. On the surface, bioaccumulation of elements in plants.

2. Bottom layer of the dump. Anaerobic conditions. Shale pyrite not yet oxidized. Some of metals and acidity from upper layer enters this layer. In case of availability of reactive limestone, acidity is neutralized. Precipitation can also occur due to anaerobic conditions only. Temperature controlled by oxygen diffusion, normally being 30–50°C in this layer. Leachate leaving this layer in short term is rich in SO_4^{2-}, Ca^{2+} and Mg^{2+}.

3. Self-ignition regions near the edges of the dump. Three stages may be separated in development of particular hot spot: incubation period with temperature rise until 70–80°C (only pyrite oxidizes), burning (active oxidation of organic matter) and cooling down. When cooled down (in order of tens of years after disposal), active leaching of metals starts from these regions, depending again from availability of limestone. Near the hot spot, thermal destruction of shale organic matter in anaerobic conditions may occur, producing liquid and gaseous organic substances-contaminants. In limestone-containing layers below cooled-down hot spot, Zn, Co and Ni are accumulating. Leaching from these regions contributes significantly to total pollution load in short term, as sulphates are formed in high rate.

4. Slopes of the dump. New-formed minerals (jarosite, gypsum, mixed-layer illite-smectite) occur in large extent. Clayey sediments are rich in Fe^{3+} (6–14%), precipitating in the form of amorphous hydroxide, and partly in jarosite, slope serving as redox front for outcoming waters. Concentration of metals (V, Mo, Cu, Ni, Zn) in these sediments on the slope of 10 years age however appear to be less than in original shale.

5. Ditches near the dump. Mine transport roads are in many cases presently serving as ditches filled or seasonally filled with water. In the bottom of these ditches, mud or peat is formed. Zn and P accumulate.

Conclusive remarks

Geochemical zonation of Maardu dump was carried out using theoretical approach and very few field analyses to describe an area of 10 sq km. These data should serve as preliminary ones for more detailed investigations. Key-question stands, how to account for buffering capacity of limestone with variable particle size in heterogeneous dump, assuming 3–6 times excess of limestone on overall scale in order to neutralize all acidity produced. Problems are not depleted in long term when all pyrite is oxidized and supposedly all acidity neutralized because of relatively low pH of natural precipitation (rainwater and snow melting water).

Regarding to pollution problems, V, Mo and U were considered as possible contaminants from the shale because of their initially high concentration in comparison with average in Earth crust. Analyses show, that these elements are not accumulating in larger concentrations as those in original shale after 10 years of changes in the dump. From environmental point however even several times lower than in the shale concentrations may possibly produce environmental hazards. This question needs to be separately discussed.

References

Allard B., Arsenie I., Håkansson K., Karlsson S., Ahlberg A.-C., Lundgren T., Collin M., Rasmuson A., Strandell E., 1991. Effects of weathering on metal releases from an engineered deposit for alum shale leaching residues. Water, Air and Soil Pollution, vol. 57–58, p. 431–440.

International Centre for Diffraction Data, 1988. Powder Diffraction File, Inorganic Phases. Swarthmore, USA.

Maremäe, 1988 – **Маремяэ Э.**, 1988. О возможности использования Эстонского диктионемового сланца в национальной экономике. Горючие сланцы, т. 5, 1, с. 407–417.

Naumov, 1991 – **Наумов Б. Е.**, 1991. Загрязнение гидросферы при выщелачивании диктионемовых аргиллитов в отвалах Маардуских фосфоритных карьеров. Горючие сланцы, т. 8, 3, с. 266–274.

Palvadre et al. 1990 – **Палвадре Р., Ахелик В., Раявее Э., Юга Р.**, 1990. Некоторые вопросы водного выщелачивания агриллитов. Изв. АН ЭССР, Хим., 39, 4, с. 235–241.

Palvadre, Kleemeier, 1982 – **Палвадре Р., Клээмейер Т.**, 1982. Выщелачиваемость некоторых тяжелых металлов из агриллитов. Изв. АН ЭССР, Хим., 31, 4, с. 243–248.

Palvadre et al, 1984 – **Палвадре Р., Утсал К., Ахелик В., Халдна Ю.**, 1984. Исследование минерального состава граптолитового аргиллита Эстонии. Горючие сланцы, т. 1, 2, с. 162–170.

Pihlak, 1986 – **Пихлак А. А.**, 1986. Критическая и допустимая температура самонагревания диктионемового аргиллита. Горючие сланцы, т. 3, 3, с. 247–155.

Pukkonen, 1989 – **Пукконен Э.**, 1989. Макроэлементы и малые элементы в граптолитовом агриллите Эстонии. Горючие сланцы, т. 6, 1, с. 11–18.

Veski et al., 1990 – **Вески Р., Щербакова Е., Баженова Л.**, 1990. Аммониево-сульфатная техногенная минерализация в горелых отвалах Маарду. Изв. АН ЭССР, Хим., 39, 3, с. 179–184.

MAARDU PUISTANGUTE GEOKEEMILINE TSONEERIMINE

Erik Puura

Resümee

Aastakümneid kestnud fosforiidi pealmaakaevandamine Maardus on viinud keskkonna reostumiseni, mille põhjustajaks on fosforiidikihi katendis sisalduv ja endisele karjäärialale tagasi kuhjatud *Dictyonema* argilliit. Argilliidis sisalduv püriit on atmosfääritingimustes ebastabiilne, reageerides hapniku ja veega. Oksüdeerumise tagajärjel tekivad sulfaadid, argilliit laguneb ja raskmetallid, mille sisaldus argilliidis on anomaalselt kõrge (U, Mo, V), vabanevad. Oksüdeerumisel eralduv soojushulk puistangute kuumenemiseni. Puistangute keskosas, kus hapniku juurdekannet kontrollib hapniku difusioon, jääb temperatuuritõus 20–30°C piiresse; puistangute äärealadel ja suurte lõhede või ebatasasuste olemasolul puistangu pinnal võivad tekkida konvektiivsed õhuvoolud. Need kiirendavad oksüdeerimisreaktsiooni, tagajärjeks on isesüttimine, kuna temperatuuridel 70–80°C algab argilliidis sisalduva orgaanilise aine (kerogeeni) aktiivne oksüdeerumine.

Puistangu üldises arengus võib eristada lühema- (aastad ja kümned aastad) ja pikemaajalisi (sajad ja tuhanded aastad) protsesse. Aastate ja kümnete aastate jooksul akumuleeruvad isesüttimiskollete alla jäävates kihtides (Zn, Fe, Co, Ni, orgaanilised ained), puistangute nõlvadel (Fe), ümbritsevates kraavides (Zn, P), isesüttimiskollete kohal (väljasettimisel gaasidest) ja puistangutaimedes (bioakumulatsioon) reoained. Toimub sulfaatiooni aktiivne väljakanne puistangualalt. Puistangute keskosas kulgeb redoksfront (keskmiselt 5 cm aastas) puistangute põhja suunas. Seoses puistangutesse kuhjatud lubjakivi neutraliseeriva toime tõttu püriidi oksüdeerumisel tekkinud väävelhappesse ja anaeroobsetele tingimuste tõttu puistangu sügavuses ei toimu esimeste aastakümnete jooksul raskmetallide aktiivset väljakannet. Puistangute heterogeensust arvestades on raske ennustada, kas lubjakivide puhverdusvõimest piisab kogu tekkinud happe neutraliseerimiseks. Arvestades aga, et 100–300 aasta pärast on redoksfront jõudnud puistangu alumistesse kihtidesse ning vihma- ja lumesulamisvesi on pidevalt happelise reaktsioo-

niga, võivad puistangud aastasadade möödudes olla ümbritsevale keskkonnale suuremaks ohuks kui praegu. Seetõttu ei ole korrektne leida mingi elemendi väljaleostumisaeg, viidates praegusele väljakande intensiivsusele.

Praegu võib puistanguala jagada viieks geokeemiliseks tsooniks: (1) ülemised kihid, kus argilliidi püriit on juba oksüdeerunud; (2) alumised kihid puistangu keskosas, kus valitsevad anaeroobsed tingimused; (3) isesüttimiskollete piirkond; (4) nõlvaalad; (5) ümbritsevad kraavid. Selle teoreetilis-praktilise tsoneerimise alusel on võimalik teha detailsemaid uuringuid selgitamaks reoainete akumuleerumist ja leostumist ning koostamaks pikemaajalisi prognoose.

COMPOSITION OF CARBONATE ROCKS OF THE IDAVERE, JÕHVI AND KEILA REGIONAL STAGES (VIRUAN, ORDOVICIAN) IN EAST ESTONIA

Leho Ainsaar

Introduction

The composition of Estonian Paleozoic carbonate rocks has been studied for long period on the level of major components. During the official geological mapping of the territory of Estonia, taken place from 1960-s to 1980-s, a huge amount of analyses was made for many microelements from hundreds of boring cores. Most of these analyses, mainly semi-quantitative spectral analyses with abbreviated chemical analyses, were made in the laboratory of Geological Survey of Estonia in Tallinn. This material is partly analyzed statistically and published by P. Vingisaar, T. Kiipli, et al. (Vingisaar et al., 1979; 1981; Kiipli et al., 1984).

The aim of this study was to follow the distribution of major and minor elements in one sedimentary complex, limited in North Estonia by considerable discontinuity surfaces in the upper and lower boundary. This complex, including the Idavere, Jõhvi and Keila stages, is described as a distinct macrocyclite (Kõrts et al., 1991) and can be possibly subdivided into two mesocyclites. The upper mesocyclite (upper part of the Jõhvi Stage and Keila Stage) differs from lower one by clear microcyclic subdivision consisting up to 25 limestone-argillaceous limestone (or marl) cycles, traced in the whole extent of North-Estonian confacies belt (Ainsaar, 1992; 1993).

Carbonate rocks of the Idavere, Jõhvi and Keila stages formed lithostratigraphically Kahula Formation (Resheniya..., 1978), or Kahula Group (Resheniya..., 1987) by previous stratigraphic charts; later this name was used only for rocks of the Jõhvi and Keila stages (Männil, 1990). In this study the name of Kahula Group is used in its initial size to mark the whole Idavere-Keila complex in North Estonia. The complex is characterized by more or less argillaceous, wavy-bedded or semi-nodular limestone

(mainly wackestone) with intercalations of marl and several thin K-bentonite layers. The thickness of the Kahula Group is 30–50 m.

Material and methods

Many boreholes were drilled through the Ordovician in geological mapping of Jõgeva District (East Estonia) of scale 1 : 50 000 by Geological Survey of Estonia in late 1980-s. For this study 93 samples were collected from 28 m of section of boring core Tähkvere-704 and 4 additional samples from the Keila Stage of boring core Vaali-707 (Fig. 1).

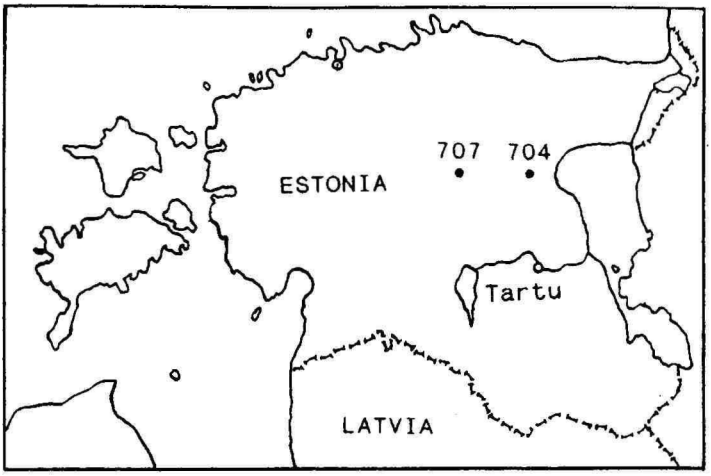

Fig. 1. Location of boreholes Tähkvere-704 and Vaali-707.

The samples were analyzed for 42 chemical elements and for insoluble residue in the laboratory of Geological Survey of Estonia in Tallinn in 1990. Main components of rock (CaO, MgO and insoluble residue) were determined by abbreviated chemical analysis. For Pb, Sr, Rb, Y and Zr the samples were analyzed by X-ray fluorescence spectroscopy and for Si, Al, Fe, Na, Ti, B, Ba, Ga, Sc, V, Cr, Mn, Co, Ni, Cu and Yb by spectral analysis. Determinations of 18 elements contained in many samples concentrations below

the limit of detection and were ignored in this study. Content of CO_2 was also excluded because it is occurring only in compounds with Ca and Mg in the limestones. The methodology, limits of detection and variations of results for spectral analysis in the laboratory of Tallinn are described by Vingisaar et al. (1981) and Kiipli et al. (1984).

The chemical data was subjected to statistical analyses. Basic statistics such as mean and variance were calculated for each element in lithologically different parts of the complex and correlation analyses were performed on the whole group. Factor analysis was used to group the elements to associations.

Statistical results

Correlation graph of linear pairways correlation coefficients and factor analysis showed the occurrence of following associations of chemical elements in the limestone and marl of the Kahula Group in East Estonia (samples of K-bentonites were excluded):

I. Terrigenous association: Rb, Zr, Ga, Cr, V, Ti, Si, B, Co, Y, Ba, Na, Sc, Fe, Yb, Ni, Cu and Al (in the order of correlation coefficient with content of insoluble residue);

I.a. Clay association: Al, Si, Ba, Rb, Cr, Ga, Yb, Zr, Ti and Sc (in the order of coefficients with Al);

I.b. Iron association (pyrite): Fe, Co, V and Ni;

II. Dolomite association: Mg, Mn, (Fe);

III. Calcite: Ca;

IV. Sr;

V. Pb.

These results are generally similar to data of the whole Ordovician and Silurian carbonate complex of Estonia (Vingisaar et al., 1981; Kiipli et al., 1984) and show that the distribution of majority of studied elements depends on content of argillaceous material in the rocks. The only notable difference is clear relation of yttrium, considered by Kiipli et al. (1984) to be related with phosphates, with terrigenous association, which may be explained by very small concentration of phosphorus (<0.06% of P) in the studied rocks.

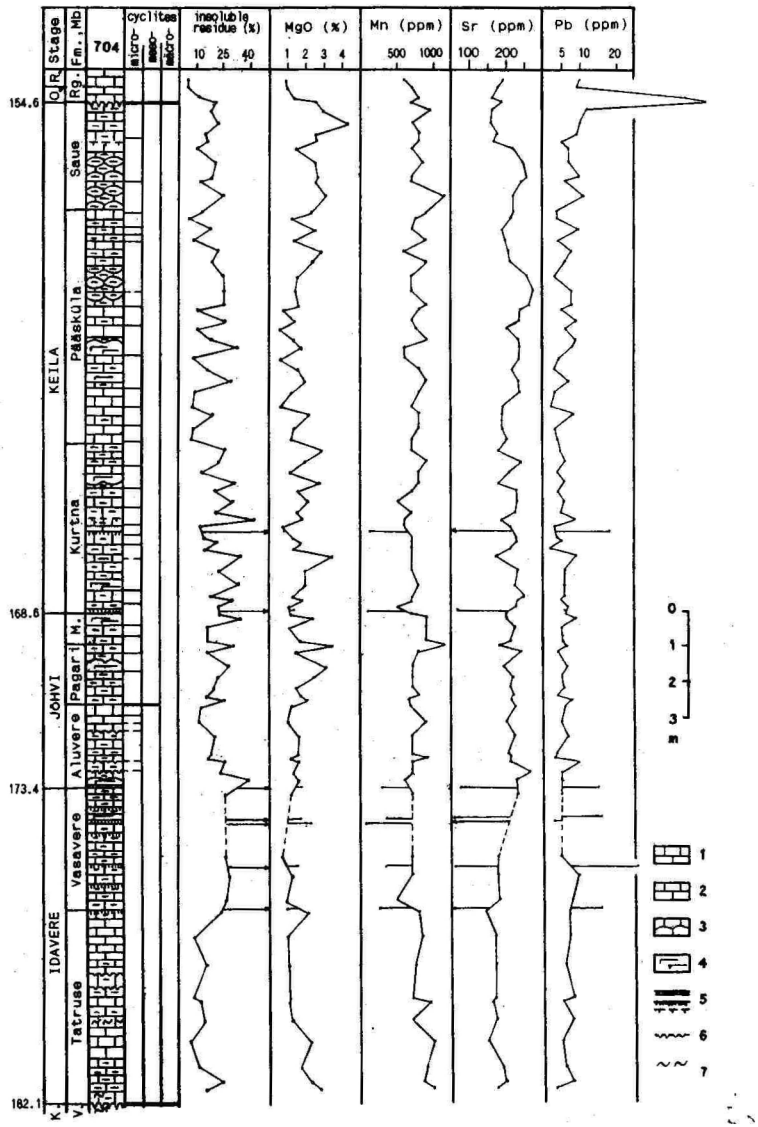

Fig. 2. Distribution of insoluble residue and elements in the boring core Tähkvere-704. Values corresponding to the K-bentonites are shown out of the curve;

1 – limestone; 2 – argillaceous limestone; 3 – semi-nodular structure; 4 – marl; 5 – K-bentonites; 6 – discontinuity surface; 7 – kukersite. Regional stages: K. – Kukruse; O. – Oandu; R. – Rakvere. Formations and members (Fm., Mb.): V. – Viivikonna; M. – Madise; Rg. –Rägavere.

Table 1. Mean and standard deviation of insoluble residue (i.r.) and elemental concentrations in boring cores 704 and 707 by traditional lithostratigraphic units, in the whole Kahula Group (carbonate rocks only) and in K-bentonites (in ppm unless otherwise noted; number of samples in parentheses; methods: oxides – by chemical analysis, * – by X-ray fluorescence spectroscopy, all others – by spectral analysis)..

	Tatruse	Vasavere	Aluvere	Pagari, Madise & Kurtna	Pääsküla	Saue	Kahula Group	K-bentonites
	(10)	(4)	(8)	(30)	(23)	(12)	(87)	(7)
1	2	3	4	5	6	7	8	9
i.r. (%)	13.9±5.9	27.0±1.3	20.5±8.9	22.7±7.7	16.2±8.3	17.7±4.1	19.3±7.9	85.9±3.0
CaO (%)	44.4±4.1	38.1±1.0	41.4±5.9	38.8±5.7	43.7±5.8	39.6±4.4	41.1±5.6	1.9±1.1
MgO(%)	1.6±0.7	1.0±0.3	1.4±0.3	1.8±0.7	1.5±0.6	3.7±2.4	1.9±1.3	1.2±0.4
Si (%)	10±5	20±8	14±5	16±6	11±7	11±4	13±6	
Al (%)	2.9±1.6	2.6±0.5	3.3±1.4	3.8±1.5	2.5±1.6	3.2±1.5	3.2±1.5	15.1±2.0
Fe (%)	1.2±0.4	1.0±0.4	1.4±1.1	1.7±0.9	1.1±0.7	1.5±0.8	1.4±0.8	5.4±2.0
Na (%)	0.10±0.02	0.12±0.02	0.10±0.03	0.12±0.03	0.11±0.03	0.10±0.02	0.11±0.03	0.16±0.01
Ti (%)	0.15±0.04	0.17±0.04	0.16±0.03	0.17±0.04	0.15±0.04	0.15±0.03	0.16±0.04	0.32±0.11
Pb*	6± 2	7±2	6±2	6±2	6±2	12±11	7±5	14±8
Sr*	166±16	190±27	220±20	214±22	220±25	186 ±52	206±33	58±11
Rb*	20±11	28±8	29±12	39±18	26±18	27±7	30±17	98±12
Y*	17±2	18±3	17±4	18±3	14±4	13±3	16±4	36±10
Zr*	66±18	72±15	72±20	76±17	67±19	68±11	71±18	273±88
B*	32±11	70±20	44±20	48±23	37±28	23±6	40±24	125±14

Table 1 (järg)

1	2	3	4	5	6	7	8	9
Ba	<110±40	130±30	170±50	170±40	<110±50	140±30	<140±50	350±50
Ga	<4±1	7±2	<5±2	6±2	<5±2	<5±1	<5±2	21±4
Sc	<4±3	4±1	<5±3	<6±3	<3±3	5±2	<5±3	14±4
V	15±4	22±4	18±7	24±9	19±7	21±5	21±7	78±32
Cr	26±8	39±11	27±10	34±12	<21±10	<21±6	<27±12	42±29
Mn	850±110	650±100	740±110	730±130	770±100	840±150	770±130	220±120
Co	<4±1	5±1	<4±2	6±2	<4±1	<4±1	<4±2	10±4
Ni	13±3	13±2	14±5	13±3	12±4	12±3	13±3	29±8
Cu	7±1	9±2	9±2	10±3	9±3	8±1	9±3	16±5
Yb	<2±1	3±0	2±1	3±1	<2±1	<2±1	<2±1	4±1
K (%)								7±2
Th*								14±3
Nb*								17±6
Zn								25±10
Be								4±2
La								24±10

The content of magnesium is slightly related with iron and terrigenous association, which is common for Estonian carbonates and can be explained by similar behaviour of many metals in sorption from seawater to clay particles and in later diagenetic transformation to dolomite (Mg), sulphides or moving to the structure of clay minerals (Kiipli et al., 1984).

Strontium has clear negative correlation with magnesium (correlation coefficient r = –0.50) and was obviously partly removed by dolomitization (Taalmann et al., 1977). Strontium has some positive correlation with several elements of terrigenous association (Ba, B, Cu, Si, Ti) but not with calcium (r = 0.04). Lead is slightly correlated with iron association (Fe, V), occurring probably with them in some sulphide-rich rocks like pyritized limestone below discontinuity surfaces.

Distribution of elements in the sequence

The mean values and standard deviations of elemental concentrations and of insoluble residue content in traditional lithostratigraphic units and in limestone and marl of the whole Kahula Group are shown in the Table. Lithologically very similar Pagari, Madise (in the Jõhvi Stage) and Kurtna "members" (in the Keila Stage) are taken together. Vasavere and Pagari-Madise-Kurtna beds represent more argillaceous parts of the lower and upper mesocyclite, respectively; Tatruse and Pääsküla beds are less argillaceous parts of them. The uppermost part, Saue "member", is argillaceous limestone differing from the rest of the complex by presence of some shell accumulations. Vertical distribution of insoluble residue and of selected elements in the Tähkvere-704 boring core is shown in Fig. 2.

Distribution of most of the elements is determined by content of argillaceous material. The variance of this component is controlled mainly by microcycles, particularly in the upper mesocyclite. Meso- and macrocyclites have also some influence to distribution of argillaceous material, as it is seen in the Table by means of insoluble residue content, but this variance is not so wide as in microcyclites. Content of argillaceous material and of most of the elements of this group varies 3–5 times in microcyclites whereas mean values for the parts of the meso- and macrocyclites vary only 1.2–2 times. For this reason, the

distribution of majority of elements in the sequence is determined by microcyclicity.

Considering the magnesium to be related mainly with dolomite, the calculated content of this mineral in the main part of the studied interval of Tähkvere-704 core is 3–15% (mean ~8%). The uppermost 1–1.2 m of Keila Stage below the significant discontinuity surface is containing dolomite 13–18% in boring core 704 and uppermost 1.4 m in boring core Vaali-707 even 40–42% (by two samples; the third sample 4 m below the discontinuity surface contained 6% of dolomite). Content of strontium in this layer is 1.5–2 times lower than average. Low values of strontium content are common for secondary dolomitized limestones (Taalmann e.a., 1977; Kiipli, 1983; Tucker, Wright, 1990). The higher dolomitization of only about meter-thick bed below the discontinuity surface, marking considerable sedimentary gap in Middle Ordovician, may refer to possible early dolomitization of limestones started already during the existence of hardground environment. This process might take place in a mixing zone of fresh groundwater (or meteoric water) and percolating seawater (Kiipli, 1983; Moore, 1989). T. Kiipli (1983) refers to examples, if upper 1–3 metres of the Pirgu and Jaagarahu stages are dolomitized below the overlying regressive beds.

The more realistic explanation for magnesium and strontium distribution pattern in the sequence (particularly in the Vaali-707 core) is secondary post-Ordovician selective dolomitization. In many boring cores of East Estonia the aphanitic pure limestone of Rägavere Formation (Voore Group), overlying the Idavere-Keila argillaceous complex, is strongly affected by post-Ordovician dolomitization. This process was usually stopped in the rapid lithological boundary between the Kahula and Voore groups (Keila and Oandu stages) and underlying argillaceous limestone remained undolomitized. However, the limit of secondary changes of limestone was not so rapid and uppermost part of the Keila Stage is often more or less dolomitized (data by Ain Põldvere). That was partly caused by absence of marl layer of the Hirmuse Formation (Oandu Stage) in this boundary in central part of East Estonia. After T. Kiipli (1983) large dolomitization of Ordovician and Silurian limestones took place under the bottom of Devonian sea in an intermixture zone of groundwater and seawater.

Very high concentration of lead (5–6 times higher than average) is related with the same discontinuity surface in the upper boundary of the Keila Stage (and of the macrocyclite). This surface is characterized by pyritized impregnation zone with thickness 15–25 cm below the surface and by long vertical and subhorizontal pyritized borings, reaching up to 15 cm from the surface. The impregnation zone is dark in colour because of fine pyrite crystals, but 20 cm of light-coloured aphanitic limestone of Oandu Stage above the surface contains big pyrite crystals of 0.5–1 cm in size. Both rocks sampled 5 cm above and below the surface have very high lead content. The abundance of pyrite with high lead content in overlying bed may be caused by replacement of sulphides from discontinuity surface impregnation zone to surrounding limestones after early diagenesis. There are described examples in the world, if formation of ore of Pb-Zn-Fe sulphides is related with discontinuity (emersion) surfaces and unconformities in the carbonate rocks (Flügel, 1982).

It must be taken into account that rapid lithological boundary between the Kahula and Voore groups might work as geochemical barrier, causing some sulphide mineralization and stratigraphically traced dolomitization in East Estonia.

K-bentonites

There are at least 17 thin (up to 10 cm) layers of K-bentonite or bentonitic marl in the Idavere, Jõhvi and Keila stages in East Estonia, 6 of which in the Tähkvere-704 core were sampled and analyzed (Table). These results are quite similar to composition of North American K-bentonites of the same age, analyzed by Kolata et al. (1986). East Estonian bentonites seem to be more rich in Na, Fe, Cr, Yb and La and more pure in Zn content than North American ones, although, the laboratory methods used are not comparable.

Conclusions

The majority of elements in the Kahula Group are related with terrigenous material and therefore their distribution in the

sequence is controlled mainly by microcyclical variation of argillaceous material. Macro- and mesocyclites in the Idavere-Keila complex control only slightly these variations. The most notable variations in magnesium, strontium and lead concentrations in the sequence are related with secondary changes of carbonate rocks nearby discontinuity surface and significant lithological boundary between the Kahula and Voore groups.

Acknowledgements

The author is thankful to Mr. Ain Põldvere (Geological Survey of Estonia) for his generous assistance with this work.

References

Ainsaar L., 1992. Jõhvi ja Keila lademe stratigraafilisest liigestamisest Põhja-Eestis. — Acta et Commentationes Universitatis Tartuensis, 956, lk. 56–68.

Ainsaar L., 1993. On the stratigraphy of the Middle Ordovician Jõhvi and Keila Regional Stages in North Estonia. — Geologija (Vilnius), 14, I, p. 109–117.

Flügel E., 1982. Microfacies analysis of limestones. Berlin e.a., Springer-Verlag, 633 p.

Kiipli, 1983 – **Кийпли Т.** О генезисе доломитов ордовика и силура в зоне контакта с перекрывающими отложениями девона. — Известия АН ЭССР. Геология, 32, с. 110–117.

Kiipli et al., 1984 – **Кийпли Т., Кивисилла Я., Винтсаар П., Таалманн В.** Эволюция химического состава известняков ордо- вика и силура Эстонии. — Известия АН ЭССР. Геология, 33, с. 120-127.

Kolata D. R., Frost J. K., Huff W. D., 1986. K-bentonites of the Ordovician Decorah Subgroup, Upper Mississippi Valley: correlation by chemical fingerprinting. — Illinois Geological Survey Circular 537, 30 p.

Kõrts et al., 1991 – **Кыртс А., Мянниль Р., Пыльма Л., Эйнасто Р.** Этапы и обстановки накопления кукеристовой (водорослевой) органики в ордовике и силуре Эстонии. В кн: Кальо Д., Модзалевская Т. Л., Богданова Т. Н. (ред.). Важнейшие биотические события в истории Эстонии. Труды XXXII сессии Всесоюзного палеонтологического общества. Таллинн, с. 87–95.

Männil R., 1990. The Ordovician of Estonia. In: Kaljo, D., Nestor, H. (eds). Field meeting, Estonia 1990, An excursion guidebook. Tallinn, Estonian Academy of Sciences, p. 11–20.

Moore C. H., 1989. Carbonate diagenesis and porosity. — Developments in Sedimentology, 46, Amsterdam e.a., Elsevier, 338 p.

Resheniya ..., 1978 – Решения Межведомственного регионального стратиграфического совещания по разработке унифицированных стратиграфических схем Прибалтики 1976 г. Ленинград, 84 с.

Resheniya ..., 1987 – Решения Межведомственного стратиграфического совещания по ордовику и силуру Восточно-Европейской платформы 1984 г. с региональными стратиграфическими схемами. Ленинград, 114 с.

Taalmann et al., 1977 – **Таалманн В., Вингисаар П., Кяйпли Т.** Геохимические особенности доломитизированных карбонатных пород Эстонии. В кн: Опыт изучения вторичных изменений в карбонатных породах Прибалтики и Белоруссии, Таллинн, с. 8–9.

Tucker, M. E., Wright, V. P., 1990. Carbonate sedimentology. Oxford e.a., Blacknell Scientific Publications, 482 p.

Vingisaar et al., 1979 – **Вингисаар П., Гулова Х., Кяйпли Т., Таалманн В.** Вещественный состав палеозойских карбонатных пород Эстонии. – Известия АН ЭССР. Геология, 28, с. 45–51.

Vingisaar et al., 1981 – **Вингисаар П., Гулова Х., Кяйпли Т., Таалманн В.** Распределение микроэлементов в карбонатных породах ордовика и силура Эстонии. Известия АН ЭССР. Геология, 30, с. 106–110.

IDAVERE, JÕHVI JA KEILA LADEME KARBONAATKIVIMITE KOOSTIS IDA-EESTIS

Leho Ainsaar

Resümee

Uuriti 23 keemilise elemendi ja lahustumatu jäägi jaotust ühte makrotsükliiti esindavas Kahula ülemkihistus kahes Ida-Eesti läbilõikes. Geokeemiliste (röntgenfluoressents, spektraal- ja lühendatud keemilise analüüsi) andmete statistilise töötluse tulemusel eraldati terrigeense komponendiga seotud ja sellest sõltumatud (Mg, Mn, Sr, Pb) elemendid ning leiti iga elemendi põhilised statistilised näitajad erinevate litoloogiliste ühikute kaupa. Terrigeense komponendiga seotud elementide sisaldust kontrollib põhiliselt sedimentatsioonniline mikrotsüklilisus, sisalduste varieeruvus makro- ja mesotsükliitide erinevate osade vahel on tunduvalt väiksem. Suurimad kõikumised magneesiumi, strontsiumi ja plii sisaldustes on seotud sekundaarsete protsessidega lubjakivis Keila ja Oandu lademe piiril, mis kujutab püriitset katkestuspinda koos suure litoloogilise muutusega.

Contents — Sisukord